

61-639 SONIC FATIGUE 1962

0-1

ASD-TR-61-639

## SONIC FATIGUE LIFE DETERMINATION BY SIREN TESTING

TECHNICAL REPORT No. ASD-TR-61-639

MAY 1962

FLIGHT DYNAMICS LABORATORY  
AERONAUTICAL SYSTEMS DIVISION  
AIR FORCE SYSTEMS COMMAND  
WRIGHT-PATTERSON AIR FORCE BASE, OHIO

Project No. 1370, Task No. 137001

(Prepared under Contract No. AF 33(616)-7147  
by Bolt Beranek and Newman, Inc.  
Authors: Preston W. Smith, Jr. and Charles I. Malme)

20100804 112

## NOTICES

When Government drawings, specifications, or other data are used for any purpose other than in connection with a definitely related Government procurement operation, the United States Government thereby incurs no responsibility nor any obligation whatsoever; and the fact that the Government may have formulated, furnished, or in any way supplied the said drawings, specifications, or other data, is not to be regarded by implication or otherwise as in any manner licensing the holder or any other person or corporation, or conveying any rights or permission to manufacture, use, or sell any patented invention that may in any way be related thereto.

Qualified requesters may obtain copies of this report from the Armed Service Technical Information Agency, (ASTIA), Arlington Hall Station, Arlington 12, Virginia.

This report has been released to the Office of Technical Services, U. S. Department of Commerce, Washington 25, D. C., for sale to the general public.

Copies of ASD Technical Reports and Technical Notes should not be returned to the Aeronautical Systems Division unless return is required by security considerations, contractual obligations, or notice on a specific document.

## FOREWORD

This report was prepared by Bolt Beranek and Newman Inc., Cambridge 38, Massachusetts, on Air Force Contract AF33(616)-7147 under Project Nr 1370, "Dynamics Problems in Flight Vehicles", Task Nr 137001, "Resonant Fatigue of Structures". This Task and Project are a part of Air Force Systems Command's Applied Research Program 750A, "Mechanics of Flight". The work was administered under the direction of Flight Dynamics Laboratory, Aeronautical Systems Division. Mr. M. J. Cote was task engineer for the Laboratory.

The studies presented began in March 1960 and were completed in October 1961. Dr. P. W. Smith, Jr., was project supervisor.

The authors acknowledge the considerable assistance in various phases of the work of Dr. Ira Dyer, Dr. Richard H. Lyon, Mr. Richard J. McQuillin, and Mr. Creighton M. Gogos, all of Bolt Beranek and Newman Inc. The valuable comments of Mr. M. J. Cote, and Dr. O. R. Rogers of Flight Dynamics Laboratory, Aeronautical Systems Division, and the able cooperation of personnel of both Flight Dynamics Laboratory and Test Operation Branch, Propulsion Division, Directorate of Engineering Test, in making available and operating the test stand at Wright Field where the jet noise tests were made, is also gratefully acknowledged.

This report concludes the work on Contract AF33(616)-7147.



## ABSTRACT

Experimental and theoretical researches were made on the problem of predicting the fatigue life of a resonant structure exposed to jet noise by testing it with intense sound from a siren. One panel design of Alclad 2024 aluminum was tested to fatigue with constant-amplitude and variable amplitude siren sounds and with jet noise. A close correlation of all three results was found.

A comparison was also made of fatigue lifetimes of a resonant cantilever beam, of plain 2024 aluminum, measured with constant excitation amplitude (pure tone) and with random excitation. Random lifetimes were found to be shorter than predictions from constant-amplitude data.

## PUBLICATION REVIEW

This report has been reviewed and is approved.

FOR THE COMMANDER:



WILLIAM C. NIELSEN

Colonel, USAF

Chief, Flight Dynamics Laboratory



## TABLE OF CONTENTS

	<u>Page</u>
I. INTRODUCTION .....	1
II. SIREN-JET EQUIVALENCES FOR FATIGUE .....	3
A. Linear, One-Mode, Non-Interacting System .....	3
B. Theoretical Equivalence for Nonlinear One-Mode, Non-Interacting System .....	16
C. Experimental Equivalence Scheme for System with Response Nonlinearity and Several Modes .....	24
D. Experimental Equivalence Scheme for System with Response Nonlinearity and Fatigue Interactions .....	27
III. FATIGUE TESTS OF RESONANT STRUCTURE UNDER RANDOM AND CONSTANT-AMPLITUDE EXCITATIONS .....	31
A. Apparatus and Test Procedures .....	31
B. Results and Analysis .....	33
C. Data for Alclad 2024 .....	40
IV. STUDIES OF PANEL RESPONSE .....	41
A. Panel Design and Mounting .....	41
B. Pure-Tone Response .....	44
C. Random Response .....	48
D. Comments on Nonlinearity .....	53
V. PROGRAMS FOR VARIABLE-AMPLITUDE FATIGUE TESTING .....	54
A. The "Ideal" Program .....	54
B. Practical Siren Control Problems .....	59
C. A Simplified Program .....	60
VI. PANEL FATIGUE TESTS .....	64
A. Constant-Amplitude Tests .....	64
B. Programmed Variable-Amplitude Tests .....	67
C. Jet Noise Tests .....	71
VII. EVALUATIONS AND COMPARISONS .....	78
A. General Comments .....	81
B. Programmed Amplitude Test Schemes - Pro and Con .....	82
C. Fatigue Interactions .....	82
D. Nonlinearity .....	82

## TABLE OF CONTENTS (Cont)

	<u>Page</u>
VIII. RESEARCH ON SIREN FATIGUE TESTING .....	83
A. Experimental Investigation of Variability for Typical Construction .....	83
B. Experimental Comparisons of Constant Amplitude, Programmed Amplitude, and Random-Resonant Fatigue Lifetimes .....	83
C. Random Response of One-Mode Resonator with Nonlinear Damping .....	84
D. Response of Nonlinearly Coupled Proximate Modes .....	84
E. Experiments on Fatigue Life of a Structure with Two Distinct Modes .....	84
F. Few-Mode Models of Practical Structures .....	85
REFERENCE LIST .....	86

## LIST OF ILLUSTRATIONS

<u>Figure</u>		<u>Page</u>
1	Phase and Magnitude Relations Between Blocked, Radiation, and Total Sound Pressure Components for Pure-Tone Testing Near Resonance .....	15
2	Average Rate of Accumulation of Damage (per cycle) in Random Response of a Hard-Spring Resonator .....	18
3	Linear Prediction of Equivalent Strain. Steady Response at Equivalent Strain Level Yields Same Lifetime as Random Response at RMS Strain Level .....	20
4	Cumulative Distribution Curves for Damage (Linear Case).	21
5	Geometric Mean of the Strains at the Quartile Points of Damage Distribution Curve, as a Function of Nonlinearity	23
6	Cantilever Test Specimen for Random and Constant-Amplitude Fatigue Studies .....	32
7	Instrumentation for Cantilever Beam Fatigue Test .....	34
8	Fatigue Curves for 2024 Aluminum. Results of Constant-Amplitude and Random Experiments on Resonant Cantilever Beam, and Predictions Therefrom .....	35
9	Probability Density of Strain in Cantilever Beam Response to Random Excitation .....	37
10	Growth of Crack Length During Steady Random Excitation of Resonant Beam (Resonance Frequency, 185 cps) .....	39
11	Design of the Structural Panel .....	42
12	The Panels in Their Field Mounting for Jet Tests (Instruments Exposed for the Photograph) .....	43
13	Pure-Tone Panel Response Data .....	46
14	Probability Density of Strain in Panel Exposed to Random Noise in the Laboratory .....	51
15	Probability Density of Strain in Panel Exposed to Jet Noise .....	52



# LIST OF ILLUSTRATIONS (Cont)

<u>Figure</u>		<u>Page</u>
16	Envelope of Pressure During One Program Block .....	55
17	Distortion of Response Envelope Near the Peak of the Pressure Envelope .....	57
18	Envelope of Pressure During One Block of the Simplified Program (Block Equivalent to $10^5$ Cycles of Random Response at 110 cps) .....	61
19	Fatigue Lives with Constant Amplitude as Functions of Strain and Blocked Sound Pressure (Seven Panels, Identified by Number).....	65
20	Fatigue Lives with Programmed Amplitude as Function of Blocked Sound Pressure .....	69
21	Fatigue Curves for Alclad 2024 Aluminum .....	70
22	Contours of Constant Sound Pressure Level in a Third-Octave Band Centered on 110 cps (J75-P19 Jet Engine at Military Power) .....	72
23	Narrow-Band Spectrum of Acceleration Response of Panel to Jet Noise (145 DB Overall) .....	73
24	Narrow-Band Spectrum of Strain Response of Panel to Jet Noise (145 DB Overall) .....	74
25	Strain-Life Fatigue Data with Jet Noise Excitation ....	76
26	Sound Pressure - Life Fatigue Data with Jet Noise Excitation .....	77
27	Jet Noise Fatigue Data, Compared with Predictions Based on Laboratory Measurements of Random Response ...	79
28	Jet Noise Fatigue Data Compared with Predictions Based on Field Measurements of Random Response.....	80

## SECTION I

### INTRODUCTION

This report describes results of experimental research, with associated theoretical investigations, on the problem of predicting the fatigue life to be expected of a resonant structure exposed to jet noise by means of the results of tests with intense sound from a siren.

Several different testing methods and prediction schemes were tried. The actual predictions are compared in section VII with life-times measured in a jet noise field.

The theoretical bases of the various prediction schemes are described in section II. One scheme depends upon standard fatigue curves, constant-amplitude fatigue tests with a siren, response measurements, and theoretical calculations. A second scheme is thoroughly experimental, being based on variable-amplitude fatigue tests of the structure with a siren and various response measurements.

Some theoretical analyses of the effect upon fatigue life of a nonlinearity of the hard-spring type are also presented in section II.

Section III contains experimental comparisons of life under constant-amplitude and random excitations for a resonant cantilever beam of 2024 aluminum alloy. The results with random excitation are compared with predictions from the constant-amplitude data. These experiments represent a test in miniature of one prediction scheme, under very carefully controlled conditions.

Results of laboratory studies of the response of the structural panels used in the full-scale tests are given in section IV, along with some response data from the field tests.

The details of the design for the program used in the variable-amplitude fatigue tests are presented in section V.

The results of fatigue tests with constant-amplitude and variable-amplitude sound from the siren and of field tests with jet noise excitation are given in section VI.

---

Manuscript released by authors October 1961 for publication as an ASD Technical Report.

The results of this research have indicated a number of areas which require detailed investigation in order to improve the reliability of siren testing methods. These areas are described in section VIII.

Throughout this report the amplitude of strain  $\epsilon$ , is reported in logarithmic measure. This "strain level" is defined as  $20 \log_{10}(\epsilon/10^{-6})$ ; the unit is the "decibel", abbreviated to db, and the reference level is 1 microstrain, i.e.,  $10^{-6}$ . This procedure is natural to persons familiar with acoustical measurements and was found almost essential, in view of the available instrumentation, in order to avoid errors.



## SECTION II

### SIREN-JET EQUIVALENCES FOR FATIGUE

In this section we consider the bases of various methods for predicting the lifetime of a structure exposed to jet noise from results of tests performed with the more-or-less pure tone sound from a siren. The purpose of any of these methods is the prediction of sound excitations in the two environments which are "equivalent" in the sense that the resulting fatigue lifetimes are equal. Alternatively, a satisfactory "equivalence" will be achieved if the two lifetimes differ by a predictable amount.

Structures susceptible to sonic fatigue damage are highly resonant, characterized by one or more resonance frequencies. The forces exerted by jet sound are random in nature. Thus any equivalence scheme must take cognizance of the differences in response to random and to pure tone forces, and also of the differences in fatigue damage done by these responses. Differing degrees of idealization of those two aspects of the equivalence question -- response and fatigue -- account for the differences between the various schemes.

There is one other important criterion for a satisfactory siren-jet equivalence scheme: It must be capable of experimental realization with a reasonable investment of equipment and effort.

In this section we describe a number of different equivalence schemes. Some are based more or less directly on methods described in the literature, while others were developed on this project.

#### A. LINEAR, ONE-MODE, NON-INTERACTING SYSTEM

This equivalence scheme is valid for a linear system resonant in a single mode when there are no fatigue interactions between peak strains of different levels (i.e., Miner's law of fatigue accumulation is valid).<sup>\*</sup> The fundamental analysis was carried out by Miles (ref. 1).

##### 1. Analysis for Fatigue Damage

We assume that the jet sound pressures are random and normally distributed with a smooth spectral density in the narrow bandwidth of the structure's resonance. These have been demonstrated to be good assumptions (ref. 2). Then the probability density of the peaks of response strain  $\epsilon$  at any point is a Rayleigh distribution curve

---

<sup>\*</sup>Throughout this report we use strain rather than stress as the measure of response for reasons that are discussed below.

$$p(x) = x \exp(-x^2/2) \quad (1)$$

where  $x$  is the ratio of the magnitude of a strain peak,  $\epsilon$ , to the rms strain  $\sigma$ :

$$x = \epsilon/\sigma \quad (2)$$

The strain cycles are fully reversed, except when the peak strain is very small, and the average interval between peaks is the period of natural vibration.

In addition to the assumption of no fatigue interactions, let us assume that the constant-amplitude fatigue curve (peak strain versus life) is a straight line in a log-log plot:

$$\epsilon^\alpha N = \text{constant}, \quad (3)$$

where  $N$  is the fatigue lifetime in cycles. Then, as Miles has shown, particularly simple results are found. The average damage per cycle of random response is the same as the damage per cycle of an equivalent response whose peak value is

$$\text{peak } x_{eq} = \sqrt{2} [(\alpha/2)!]^{1/\alpha}, \quad (4a)$$

and whose rms value is

$$\text{rms } x_{eq} = [(\alpha/2)!]^{1/\alpha}. \quad (4b)$$

Steady sinusoidal excitation to this equivalent response level, with fully-reversed cycles, should therefore yield the same lifetime as the random excitation.

In view of the curvature that appears in experimental constant-amplitude fatigue curves, it is reasonable to modify this procedure by substituting the experimental curve for Eq. (3). By Miner's law, the fractional damage per cycle of peak strain  $\epsilon$  is  $[1/N(\epsilon)]$ . Therefore the average damage per cycle of random response is the integral

$$1/N_R = \int_0^\infty [1/N(\epsilon)] p(x) dx \quad (5)$$

and equals the reciprocal of the expected random lifetime in cycles,  $N_R$ . This procedure has been developed, discussed, and applied by a number of researchers (refs. 3, 4, 5). The result of the integration is a value of random lifetime  $N_R$  for each value of rms response strain  $\sigma$ . Specific examples of such calculations will appear in later sections of this report. (Figs. 8 and 21 below.)



## 2. Stress-Life or Strain-Life?

In actuality, previous researchers have uniformly used a stress-lifetime fatigue curve in these computations, whereas we recommend the use of strain-lifetime curves. There is, of course, no difference as long as the strain in the fatiguing area is below the yield point. However, beyond the yield point, the peak stress and peak strain are nonlinearly related; an essential conflict arises with the assumption of linearity of response, made in the preceding analysis. The question to be answered is: Which, if either, of the two quantities, local stress and local strain, can be considered linearly related to the overall structural response?

The answer depends on the structure involved. In most cases of sonic fatigue, the area of large strains is very localized. First, the structure itself is a sort of strain-concentrating mechanism in the sense that the gross strain, such as might be measured by a strain gage, varies from area to area on it. Secondly, the fatigue damage usually occurs in a very localized region of further strain concentration, at the edge of a hole or in a sharp bend. In these circumstances, it appears reasonable to assume, as a first approximation, that yielding in the small fatiguing area does not affect the surrounding material and that the local strains in the fatiguing area are linearly related to the response.\* We note that Gunn has successfully used a similar approximation in his analysis of fatigue of specimens with a stress concentration (ref. 6).

The distinction between stress and strain becomes of particular importance at short lifetimes when a significant proportion of damage is due to strains above the local yield point. Whereas a constant-amplitude stress-lifetime curve rapidly becomes flat in this region, the corresponding strain-lifetime curve continues to rise smoothly toward the ultimate strain (the strain for failure in a "static" tensile test) (ref. 7). Because of this difference, computations of a random fatigue curve based on Eq. (5) and constant-amplitude stress-life curves should yield a predicted life that is very much too small at the short lifetime end. Just such a difference between predictions and measurements has been found in some experiments (ref. 5).

---

\*In the language appropriate to impedance concepts, the structure as a whole may be considered a "source", delivering strains to the "load", i.e., the local fatiguing area. We believe that the source impedance is large, the source acts as a constant-strain source, and that the strains at the interface are not significantly affected by the decrease in load impedance which local yielding represents.



### 3. Fracture by Rare, Large Response Peaks

The distinction between stress and strain is also important in settling the questions of damage due to rare, very large responses. In random response, response levels of indefinitely large values must be expected, although only with very small probability. A response exceeding the ultimate strength of the material will cause immediate fracture. How does one assess the probability of such damage by fracture, as contrasted with cumulative fatigue damage? The procedure we illustrate here is, admittedly, rather rough, but should give approximately correct answers. Any more exact assessment, incorporating all the nonlinearities of material and response, would be extremely complicated.

Consider a resonant structure of 2024 aluminum failing without the benefit of stress concentrations. Computations can be made by means of Eq. (5) using the strain-life failure curves of Freudenthal (ref. 8), and D'Amato (ref. 7). For an rms strain of  $1.9 \times 10^{-3}$  (rms stress of 20,000 psi) one computes an expected lifetime of  $1.6 \times 10^5$  cycles if he ignores the rare, very high strains. However, in this case the ultimate strength (64,000 psi) is only 3.2 times the rms stress. If the Rayleigh distribution [Eq. (1)] were valid for stress, cycles of peak stress exceeding the ultimate strength would be expected to occur 6 times in every 1000 cycles.\* Clearly, immediate fracture from such "rare" response levels would be much more likely than failure by the gradual accumulation of fatigue damage.\*\* The lifetime of the structure would not be determined by the rate of accumulation of fatigue damage but rather by the rate of occurrence of large responses. In the example cited above, measured lifetimes for an ensemble of identical structures would show a broad, flat distribution (equal probability density in lifetime) from zero to about 300 cycles (half the average interval between peaks exceeding the ultimate strength), with larger lifetime becoming gradually less probable.

---

\*The probability of exceedances of a response value  $x$  is  $\exp[-x^2/2]$ .

\*\*If cycles of large response levels occur in clumps, the probability of occurrence of a clump is less than the probability of exceedances by a factor which is, as a first approximation, the average number of cycles in a clump. The average clump size has been determined by analysis, for both linear and nonlinear systems (ref. 9). For practical values of damping, there is no significant tendency to clumping of peaks exceeding 3 times the rms response.

The fact, demonstrated in the literature (refs. 3, 5) and in this project, that random fatigue tests of resonant structures can be made at short lifetimes without any suggestions in the results of failure by rare exceedances of the ultimate stress, is positive evidence of the falsity of using stress as the independent variable in Eqs. (1) and (5).

If the independent variable in Eqs. (1) and (5) is taken to be strain, the problem of failure by rare exceedances of the ultimate strength does not arise. In the numerical example used above, the strain resulting in fracture on the first cycle (about 0.19 for 2024 aluminum) so far exceeds the rms strain,  $1.9 \times 10^{-3}$ , that a computed probability of exceedance (1 in  $10^{2171}$ ) is undoubtedly meaningless. In this view, the only significant failure mechanism is accumulative fatigue.

#### 4. Analysis for Response

The preceding discussion (subsection 1) has outlined the evaluation of a lifetime for random fatigue from (1) the rms value of response strain and (2) failure curves (peak strain-lifetime) for fully reversed strain cycles of constant amplitude. A complete equivalence scheme must also include a means of relating the rms response to the sound pressures exciting the structure.

We shall not consider methods for solving the response problem by pure computation. To some extent this is due to the natural bias of an experimenter; such a procedure seems only to add one more hazard to a long chain of hazardous predictions. In any case, a number of reasonable experimental methods for solving the response problem are available. (Computational methods have been adequately treated elsewhere (ref. 10).)

In the immediately succeeding paragraphs we summarize the equations governing the one-mode linear response of a structure to sonic excitation. Both pure tone and random excitations are considered.

The dynamical equation for one-mode response of a structure to pure tone sonic excitation can be written (ref. 11)

$$vZ_{\text{mech}} = F_{\text{tot}} = Tp_{\text{tot}} \quad (6)$$

where  $v$  is the response velocity,

$Z_{\text{mech}}$  is the in vacuo mechanical impedance,

$F_{\text{tot}}$  is the generalized force,

$T$  is a transfer function, with units of area, and

$p_{\text{tot}}$  is the sound pressure acting on the face of the structure.



If the structure is large or the motion complicated, consideration must be given to the dependence of  $T$  upon the spatial characteristics of the sound field (ref. 12). We shall assume here that the structure is small and that the sound pressure is sensibly constant over the face of the structure, so that  $T$  is therefore a constant in all environments.

The total sound pressure can, by superposition, be decomposed into the sum of the sound pressure measured when the structure is blocked (kept from vibrating) and the radiation sound pressure, measured with the structure vibrating but with the external sound source turned off:

$$P_{tot} = P_{bl} + P_{rad}, \text{ or}$$

$$F_{tot} = F_{bl} + F_{rad} \quad . \quad (7)$$

The radiation pressure is related to the radiation impedance:

$$F_{rad} = T p_{rad} = - v Z_{rad} \quad , \quad (8)$$

so that Eq. (6) can also be written

$$v(Z_{mech} + Z_{rad}) = v Z_{tot} = T p_{bl} = F_{bl} \quad . \quad (9)$$

The sum of mechanical (in vacuo) impedance and radiation impedance is the total impedance for vibration in the acoustical environment. The radiation impedance may change when the environment is changed.

The two dynamical equations, Eqs. (6) and (9), are perfectly equivalent, differing only in the treatment of the radiation pressure. In Eq. (6) the radiation pressure appears on the right side; in Eq. (9) it appears on the left in the guise of radiation impedance. The two equations have the same general form:

$$vZ = T p \quad . \quad (10a)$$

For the one-mode case we can write the impedance as

$$Z = R + j(\omega M - K/\omega) \quad , \quad (10b)$$

where  $R$ ,  $M$ , and  $K$  stand for modal resistance, mass, and stiffness, and where  $\omega$  is the frequency (radians per second). The response strain  $\epsilon$  is proportional to displacement, so that

$$\epsilon = C v/\omega \quad , \quad (11)$$

where  $C$  is an appropriate constant depending on mode shape.



The response to pure tone excitation at the resonance frequency  $\omega_0 = (K/M)^{1/2}$ , is the well-known solution of Eq. (10):

$$\epsilon = C v / \omega_0 = C T p / \omega_0 R, \text{ or}$$

$$\overline{\epsilon^2} = \overline{p^2} (CT / \omega_0 R)^2 \quad (12)$$

where we use the superscript bar to represent the time average.

The mean square response to random excitation is an equally well-known solution of Eq. (10) in the special case where the spectral density of  $p$  is essentially constant within the bandwidth of response (Ref. 1). That solution is

$$\overline{\epsilon^2} = C^2 \overline{v^2} / \omega_0^2 = S_p C^2 T^2 / 4RK \quad (13)$$

where  $S_p$  is the spectral density of the pressure  $p$  (units of pressure-squared<sup>p</sup> per cps).

We now turn to various schemes for predicting the rms response of a structure in a realistic jet environment from measurements in an artificial environment.

#### a. Low-Level Random Excitation

One experimental procedure for predicting the response involves the excitation of the actual structure by a moderately low level of random noise and measuring the corresponding low level of response. Then if, and only if, the test environment is essentially identical to the realistic environment, the ratio of rms response to rms excitation will be constant in a linear structure. If the two environments differ, a suitable correction must be made. We investigate here the nature of the correction for changes in the acoustic environment, that is in the radiation impedance.

(1) Measuring blocked pressure: If the excitation is characterized by the blocked sound pressure, the proper dynamical equation is Eq. (9). The prediction equation is then [see Eq. (13)]

$$\frac{\overline{\epsilon^2}_{(a)}}{\overline{\epsilon^2}_{(b)}} = \frac{S_p^{(bl)}_{(a)} R_{(b)} K_{(b)}}{S_p^{(bl)}_{(b)} R_{(a)} K_{(a)}} \quad (14a)$$

where  $R$  and  $K$  are total resistance and total stiffness and the subscripts  $(a)$  and  $(b)$  refer to the test and the realistic environments.

In normal circumstances, the total stiffness and total mass are negligibly affected by the radiation impedance. (This would not necessarily be true if the test environment is an acoustical resonance chamber.) In such cases we may approximate Eq. (14a) by

$$\frac{\overline{\epsilon^2}_{(a)}}{\overline{\epsilon^2}_{(b)}} \approx \frac{S_p^{(bl)}(a)}{S_p^{(bl)}(b)} \frac{\eta(b)}{\eta(a)} \quad (14b)$$

where  $\eta$  is the total loss factor, such as can be determined from the rate of decay of vibrations in the absence of external sound. (The quantity  $\pi\eta$  is the logarithmic decrement in nepers per cycle.)

(2) Measuring total pressure: If the excitation is characterized by the total sound pressure at the face of the vibrating structure, the proper dynamical equation is Eq. (6). A different approach is in order.

The first problem that arises is that the total sound pressure does not necessarily have a flat spectral density; a flat spectral density is required in order to use the simple expression, Eq. (13), for mean square response. Only if the radiation pressure is essentially negligible is one justified in using Eq. (13). We now consider one typical case in more detail.

In a common case of an aircraft panel vibrating in its fundamental mode, the radiation impedance includes a resistance which is small compared with the mechanical (internal) resistance, and a reactance corresponding to a virtual mass which is small compared with the mass of the structure. However the radiation reactance is, in the common case, large compared with the radiation resistance.

When the excitation is random, the previous dynamical impedance equations go over into equations between the spectral densities of the variables (Ref. 13). Thus, from Eq. (9) we have for the spectral density of blocked pressure

$$S_p^{(bl)} = S_v \left| Z_{tot} \right|^2 / T^2$$

where  $S_v$  is the spectral density of response velocity. At the resonance frequency  $\omega_0$ , the total impedance equals the total resistance and

$$S_p^{(bl)}(\omega_0) = S_v(\omega_0) R_{tot}^2 / T^2 \quad (15a)$$

Correspondingly, from Eq. (8), we have for the spectral density of radiation pressure

$$\begin{aligned} S_p^{(\text{rad})}(\omega_o) &= S_v(\omega_o) \left| Z_{\text{rad}}(\omega_o) \right|^2 / T^2 \\ &\approx S_v(\omega_o) \omega_o^2 M_{\text{rad}}^2 / T^2, \end{aligned} \quad (15b)$$

where in writing the last line we neglect the radiation resistance as small compared with radiation reactance.

Now let us look at the ratio of Eqs. (15a) and (15b):

$$\frac{S_p^{(\text{rad})}(\omega_o)}{S_p^{(\text{bl})}(\omega_o)} \approx \left( \frac{\omega_o M_{\text{rad}}}{R_{\text{tot}}} \right)^2 = \left( \frac{M_{\text{rad}}/M_{\text{tot}}}{\eta_{\text{tot}}} \right)^2 \quad (15c)$$

where we write the loss factor  $\eta$  for  $R/\omega M$ . This ratio, Eq. (15c) is not necessarily small. Typical values for loss factor are

$$\eta \approx 0.02 \text{ to } 0.04,$$

while typical magnitudes of the mass ratio for thin panels have been estimated to be (Ref. 14)

$$M_{\text{rad}}/M_{\text{tot}} \approx 0.01 \text{ to } 0.1.$$

Thus we conclude that the spectral density of radiation pressure may easily equal or exceed the spectral density of the blocked pressure, at the resonance frequency.

Note that the spectrum of the radiation pressure has essentially the same shape as the spectrum of the response velocity. [See Eq. (15b) and note that the radiation impedance usually varies only slowly with frequency.] Thus the energy of radiation pressure is essentially limited to a small frequency band,  $\Delta = \eta_{\text{tot}} f_o$  cps. On the other hand the spectral density of sound pressure is seldom determined with a filter having such a narrow bandwidth. Consider the relative contributions of radiation and blocked pressures to the total rms pressure measured in a bandwidth  $\Delta' = k f_o$ :

$$\text{in } \Delta': \quad \frac{\overline{p^2}^{(\text{rad})}}{\overline{p^2}^{(\text{bl})}} \approx \frac{\Delta S_p^{(\text{rad})}(\omega_o)}{\Delta' S_p^{(\text{bl})}} = \frac{(M_{\text{rad}}/M_{\text{tot}})^2}{k \eta_{\text{tot}}}. \quad (16)$$



If measurements are made with filters common in acoustical research, we have:

octave-band filter:  $k = 0.707$   
 third-octave filter:  $k = 0.236$

These values are so much larger than reasonably expected loss factors that the ratio of mean-square pressures in Eq. (16) is usually a small fraction.

From this analysis we conclude that the spectral density of radiation pressure at the resonance frequency is not necessarily negligible compared with the spectral density of blocked pressure. Even if the blocked pressure has a flat spectrum, the usual case, the total pressure may well not. Analyses such as that of Miles (ref. 1) may therefore not be strictly pertinent. On the other hand, the "spectral density" inferred from measurements of total sound pressure in a band much wider than the resonance band of the structure is often a good estimate of the true spectral density of blocked pressure. Its use in analyses such as Miles', using equations such as Eqs. (13) or (14), can thereby often be justified.

However, if in either the test or the realistic environments the radiation impedance (particularly the reactance) is abnormally high, a more detailed analysis may be required.

#### b. Low-Level Pure Tone Excitation

In many cases, determination of the rms response of measurements using low-level excitation with a band of random noise is not convenient. Then low-level pure tone sound, adjusted to the resonance frequency of the structure, may be used in the test environment. The rms response in the realistic environment (jet noise) can then be predicted from a combination of Eqs. (12) and (13):

$$\frac{\overline{\epsilon_r^2}}{\overline{\epsilon_t^2}} = \frac{S_p}{p_t^2} \frac{\omega_o^2 R_t}{4R_r K_r} , \quad (17a)$$

where the subscripts r and t are used to distinguish the "random", or realistic, and "tonal", or test, environments.

We now assume that the resonance frequencies and the modal masses are essentially the same in each environment. (This is generally found to be a good assumption except when the tonal test environment involves a resonant acoustic system.) Then Eq. (17a) can be rewritten:



$$\frac{\overline{\epsilon_r^2}}{\overline{\epsilon_t^2}} = \frac{S_p}{p_t^2} \frac{\omega_o \eta_t^2}{4 \eta_r} \quad (17b)$$

In the special case where the loss factor  $\eta$  is the same in both environments, this expression becomes

$$\frac{\overline{\epsilon_r^2}}{\overline{\epsilon_t^2}} = \frac{S_p}{p_t^2} \frac{\omega_o \eta}{4}, \quad (17c)$$

a form equivalent to results appearing widely in the literature (Refs. 1, 14, 15).

(1) To measure blocked or total pressure? The same question arises in this case of tonal excitation as did in the previous case of random excitation: Should one measure the blocked sound pressure or the total pressure (structure vibrating)? The answer is somewhat different in this case.

From Eq. (12) governing response to a tone, it is evident that the ratio

$$(\epsilon_t \eta_t / p_t)$$

is the same in either case; the same prediction of response will be made. However, if blocked pressure is measured, the sum of mechanical and radiation damping must be used in the calculation. [See Eq. (9).] If total pressure is measured, then the mechanical (in vacuo) damping alone must be used in the calculation. [See Eq. (6).] The difficulty with the latter procedure is that the in vacuo damping cannot be measured; the damping determined in the test environment is the sum of mechanical and radiation damping. (Any of the standard techniques may be used.)

An important simplification occurs if it can be assumed that;

- 1) the radiation damping in the random environment is negligible;
- 2) the mechanical damping is the same in both random and tonal environments.

Then the total pressure technique may be used with the simpler Eq. (17c) to predict the random response, even when the radiation damping is large in the tonal test environment. In the same situation, the blocked pressure technique requires that Eq. (17b) be used in order properly to account for radiation damping.

In contrast to this simplification resulting from the use of total pressure, there is some question about experimental precision arising from the use of this technique. In some cases the radiation damping dominates internal mechanical damping in the test environment; this occurred in the siren experiments reported below. Then the total pressure is much smaller than the blocked pressure. The total pressure is the vectorial sum of the blocked pressure and the radiation pressure. At resonance all three components are in phase (or anti-phase) as shown in Fig. 1. The blocked pressure is essentially constant, for small changes in frequency near resonance. However the radiation pressure, being proportional to response velocity, varies both in phase and magnitude; its trace in the vector plot (Fig. 1) lies on a circle passing through the end of the blocked pressure vector.

Now, the response strain is proportional to the response velocity and, therefore, to the radiation pressure. It appears from Fig. 1 that the magnitude of the ratio  $\epsilon^2/p^2$ , which appears in the prediction formula, Eq. (17), may be very sensitive to tuning in some circumstances; the fractional change in this ratio may be much larger than the fractional change in response. Therefore a slight detuning, not noticeable in the tuning procedure, may lead to larger errors in the prediction when the total pressure technique is used. This effect should be investigated qualitatively. (Note that tuning with phase measurements would minimize this source of error.) We believe this effect was responsible for some of the scatter observed in the measurements reported below.

To conclude this discussion, either the blocked pressure technique or the total pressure technique can be used in the prediction, if one is sufficiently careful to verify the assumptions. The choice is intimately related to the problems of determining the damping factor and of the variation in damping with acoustic environment.

## 5. Summary of Equivalence Scheme

The equivalence scheme described above is based on an analysis which assumes both a linear, one-mode structure and fatigue accumulation without interactions between the damage done by successive peaks of strain. The procedure for applying this scheme can be summarized into three steps.

Step 1. Pressure-Nominal Strain: The rms value of nominal strain (as measured by a strain gauge at any convenient spot on the structure) which will result from excitation by a specified random (jet) noise level is predicted by response measurements. These tests can use a pure tone exciting the structure at resonance, in which case Eq. (17) is used for the prediction. Alternatively, these tests can use a random sound, in which case Eq. (14) is used for the prediction. Some care is required to get an accurate prediction if the acoustical environment of the structure in these response tests is not realistic.

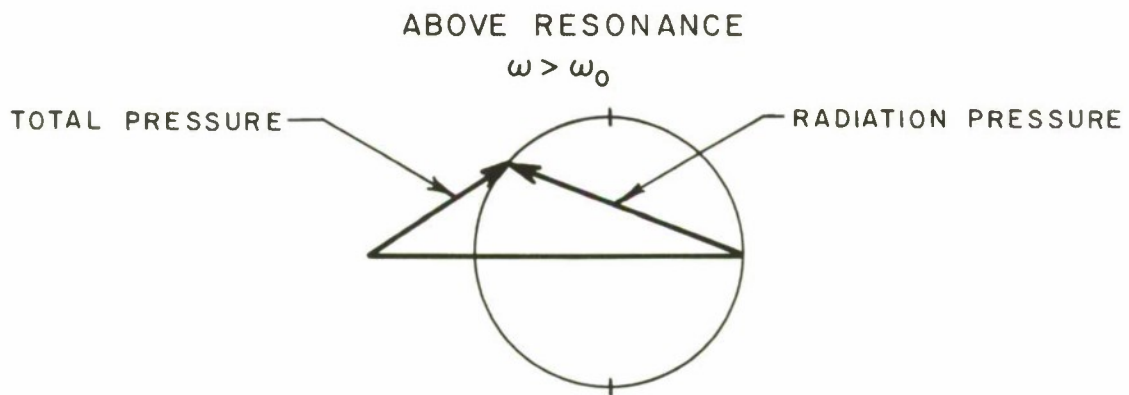
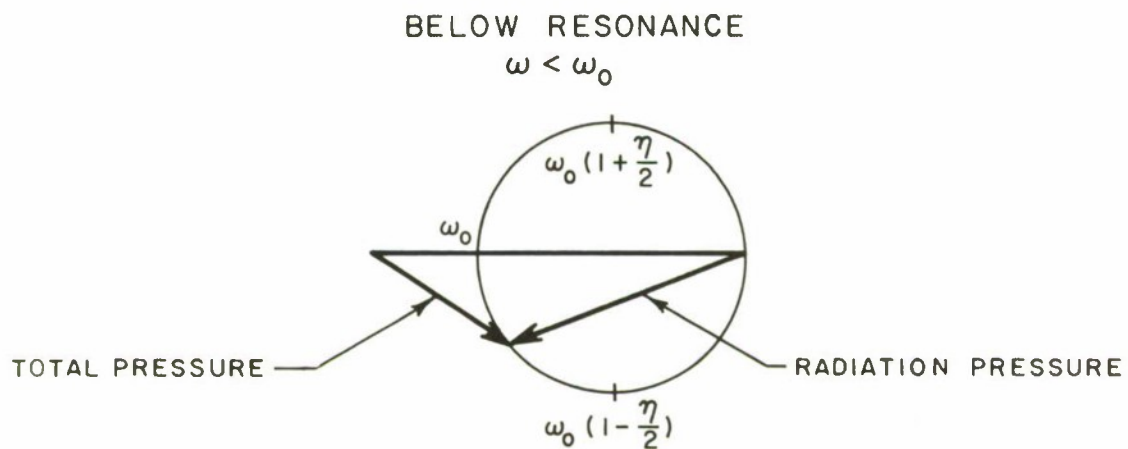
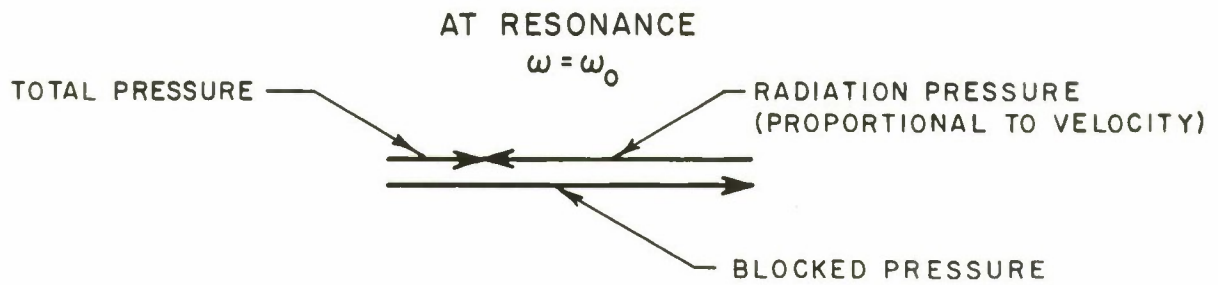


FIG.1 PHASE AND MAGNITUDE RELATIONS BETWEEN  
BLOCKED, RADIATION, AND TOTAL SOUND PRESSURE  
COMPONENTS FOR PURE-TONE TESTING NEAR  
RESONANCE



### Step 2. Nominal Strain - Fatigue Life (Constant Amplitude):

The structure is excited by a siren to a constant amplitude of alternating strain, and the fatigue life is determined. From this data, a constant amplitude fatigue curve is constructed. One may use fatigue curves derived for the material by measurements on small specimens, assuming that the strain concentration factor (between nominal strain and fatiguing strain) is a constant. Alternatively, one may excite to failure many nominally identical structures and construct a fatigue curve directly.

Step 3. RMS Random Nominal Strain - Fatigue Life: The last step is the computation of a "random S-N" curve in which the ordinate is the rms value of the nominal strain. The computation is based on the assumed Rayleigh distribution of strain peaks [Eq. (1)] and the integral formulation of Miner's law, Eq. (5).

## B. THEORETICAL EQUIVALENCE FOR NONLINEAR ONE-MODE, NON-INTERACTING SYSTEM

An analytical investigation was carried out, with the aid of a digital computer, to determine the effect of nonlinearities in the response of a structure upon the fatigue life (ref. 16). The presence of nonlinearity leads to a change in the probability density of strain peaks in the response to random excitation. These changes can lead to a rate of accumulation of damage which is different than that for the linear structure, even though the excitation is the same. We summarize that investigation here.

The analysis maintains the assumption that only one mode of response is excited. Neither is any attempt made to correct for fatigue interactions between different strain levels, except to the extent that the correction can be properly represented by a "fictitious S-N curve", as suggested by Freudenthal (ref. 17).

The analysis takes as a model for the nonlinear structure a beam with pinned ends, responding in its fundamental mode. The displacement  $s(t)$  at the center of such a beam satisfies the nonlinear equation of a hard-spring resonator:

$$M\ddot{s} + R\dot{s} + Ks(1+s^2/l^2) = F(t) \quad , \quad (18)$$

where mass  $M$ , resistance  $R$ , low-level stiffness  $K$ , and the "characteristic displacement"  $l$  are constants. The quantity  $F(t)$  is the generalized force. As long as  $s$  is small compared with  $l$ , this is the linear one-mode equation. The characteristic displacement  $l$  equals twice the radius of gyration of the beam's cross section if the ends of the beam are firmly pinned. Thus, in a flat plate of thickness  $t$ ,  $l = t/\sqrt{3}$ .

The surface strain  $\epsilon$  in the center of the beam (the point of maximum strain) is nonlinearly related to the displacement  $s$  by the equation

$$\epsilon = cs(1+s/2\sqrt{3} \ell) , \quad (19)$$

where  $c$  is a constant of proportionality. The linear term in Eq. (19) represents the usual bending strain which results from a transverse displacement of the beam's center. The nonlinear term represents the membrane strain due to the elongation of the beam when the transverse displacement is large.

### 1. Average Damage Per Cycle

The average fatigue damage per cycle was computed by Miner's law with the further assumption that the constant-amplitude fatigue curve is a straight line, in a log-log plot, with a slope  $(-\alpha)$ . These are the assumptions used to derive Eqs. (3) and (4) above. However the exact probability density of peaks was used instead of the Rayleigh distribution, Eq. (1), which holds for the linear structure.

The results of these computations are presented in Fig. 2. The ordinate in Fig. 2 is the ratio of the average damage per cycle in nonlinear random response to the "linear estimate" of average damage per cycle. The linear estimate is the damage that would be sustained by the same structure if the characteristic displacement  $\ell$  were very large; it is the value that would be predicted by the procedure outlined above in subsection A [Eqs. (4) and (13)]. The abscissa in Fig. 2 is a linearity parameter  $y$  defined by

$$y = 2\ell/\sigma_0 \quad (20)$$

where  $\sigma_0$  is the linear estimate of the rms of the displacement  $s$ . Linear response is represented by  $y = \infty$ .

The three top curves in Fig. 2, labelled CASE B, are the results for the pinned-beam, for values of  $\alpha = 4, 8, \text{ and } 16$ . The curves show that the damage rate increases with increasing nonlinearity (smaller  $y$ ) when the nonlinearity is small. There is a maximum point in each case. Thus for a value  $\alpha = 16$  (appropriate to 2024 aluminum near the endurance limit), the maximum effect is a factor 3.4; the actual nonlinear lifetime would be  $(1/3.4) \approx 0.3$  times the linear estimate of lifetime. We note that these effects are small when expressed in terms of the estimated response; the maximum effect of nonlinearity on lifetime corresponds to an increase of 8% (0.7 db) in the rms response.

The three curves labelled CASE A in Fig. 2 show the effect of nonlinearity on damage rate when the membrane strain (the nonlinear term in Eq. (19)) is neglected and the fatiguing strain is linearly proportional to displacement. Because nonlinearity diminishes the probability of large displacements, the damage rate is uniformly diminished in Case A. Asymptotic expressions for the ratios of damage rates for Cases A and B, valid for extreme nonlinearity, have been computed and published (ref. 18).



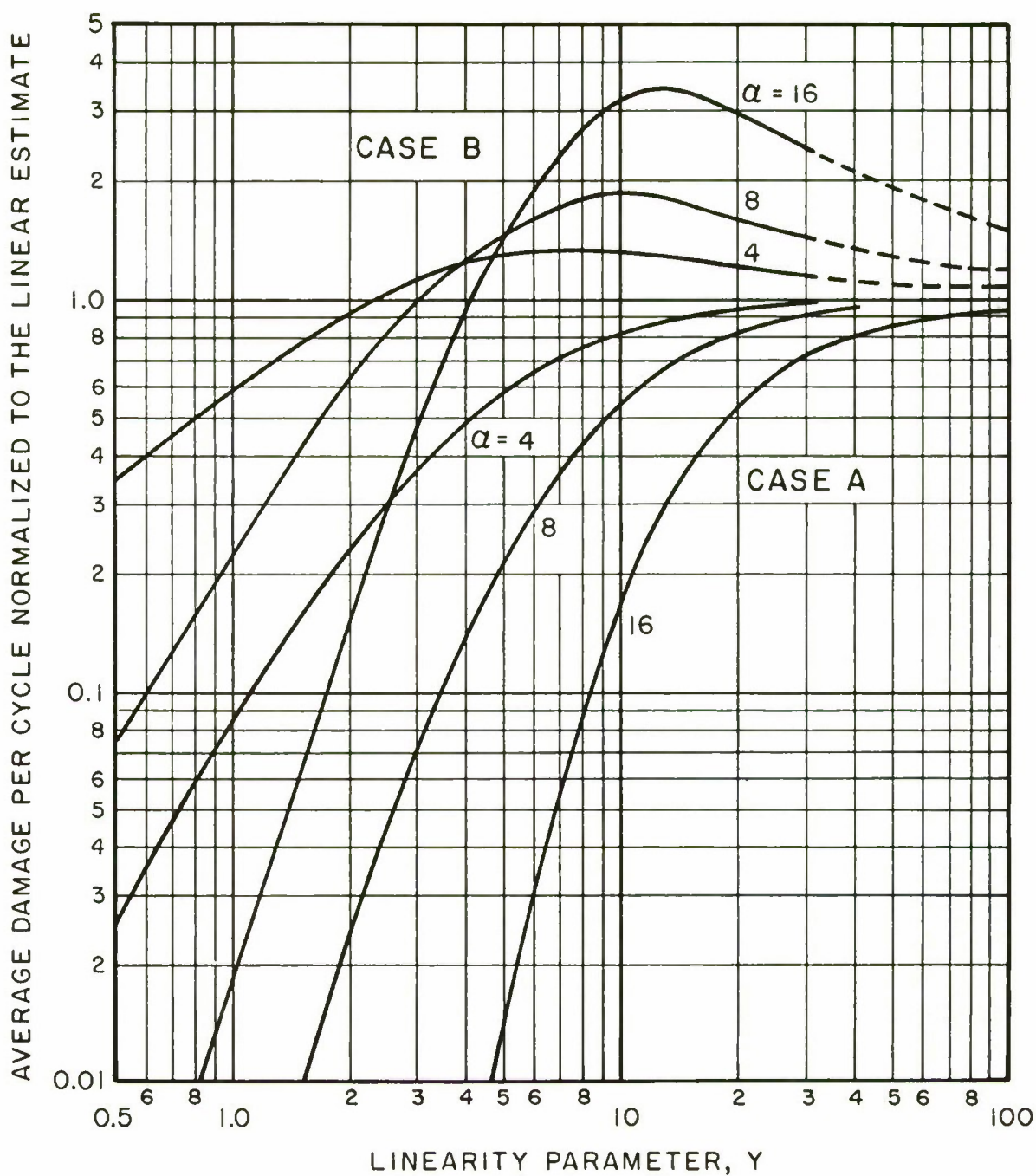


FIG. 2 AVERAGE RATE OF ACCUMULATION OF DAMAGE (PER CYCLE) IN RANDOM RESPONSE OF A HARD-SPRING RESONATOR



The curves in Fig. 2 only show changes from the linear prediction of the damage rate. The linear prediction of damage rate was discussed in subsection A above. It is encompassed in the "equivalent strain level" [Eq. (4)], which is defined as the steady response level that has the same lifetime as the specified rms strain response to random excitation. The difference (in decibels) between the equivalent strain level and the rms strain level is plotted in Fig. 3 against  $\alpha$ , the slope of the  $\log \epsilon - \log N$  curve.

## 2. Range of Damaging Strains

We consider here ways of characterizing the ranges of values of strain peaks which are responsible for the greatest part of the fatigue damage.

In the linear case this information is readily shown by plotting the cumulative distribution function of fatigue damage. These curves show as ordinate the percent of total damage which is attributable to response strain peaks smaller than the abscissa value. Such curves are shown in Fig. 4, where the abscissa is the strain level in db re the rms value of strain. For consistency with the nonlinear results, Fig. 4 is based on assumptions of

- Miner's law of damage accumulation [Eq. (5)]
- straight fatigue curve in a log-log plot [Eq. (3)]
- Rayleigh distribution of strain peaks [Eqs. (1) and (2)].

The resulting damage distribution function is an Incomplete Gamma function, for which tables exist.\*

Also plotted on Fig. 4 are the points of maximum damage density. These are the points at which the damage density -- the integrand

$$x^\alpha p(x) = x^{\alpha+1} \exp(-x^2/2)$$

in the integral, Eq. (5), for total damage -- has its maximum value. (Thus it is the "mode" of the damage density curve.) Analytically, the point of maximum damage (sometimes called "peak damage point") is

---

\*The function plotted in Fig. 4 is, in the notation of Pearson's Tables (ref. 19),

$$I\left[\frac{x^2}{\sqrt{2\alpha+4}}, \frac{\alpha}{2}\right].$$

It is plotted against  $20 \log_{10} x$ .

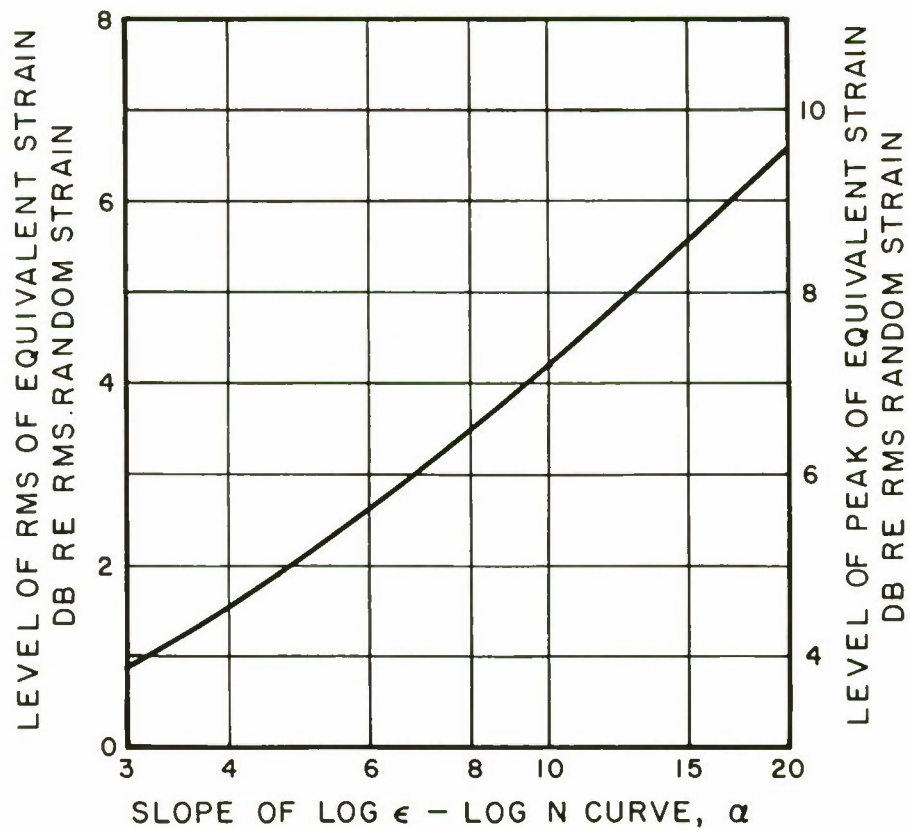


FIG. 3 LINEAR PREDICTION OF EQUIVALENT STRAIN. STEADY RESPONSE AT EQUIVALENT STRAIN LEVEL YIELDS SAME LIFETIME AS RANDOM RESPONSE AT RMS STRAIN LEVEL

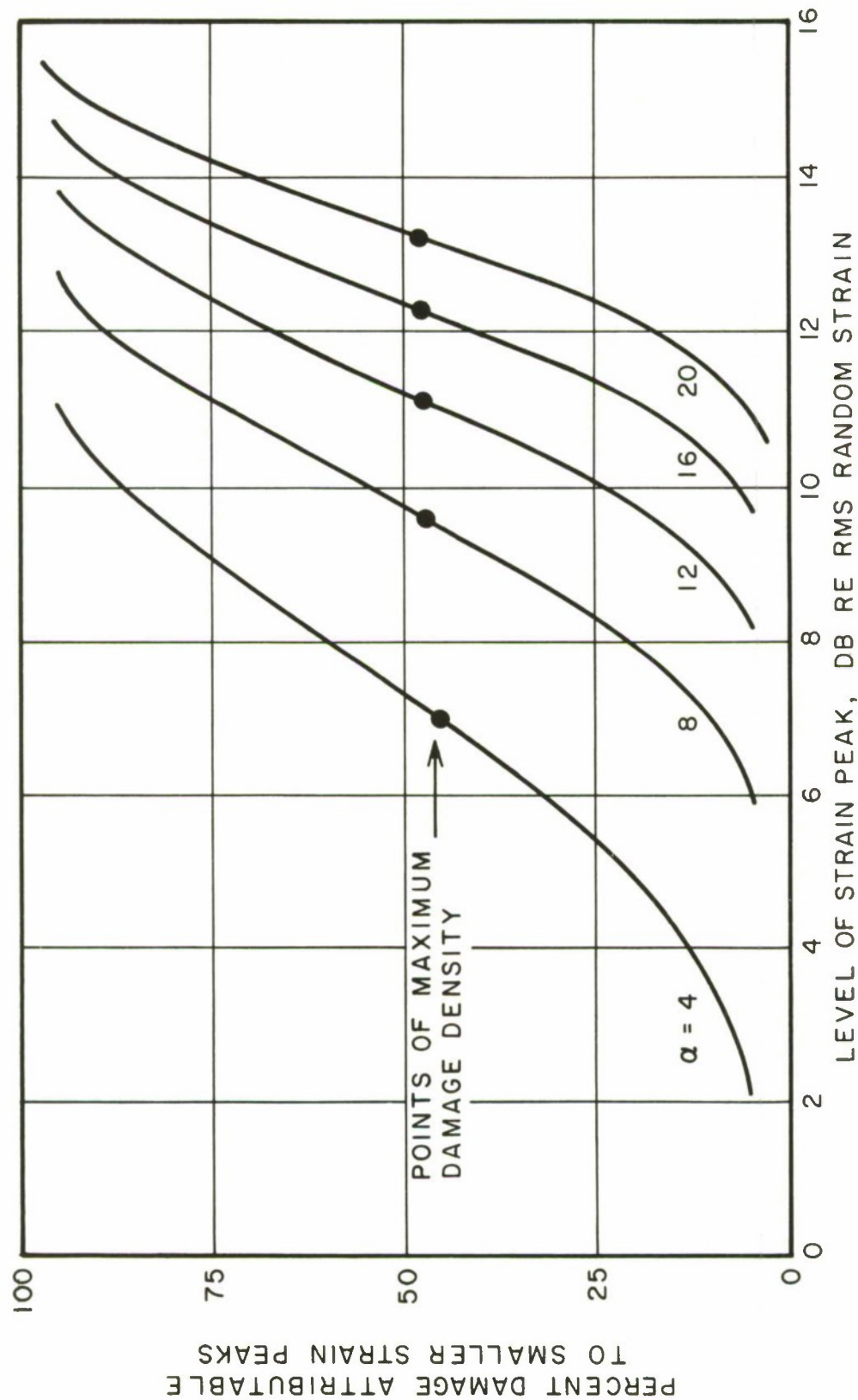


FIG. 4 CUMULATIVE DISTRIBUTION CURVES FOR DAMAGE (LINEAR CASE)



$$x_{PD} = (\alpha + 1)^{1/2} \quad (21)$$

where  $x = \epsilon/\sigma$ , is the ratio of strain to the rms value of strain. This point is seen to lie very close to the median of damage, i.e., the 50% point in Fig. 4.

Comparable detail about the distribution of damage in the non-linear random response is not available. However some comparisons between linear and nonlinear cases can be made. The most important range of values of response strain is conveniently characterized by the values of the quartile points on the distribution curves, the points which have ordinate values of 25% and 75% on Fig. 4. We shall use here the difference in the levels of the quartile strains (that is, 20 times the logarithm of their ratio) as a measure of the range of damaging strains. It was found, by hand calculations from the results of the digital computer analysis, that this range of damaging strains is essentially constant, as shown in Table I. The differences shown (0.3 db or less than 4%) are not significant in view of the possible errors in hand manipulation of the data.

TABLE I

THE INTERQUARTILE RANGE OF DAMAGE, IN DECIBELS:  $20 \log_{10}(x_{3/4}/x_{1/4})$ .

Values for nonlinear response were computed for values of linearity parameter  $y$  [Eq. (20)] from 4 to 32, and varied no more than  $\pm 0.1$  db.

slope $\alpha$ of fatigue curve:	4	8	16
linear range	3.6	2.8	2.0
nonlinear range	3.9	2.9	2.1

As a measure of central tendency of the damage distribution curves in the case of nonlinear response, we shall use the geometric mean value of the strains corresponding to the quartile points (25% and 75%) on the curve.\* In the linear case the geometric mean of the quartile points is very close (within 0.1 db or 1%) to the median (50% point). In the presence of response nonlinearity, the geometric mean value is slightly larger than for the corresponding linear structure (Fig. 5). The amount of change correlates quite well with the change in damage rate shown in Fig. 2 (Case B).

---

\*This somewhat unusual choice was dictated by the availability of data. Values of the median of the nonlinear damage curve were not recorded in the course of computations. The point of maximum damage density (the mode) suffers from the disadvantage of being sensitive to the choice of independent variable. However some values are given in Fig. 5 of reference 16.

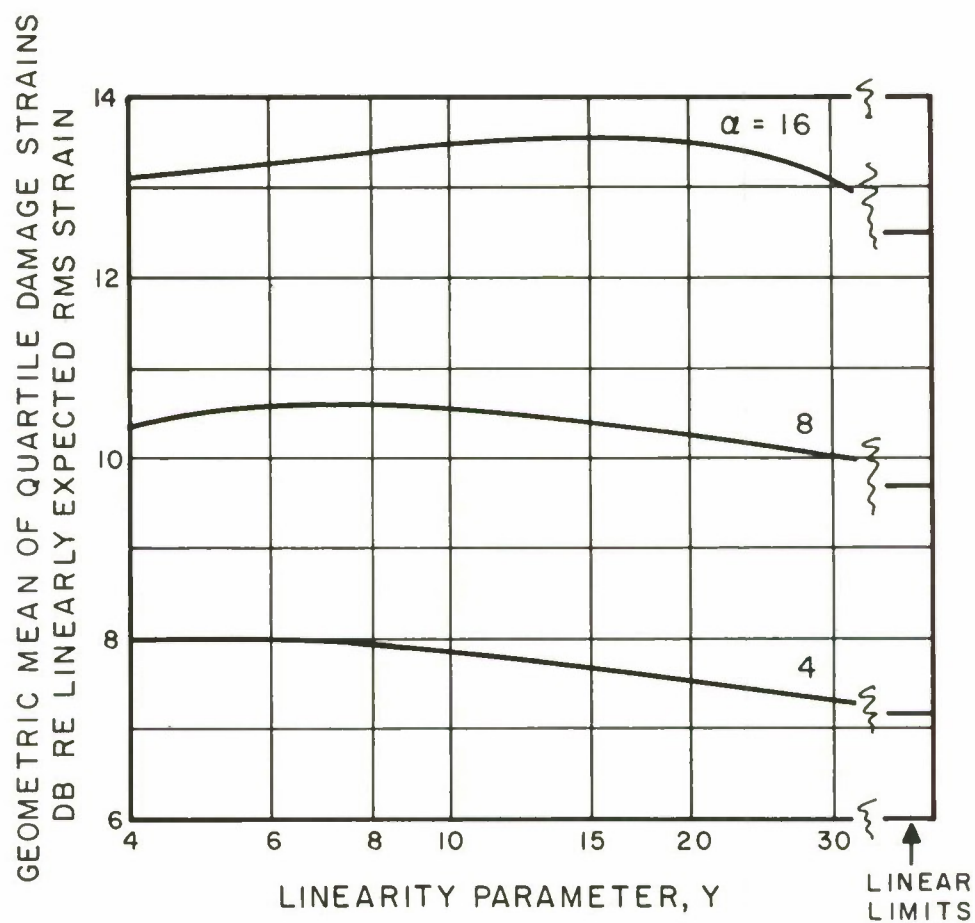


FIG. 5 GEOMETRIC MEAN OF THE STRAINS AT THE QUARTILE POINTS OF DAMAGE DISTRIBUTION CURVE, AS A FUNCTION OF NONLINEARITY

### 3. Summary

An analysis was made of the effects of dynamic nonlinearity upon fatigue damage from random excitation. The results are strictly pertinent only to a particular model of the structure: A beam with pinned ends, vibrating in its fundamental mode, with fatigue damage occurring on the beam's surface at midspan. However, it is expected that the present results would be qualitatively pertinent to other nonlinear structures wherein the response nonlinearity arises from a similar cause, namely a symmetric but nonlinear spring force. (Other structures with similar dynamical equations are discussed in a recent review paper (ref. 20).)

It was found that, with moderate nonlinearity, the rate of accumulation of damage is increased but slightly from the rate one would estimate by ignoring the nonlinearity (Fig. 2). The change in damage rate depends upon the extent of nonlinearity and the slope of the fatigue curve. For values of slope from 4 to 16, the change in damage rate corresponds to a change in excitation not exceeding 0.7 db (8%).

Secondly it was found that nonlinearity causes very little change, from the linear estimate, in the absolute values of the strains that do the most damage. This fact was shown both by the essential constancy in the ratio of the quartile strains in the damage distribution (Table I) and by the small changes in the geometric mean of the quartile strains (Fig. 5). These latter changes (small increases) have about the right magnitude to account for the changes in damage rate shown in Fig. 2.

#### C. EXPERIMENTAL EQUIVALENCE SCHEME FOR SYSTEM WITH RESPONSE NONLINEARITY AND SEVERAL MODES

An equivalence scheme using experimentally-determined engineering corrections for nonlinearities of response, and for the presence of more than one mode, has been outlined in a number of reports (ref. 4). Basically this procedure is an adaptation and modification of the scheme outlined in subsection A above.

Suppose that it is required that a structure withstand a certain jet noise environment (specified spectral density). A structure has been designed and samples of it built. One wishes to specify response and fatigue tests using a pure tone siren and a computation procedure that will determine the average life to be expected of the structure in the given environment. The determination would proceed in the following manner.\*

---

\*It is not entirely evident from the reports (ref. 4) that the test procedure described here is that which was actually used in practice. However we have attempted here to be faithful to the principles described in the references.



## 1. Response Tests and Linear Prediction of Random Response

By a combination of prior experience, numerous measurements (including, perhaps, strain gauges in many places, strain-sensitive lacquer, and qualitative fatigue tests using the siren), and good luck, a single location and orientation for a reference strain gauge is chosen; its output represents the nominal response strain used in calculations. The response of the structure to pure tone (siren) excitation is investigated as a function of frequency, to detect the various modes of response, and as a function of sound pressure level to detect nonlinearity in the various modes. The latter tests are made with sound frequencies equal to the resonance frequencies of the various modes. Generally it is found that motion in one of the modes predominates.\*

A linear prediction of the rms nominal strain in the random environment is made by the techniques discussed in subsection A Eq. (17), based on the results of the response measurements. This prediction is made for each important mode.

## 2. Correction for Extra Modes

When more than one mode is apparent in the response, the predicted mean-square responses for the various modes are simply added to yield a prediction of the total mean-square response in the random environment.

## 3. Correction for Response Nonlinearity

The linear prediction equation, Eq. (17), for the rms of nominal strain in random response depends upon the ratio of nominal strain to sound pressure which is found by pure tone response measurements at resonance. When the response of a mode is nonlinear, that ratio varies with strain level.

In the present equivalence scheme, compensation is made for such nonlinearity by requiring that the strain-pressure ratio be evaluated at the "peak-damage strain", i.e., the level of nominal strain which lies at the maximum of the damage density curve. (See subsection B-2, Eq. (21), and Fig. 4, above.) Of course this level cannot be predicted exactly at this stage, since the ratio of peak-damage strain to rms strain depends on lifetime and the lifetime depends on the strain concentration factor which has not been determined. However a fairly good estimate can usually be made.

---

\*In the present context, "mode" refers to a single, narrow peak in the response curve.

After a strain concentration factor has been determined by pure-tone fatigue testing (subsection 4, below), a corrected estimate of the value of the peak-damage strain is made and the prediction of rms random response is corrected according to the change in nonlinearity of pure-tone response.

The order in which corrections should be made for extra modes and for nonlinearity, and the manner in which these corrections may interact, are not entirely clear. When one mode is dominant, these problems are probably of little importance. The correction for extra modes should then be a small correction.

#### 4. Fatigue Tests and Prediction of Life in Random Environment

From constant-amplitude mechanical fatigue tests on specimens of the material, designed with no strain concentrations, a fatigue curve is determined. These data may come from the available literature.

A constant-amplitude fatigue test is made on the structure, excited by sound from the siren, at a (peak) nominal strain equal to the expected peak-damage nominal strain. The lifetime is measured. The difference between the experimental nominal strain and the strain on the fatigue curve which corresponds to the same lifetime represents the strain concentration factor. This factor is applied uniformly to the old fatigue curve to generate a new fatigue curve relating nominal strain and lifetime.

On first thought, it might seem desirable to try to generate a fatigue curve for nominal strain by repeated fatigue tests on nominally identical structures. However, the structural variability which must be expected between specimens and the relative awkwardness of the leviathan which is a siren "facility" militate against such a procedure.

From the constant-amplitude fatigue curve for nominal strain which has now been constructed, the lifetime for random response with the predicted rms nominal strain is computed by the procedures of subsection A-1 above [Eq. (5)], assuming a Rayleigh distribution of strain peaks and ignoring any fatigue interaction effects.

#### 5. Comments

The equivalence scheme described in this subsection has, through its use in the aircraft industry, been proved a practical engineering procedure although some questions have been raised over its accuracy. It is evident that no attempt is made to compensate for any fatigue interactions between response peaks of different amplitude.

The correction for the presence of more than one response mode is very much an ad hoc procedure with little analytical basis. When the several resonant response modes are well separated, the procedure of summing mean-square responses in the separate modes yields correct



predictions of the total mean-square response. However, there is no available information to indicate, one way or the other, whether the relationship between fatigue life and total mean-square response is the same for one and for several resonant modes. Use of the correction is at least a more conservative procedure than the ignoration of extra modes.

The correction for nonlinearity can be based on two hypotheses concerning the random nonlinear response mechanism:

(1) Insofar as significant fatigue damage is concerned, the nonlinear distribution of strain peaks can be represented as a Rayleigh distribution with a new value of rms strain. Thus, if the peak density curve is plotted on a logarithmic scale (e.g., linear in decibels), the effect of nonlinearity is merely a displacement of the curve without distortion.

(2) The extent of this displacement is equal to the deviation from linearity of the strain-pressure ratio, measured at pure-tone resonance at the "peak-damage" strain.

The exact nonlinear analysis given in the previous subsection can be used to check these hypotheses, for the case of one special type of nonlinearity. The validity of the first hypothesis is fairly well borne out by the observed near-constancy of the inter-quartile range of damage [subsection A-2 and Table I]. The validity of the second hypothesis has not been checked in detail. A few computations have been compared with the results given in Fig. 5. They show that the second hypothesis gives the correct direction for the displacement of the damage curve, but underestimates the magnitude of the displacement (in logarithmic measure, i.e., in decibels) by a factor of about  $1/2$ . [The calculations are made from Eqs. (7) and (11) of reference 16.]

However, it must be noted that the hard-spring model of a nonlinear structure used in these calculations is a very idealized and specialized case of nonlinearity. Other types of response nonlinearity may be presented and may dominate; nonlinearity of damping is particularly notable in experimental measurements (ref. 21). There is no analytical basis for verifying these hypotheses in the case of nonlinear damping.

#### D. EXPERIMENTAL EQUIVALENCE SCHEME FOR SYSTEM WITH RESPONSE NONLINEARITY AND FATIGUE INTERACTIONS

We outline in this section a new siren-jet fatigue equivalence scheme which does not depend upon calculations based on the absence of fatigue interactions, i.e., on Miner's rule [Eq. (5)]. Moreover, the effects of nonlinearity of response are included.



The proposed procedure is, in essence, to use an experimentally-determined programmed fatigue test in which the structure is driven at resonance by a sound pressure whose amplitude varies in time according to a predetermined program. The expected total test time is divided into a number of equal, nominally identical blocks. Within each block the excitation and response increase to a maximum value and then decrease to zero (or a close approximation thereto). The variations may be continuous or in steps chosen to approximate the proper continuous curve.

The program of pressure is to be chosen so that its probability density reproduces the probability density of strain in random response (except for a uniform scale change) when the response is linear. Thus if the overall excitation is small so that response is linear, the pressure program is chosen so that the long-time (one block) probability density of strain is identical with the density of strain under random excitation by some one value of rms random sound pressure.

Experimentally, the program can be designed as follows. The structure is exposed to a low level of random noise while it is mounted in an environment essentially identical to the jet-noise environment. Measurements are made of the rms sound pressure, the rms strain response, and the density of peaks in that response.

Then the structure is mounted in position for the intense pure-tone (i.e., siren) fatigue test. It is excited by a low-level pure tone. The sound pressure is adjusted until the rms strain in this test equals the rms strain in the previous random test. The rms value of the adjusted sound pressure is defined as the equivalent of the rms sound pressure in the random test.

Now, with linear response, the pure-tone response is proportional to the pure-tone sound pressure. Therefore the desired program of sound pressures is one having the same peak statistics (relative to the equivalent rms pressure) as the peak statistics of the random strain (relative to the rms random strain). Analytical and practical details are discussed in section V below.

By following these steps we have determined a program of low-level pure-tone sound pressures which, in the siren environment, is equivalent to a measured rms random sound pressure in the jet environment. We postulate that the equivalence of responses will be maintained if the pure-tone and random sound pressures are all scaled up by the same factor (i.e., all sound pressure levels increased by the same number of decibels). We further postulate that the fatigue lifetimes in siren and jet environments will be equal, if the scale factor brings the response into the fatigue region.

One of the major purposes of this study is to check these postulates experimentally. There are two underlying aspects to them that can be discussed before the data are presented. These are (1) the influence of any fatigue damage interactions between strain peaks of different amplitudes, and (2) the influence of response nonlinearities. Those discussions follow the next paragraph.

The preceding exposition of procedure for determining the pressure program was made simple by ignoring any practical problems. Preliminary testing to help choose a position for the strain gauge is as important as in the preceding scheme (subsection II-C). The choice between measuring pressures with the panel's motion blocked or with the panel moving must be made (subsection II-A). Moreover an experimenter would certainly measure the ratio of pure-tone pressure to strain at more than one amplitude. Further belaboring of such points is unnecessary for experimentally inclined readers and unrewarding to the theoretician.

## 1. Fatigue Interactions

Fatigue experiments made in the laboratory with strain cycles of varying amplitude have long been notorious for their disagreement with predictions of lifetime based on so-called "linear damage laws", i.e., theories that neglect fatigue interactions between cycles of different amplitudes. Freudenthal's results, for example, have demonstrated the importance of such effects in his tests on aluminum alloys 2024 and 7075 and on SAE 4340 steel alloy where he generally used a random response with an exponential density of stress peaks (refs. 8, 17, and 22-25).

The various formalisms which have been proposed to match the experimental data -- fictitious S-N curves, etc. -- do not take a form which is generally useful for predicting fatigue life, for a variety of reasons. Some involve parameters not experimentally verifiable. In other cases the dependence of the parameters upon the distribution of the random loading is unknown. Such a readily adaptable procedure as the fictitious S-N curve, with a constant slope in a log-log plot, may yield a conservative estimate of fatigue lifetime, but it may also be so conservative as to constitute an unwanted design penalty. Formalisms dependent on a value called "maximum stress" lead to special frustration when only statistical probabilities for the occurrence of given response levels are known.

In the present siren-jet fatigue equivalence scheme, we have proposed to use the method of "programmed loading" to incorporate the effects of fatigue interactions in the siren tests.

Unfortunately the literature does not present a single picture of the success of such programmed loading in reproducing the fatigue effects of random loading. Where some tests of programmed loading yield shorter lifetimes than random loading (ref. 22, Fig. 2), others show the opposite trend (ref. 26, Fig. 14). These differences may very well be related to differences in the distributions of the random strains and to differences in the short-time correlation between strains of different levels in the random signal.



## 2. Response Nonlinearity

We now consider the effect of response nonlinearity on the postulate that the equivalence between programmed response and random response is invariant under a uniform scaling of the excitations. First consider the case of a structure with nonlinear stiffness, for which exact statistical solutions are available.

The analysis for random response in one mode with a nonlinear stiffness was summarized in subsection II-B above. The following points are pertinent. The probability density of the velocity (time rate of change of displacement) is Gaussian and its rms value is linear in the strength of excitation (ref. 27). Therefore the density of velocity peaks is a Rayleigh distribution at all levels of excitation. The density of displacement peaks is not Rayleigh. However, if the relation between peak displacement and peak velocity which is valid for pure-tone steady-state vibration at resonance is used to transform the (Rayleigh) density of velocity peaks, then the correct density of displacement is obtained (ref. 20).

Now, the peak velocity of nonlinear response to pure-tone steady-state excitation at resonance is linear in the strength of excitation (ref. 21). If, therefore, the nonlinear structure is excited to quasi-steadystate resonance by a pure-tone excitation whose strength is varied so as to result in a Rayleigh distribution of peak values, then the long-time density of its displacement peaks will have the same distribution as in the case of random excitation. Since the peak strain is uniquely determined by peak displacement, the peak strains must also have the same statistics with random and programmed excitations. This completes the proof of the equivalence scheme for structures with nonlinear stiffness.

Other types of nonlinearity, for example in damping, are significant in many structures, as we remarked in subsection II-C. There is no analysis by which the effects of such nonlinearity on the response statistics can be assessed. However the random response of a highly resonant structure, on the average, probably resembles closely a sequence of natural vibration cycles whose peak amplitude varies slowly in time. (See the discussion in ref. 20.) Retention of the present equivalence scheme under these circumstances is intuitively attractive until some pertinent analytical or experimental evidence to the contrary is found.



## SECTION III

### FATIGUE TESTS OF RESONANT STRUCTURE UNDER RANDOM AND CONSTANT-AMPLITUDE EXCITATIONS

A series of fatigue tests were made with a simple resonant structure excited mechanically by random forces and by sinusoidal forces of constant-amplitude. The basic design of these tests is very similar to those used by Head and Hooke (ref. 3) and Fralich (ref. 5).

The majority of these tests were made on beam specimens of plain 2024 T3 aluminum alloy, sheet, excited to bending vibrations. The results of the constant-amplitude tests, with failure occurring at a transverse hole, are compared with constant-amplitude tests reported in the literature, to determine a value of strain concentration due to the hole. The constant-amplitude results are also combined according to Miner's rule [Eqs. (1) and (5), subsection II-A] to yield predictions of fatigue life with random excitation which are compared with the results of the random experiments.

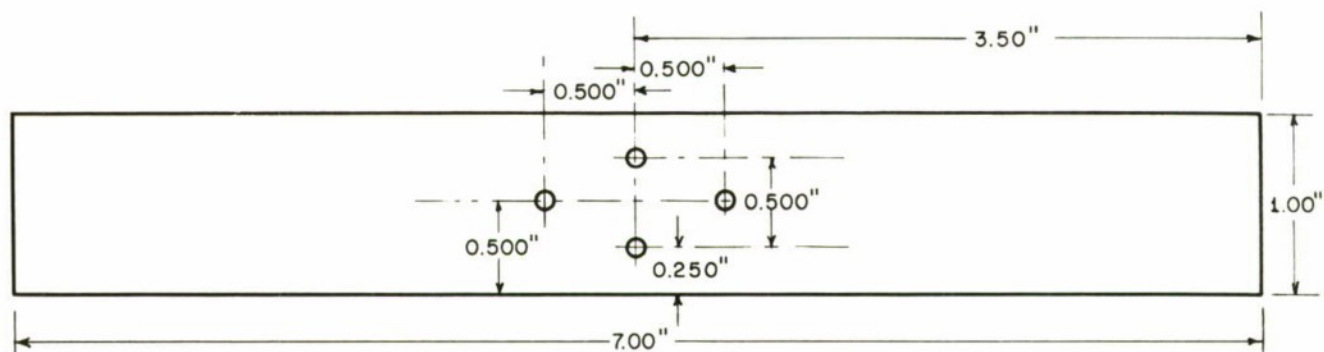
Other tests were made with random excitation of similar specimens of Alclad 2024 aluminum alloy to determine a relation between fatigue lifetime and rms response. This relation will later be compared with results of excitation by jet noise of the larger structural panels, which were made of this material.

#### A. APPARATUS AND TEST PROCEDURES

The test specimens are simple rectangular beams cut from commercial sheet stock (0.063 in. thick) to the dimensions given in Fig. 6. For the tests, a specimen is clamped across the center between two 1/4-in. bars which form the support by which it is forced. The two middle holes in Fig. 6 are positioning holes covered by this support. Thus the specimen and the supporting clamp form a double cantilever beam system. When the clamp is forced at a suitably chosen frequency the two ends of the specimen vibrate with large amplitudes while the clamp itself moves very little. The response is principally in the fundamental cantilever mode, with a slight amount of rigid body displacement superposed.

The two 1/8-in. holes drilled through the specimen at distances of 0.5 in. from the transverse center line (Fig. 6), provide controlled strain concentrations. They are necessary to prevent unobservable fatigue failures at the edge of the clamp; moreover, failure in bending at a hole is a common occurrence in aircraft structures (e.g., at rivet holes).

The specimens were made with normal care for dimensions, etc., in our machine shop. Batches were milled and drilled together; no variations between batches were noted in the fatigue tests. The



ALUMINUM 2024 T3 0.063"  
ALL HOLES 0.125" DIA.

FIG. 6 CANTILEVER TEST SPECIMEN FOR RANDOM AND  
CONSTANT-AMPLITUDE FATIGUE STUDIES

long side of the beams was parallel to the direction in which the plate stock was rolled. The strain concentrating holes were drilled to size in stages, with care taken to avoid burrs, however no attempt was made to polish or otherwise finish them.

Instrumentation and test procedures are illustrated in Fig. 7. The central supporting clamp of the test specimen is screwed securely to the voice coil of a Goodmans Type 390A shaker, driven electrically by the chosen signal. A nominal strain response is measured by a strain gauge in the transverse plane containing one of the strain concentrating holes.

The response level is also determined by measuring the displacement of the end of the beam. The value of strain calculated from the displacement, using the theoretical shape for the lowest mode of a cantilever, was found to be in good agreement with that measured by the strain gauge, after a correction was made for the amplitude of clamp displacement. Measurement of displacement was found to be essential for monitoring strain level during fatigue tests because the strain gauges usually failed after a few minutes at the higher test levels.

In fatigue tests with random excitation, electrical noise from a random noise generator is passed through a band-pass filter tuned to a broad frequency region centered on the fundamental resonance frequency of the beams. This procedure limits low-frequency signals that might cause too large a displacement of the voice coil and limits the amplitude of response in the higher cantilever modes. A 300-watt power amplifier drives the shaker.

Basic measurements of strain response are made with a Ballantine Model 320 true rms voltmeter. A long averaging time (8 sec time constant) is required to obtain reasonably precise measurements because of the narrow bandwidth of the beam's resonance ( $Q \approx 45$ ,  $c/c_c \approx 0.01$ ). So that the beam should not suffer significant fatigue damage while the response level is being set and measured, it is necessary to make the measurement at a slightly lower level and then increase the excitation by a known amount with an accurate attenuator. Tape recordings of the random response strains are made, as long as the strain gauge lasts, for subsequent statistical analysis.

## B. RESULTS AND ANALYSIS

### 1. Constant-Amplitude Tests

The results of these fatigue measurements on the beams of plain 2024 aluminum alloy are summarized in Fig. 8. Three samples were fatigued at each of four levels with constant-amplitude vibrations. Through these points is drawn the smooth curve B.



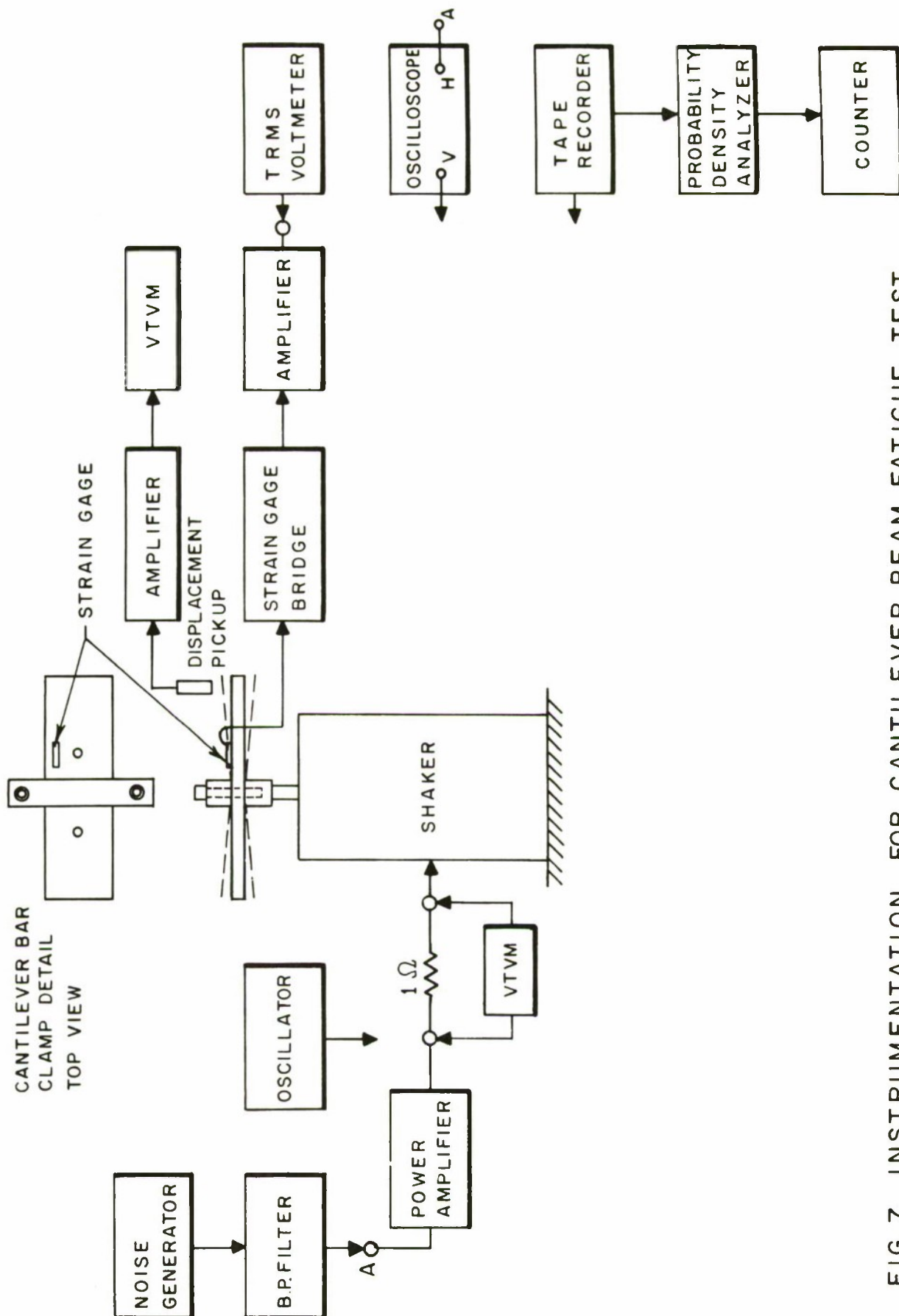


FIG. 7 INSTRUMENTATION FOR CANTILEVER BEAM FATIGUE TEST

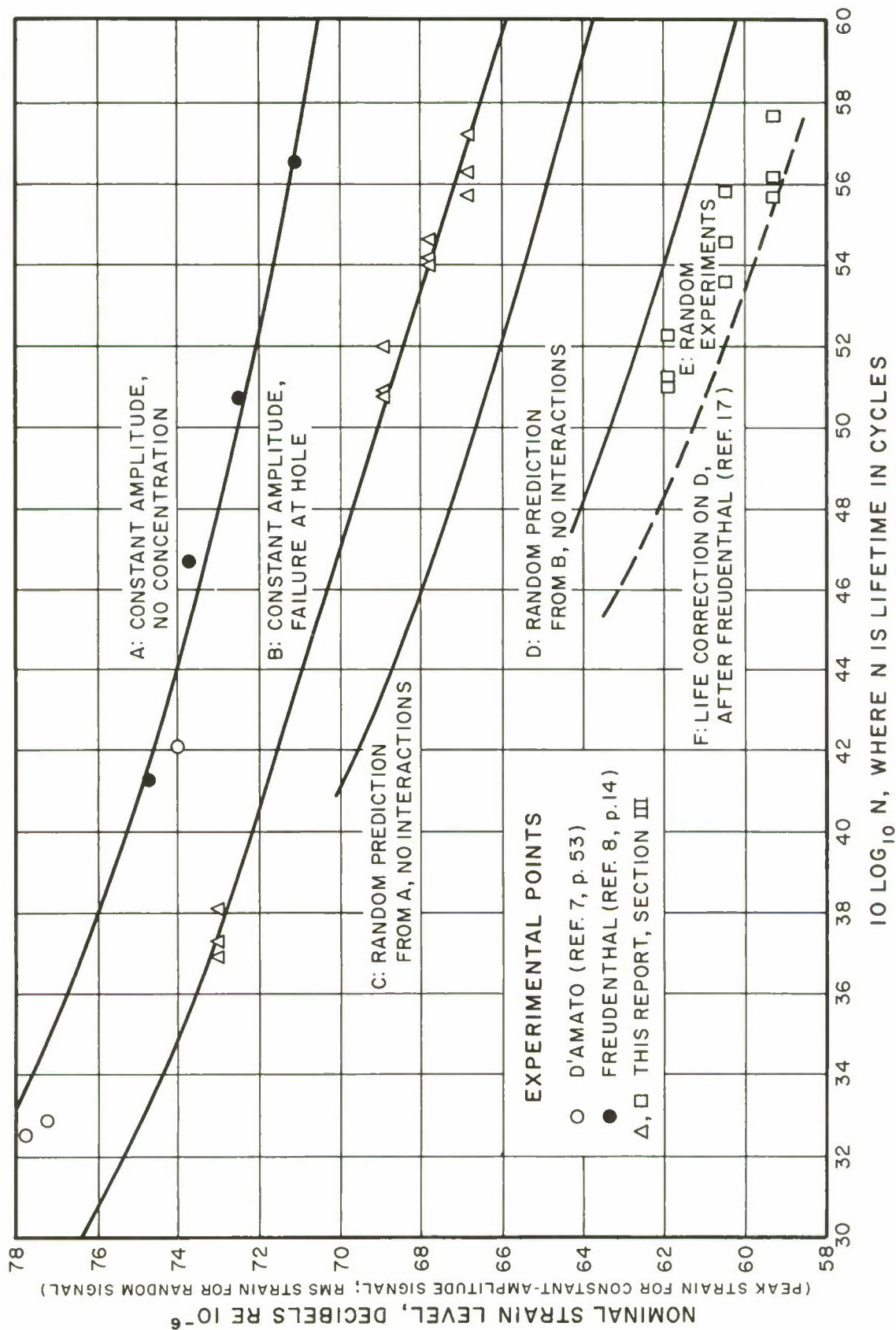


FIG. 8 FATIGUE CURVES FOR 2024 ALUMINUM. RESULTS OF CONSTANT-AMPLITUDE AND RANDOM EXPERIMENTS ON RESONANT CANTILEVER BEAM, AND PREDICTIONS THEREFROM.

The fatigue curve A is determined by the experimental data obtained by Freudenthal (ref. 8) and D'Amato (ref. 7) for test specimens without marked concentration factors. Freudenthal's data were acquired by the rotating-beam method. His values of stress were converted to strain by the Young's modulus:  $1.06 \times 10^7$  psi. D'Amato's results, taken in tensile tests, were used to extend the curve beyond the yield point, for reasons explained in subsection II-A-2, above.

The difference between the curves is an experimental strain concentration factor for fatigue, in logarithmic measure. The values vary from 4.1 db at the lowest test level to 3.0 db at the highest level. The classical elastic stress concentration factor for a hole in a very wide plate in bending (Poisson's ratio of  $1/3$ ) is 1.9, corresponding to 5.5 db (ref. 28). However, Peterson (ref. 29) has proposed a formula for estimating the effective strain concentration factor for fatigue:

$$K_f = \frac{K_t + \alpha/r}{1 + \alpha/r}$$

where  $K_t$  is the elastic concentration factor,  $\alpha$  is a material constant, and  $r$  is the radius of the hole. For 2024 aluminum alloy, Peterson estimates that  $\alpha$  is 0.05 in. Therefore, with a hole radius of 0.0625 in., Peterson's formula yields a fatigue concentration factor of 1.4, or 3.0 db in logarithmic measure. This prediction compares quite well with the experimental values, especially at the higher levels. (The precision of measurement of strain is estimated to be  $\pm 0.2$  db.).

It is interesting to note that the fatigue curve obtained by these measurements is parallel to and approximately 0.5 db lower than the results of earlier tests made in these laboratories on the fatigue life of a cantilever bar held by a line of idealized rivets in  $1/8$ -in. holes (ref. 30).

## 2. Random Excitation Tests

Three cantilever test specimens were fatigued at each of three rms strain levels; the results of these tests are the data points labelled E in Fig. 8. The probability density of a 15 min. sample of the nominal strain (about  $1.6 \times 10^5$  cycles) is plotted in Fig. 9. The agreement between measurements and the theoretical density of normal (Gaussian) noise is quite good.

Fatigue lifetime as a function of the rms strain was computed from the constant-amplitude fatigue curves in Fig. 8 by the simple theory of subsection II-A above [Eqs. (1) and (5)], assuming a Rayleigh distribution of the strain peaks and ignoring fatigue interactions. The resulting random fatigue curve for plain 2024 aluminum alloy without strain concentrations is labelled C. The random fatigue curve computed from the experimental constant-amplitude data is labelled D in Fig. 8.



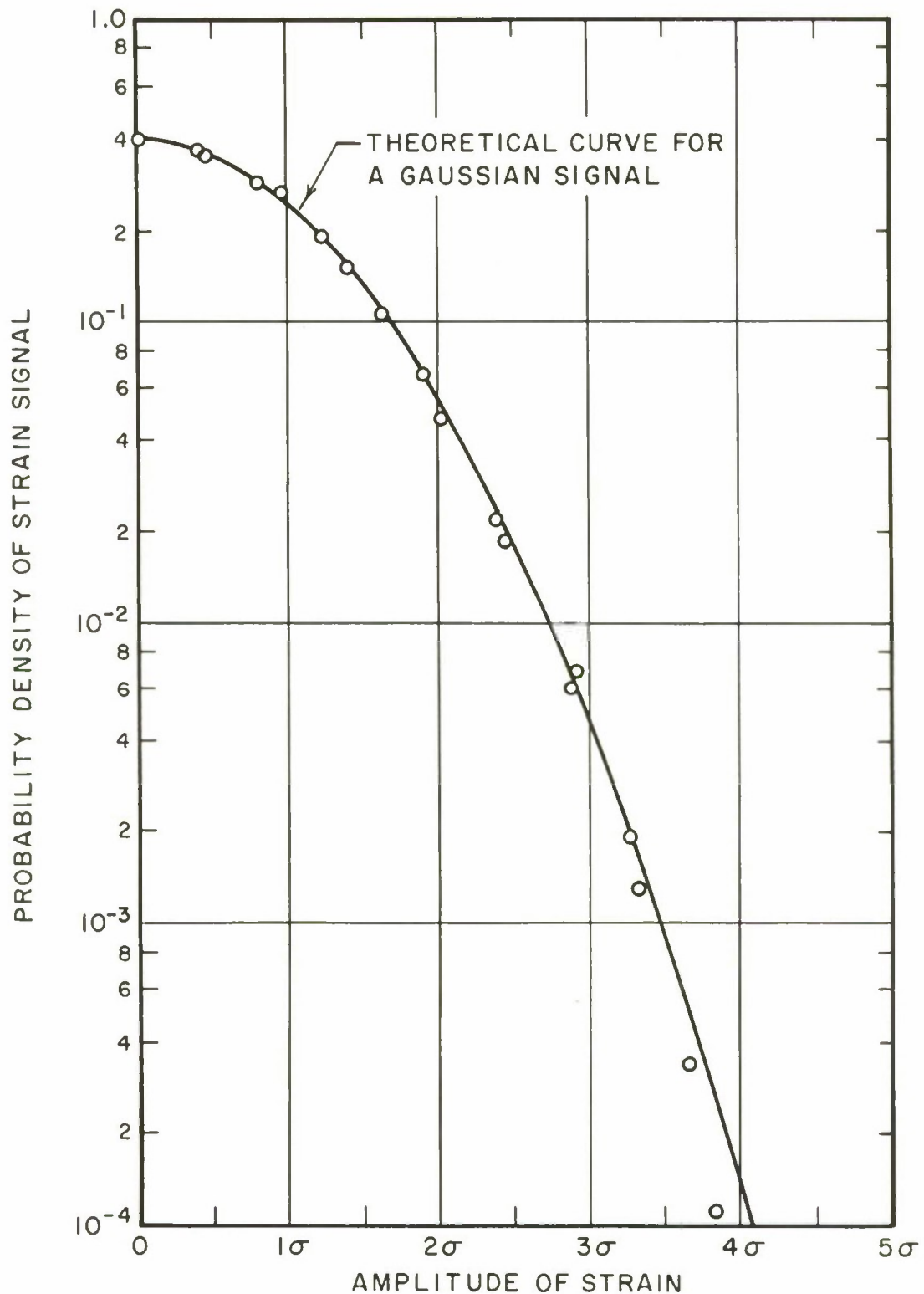


FIG.9 PROBABILITY DENSITY OF STRAIN IN CANTI-LEVER BEAM RESPONSE TO RANDOM EXCITATION

It will be noted that the experimental lifetimes with random excitation are shorter than the prediction which ignores fatigue interactions; the differences are greatest at the longest lifetimes. Freudenthal's detected qualitatively similar differences in his tests, made with the same material but with no strain concentration and with a response which differed in both its long- and short-time statistics. His results could be represented fairly well by a simple analytic expression and by a smooth curve showing the difference between experimental and predicted lifetimes as a function of predicted lifetime [ref. 17, Eq. (6.10) and Fig. 16]. If the present predicted lifetimes (curve D) are "corrected" by the factor given in Freudenthal's smooth curve, the curve labelled F in Fig. 8 is obtained. The present experimental results lie between the two curves D and F.

There is some opportunity for uncertainty inherent in the detection of a fatigue crack. In constant-amplitude tests, the change in resonance frequency and the consequent drop in amplitude if frequency is not readjusted are very sensitive indicators of a crack's existence. They are supplemented by visual inspection under stroboscopic light. However, neither of these techniques is adequate when the excitation is random; then the excitation must be turned off and the stationary specimen inspected visually. Thus, in the random fatigue test, the minimum uncertainty in life measurement is set by the time interval between inspections.

However, the rate of growth of crack length, measured in real time, is quite slow in random tests. This reflects the fact that most response cycles are too small to do much damage. Some measurements made on one specimen are shown in Fig. 10. The random excitation was turned off from time to time and the specimen's surface examined, with a good light and a five-power magnifying glass. The lengths of any cracks were measured by comparison under the glass with a rule graduated to 0.020 in. In Fig. 10, these data are plotted for each of the four fatiguing points (the four edges of the strain concentration holes which lie on transverse diameters).

The slow rate of crack growth in random response, possible variations in this rate with level of response, the impossibility of continuous inspection, and the dependence of the visibility of a given crack upon lighting conditions - these factors can create quite significant errors in lifetime. The various factors may bias the data in different directions, favoring early detection of cracks in either the long or the short tests. They may introduce differences between laboratory and field data, or between field measurements at different times. As an example, in one field test reported below, two specimens were exposed to the same noise field; the test was concluded when a crack was apparent in one specimen and not the other. On laboratory inspection, out of the bright sun, noise, and other distractions, one could readily see the "missing" crack with the unaided eye.

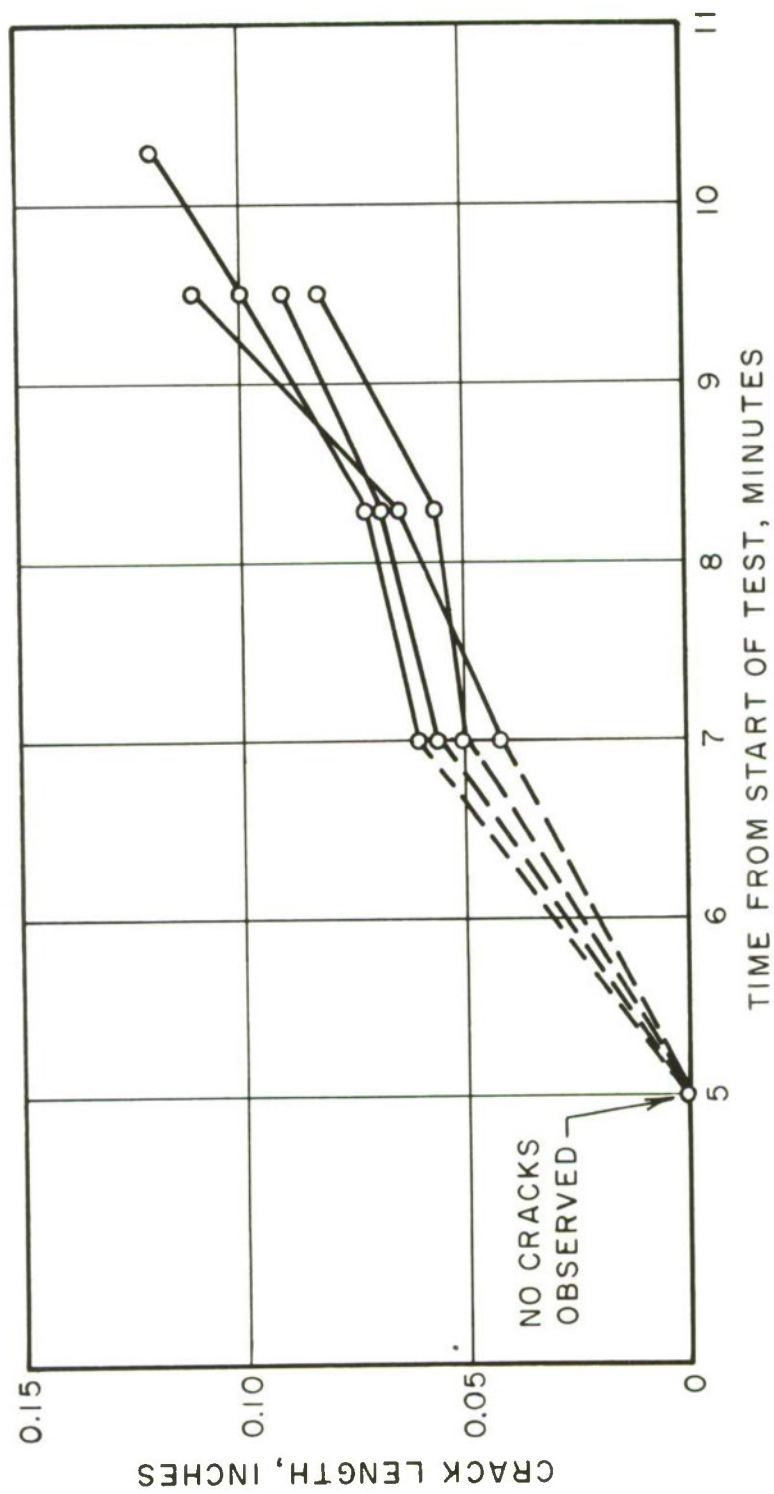


FIG. 10 GROWTH OF CRACK LENGTH DURING STEADY RANDOM  
EXCITATION OF RESONANT BEAM  
(RESONANCE FREQUENCY, 185 CPS)



There is, therefore, a very real question about the precision of the recorded lifetimes, and not much to guide one's judgement. However, the trend of the curves in Fig. 10 does not much reassure a natural skeptic of the reliability of a 50% difference in life recorded in a field test.

### C. DATA FOR ALCLAD 2024

A more limited investigation of the same kind was made with cantilever beam specimens of Alclad 2024 aluminum alloy. The design of specimens and apparatus was the same as in the earlier tests with plain 2024.

The purpose of these experiments is to determine the slope of the random fatigue curve on small specimens and to compare this slope with the slope determined in the jet-noise fatigue tests. Satisfactory correlation of results will indicate that the small specimen tests could have been used for prediction.

Three specimens were excited by steady random forces at each of two rms strain levels. The data and the computed average slope are given in Table II.

TABLE II  
FATIGUE DATA FOR CANTILEVER BEAM  
SPECIMENS OF ALCLAD 2024

Nominal Strain Level (db re $10^{-6}$ )	Specimen Number	Fatigue Lifetime ( $10 \log N$ )
56.0 db	1	59.2
	2	59.2
	3	58.9
	geometric mean life:	59.1
61.0 db	4	49.4
	5	49.8
	6	48.6
	geometric mean life:	49.3
5.0 db . . .	changes . . .	9.8
inferred slope of fatigue curve:		$\alpha = 3.9$

## SECTION IV

### STUDIES OF PANEL RESPONSE

#### A. PANEL DESIGN AND MOUNTING

A structural panel, representative of flight vehicle construction, was designed and a number of specimens were made by the California Division of the Lockheed Aircraft Corporation. A drawing of this panel is reproduced in Fig. 11. Certain somewhat unusual aspects of the design were dictated by the available siren apparatus and by the desire to eliminate, in so far as possible, complicating factors such as effects of angle of incidence of sound, extremely nonlinear response, numerous modes, etc.

The panel is made by riveting together two 0.020-in. sheets of Alclad 2024 aluminum alloy. The flat sheet has T-3 temper. The beads in the other sheet are formed when the sheet is in a soft condition and the piece is then heat treated to T-42. A transverse stiffening angle of 1/16-in. aluminum (5/8 in. high by 3/8 in. wide) was added at midspan to the design shown in Fig. 11. The ends of the assembled beaded panel are riveted to strips (0.125 x 2.00 in.) of aluminum. In testing, these strips are bolted securely by five 5/16-in. bolts to the mounting structure.

Two mountings are used, one for pure-tone excitation and one for random noise excitation. For pure-tone tests, each of the aluminum strips at the ends of the panel (Fig. 11) is bolted to a sturdy iron angle (2"x2"x1/4") which is in turn bolted to the sides of the 1 ft by 1 ft duct down which sound propagates from the siren.\* The inside face of the panel is thus exposed directly to the sound pressure, which propagates in a direction parallel to its surface. The outside face (the beaded side) is open to the room and exposed only to the relatively low level of ambient noise.

For random noise experiments the aluminum strips at the ends of the panels are bolted to a framework of iron angles which is secured to the open top of a plywood box. The box is made of one-inch plywood and has dimensions 14" x 21" x 13". The purpose of the box is to protect one side of the panel from sound pressures. In laboratory measurements a single box is used. In the field measurements behind a jet engine, three boxes are secured side by side on a 5 ft by 11 ft cast iron bed-plate. Diagonal baffles of 1/2-in. plywood are arranged at the sides of the boxes, making a smooth transition to the bed-plate (see Fig. 12). It is thought that the baffles cause less disturbance to the jet sound field than the boxes alone; no experimental comparison was made.

---

\*The siren facility used in these tests is described in detail in Reference 31.





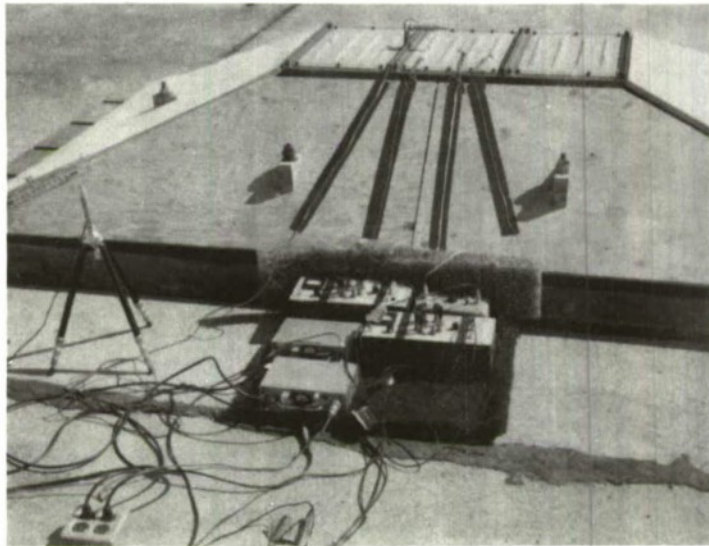


FIG.12 THE PANELS IN THEIR FIELD MOUNTING  
FOR JET TESTS (INSTRUMENTS EX-  
POSED FOR THE PHOTOGRAPH)

## B. PURE-TONE RESPONSE

The response to pure-tone excitation of the panels, mounted in the siren's duct, was investigated at some length with sound from a loudspeaker in the duct as well as with the sound generated by the siren. The motion was studied by eye, with stroboscopic light, and by measurements with accelerometers and strain gauges in many places.

It is found from low-level measurements that there are two principal modes of response. The first is essentially a simple beam motion, the panel moving in and out of the duct with no nodes of motion. The second is a twisting motion with a nodal line running lengthwise down the center of the panel. Thus, in this mode, one free edge of the panel moves into the duct while the other free edge moves out.

In response curves taken with a constant low level of sound pressure, two resonant peaks are found. One peak, typically at about 110 cps, corresponds to motion principally in the beam mode. The second peak, typically at about 120 cps, corresponds to motion principally in the twisting mode. (A third peak at about 270 cps corresponds to the second mode of the beam motion, but the response at this frequency is very much smaller than the response in the other modes.) Subsequent investigations with more intense excitation and consideration of the effects of the abnormal environment in the siren's duct (a point discussed later) indicated that the lower frequency, beam-like mode was the one of principal interest. Therefore the response data reported below all pertain to that mode.

The precise frequencies of the resonance peak and the relative proportions of beam motion and twist were found to vary considerably from panel to panel. For example, the differences in the strain levels measured on the top and the bottom beads at the lowest resonance frequency ranged from less than 1 db to 10 db for different panels, when measured at low levels (sound pressure levels of about 130 db re 0.0002 microbar). There was at the same time considerable variation (about  $\pm 3$  db) in the ratio of the sound pressure to the largest response strain from panel to panel.\*

On the other hand, much "cleaner" response was found in all respects at higher levels of excitation, approaching and into the fatigue range. Only a single peak of response was found, lying at a frequency intermediate between the frequencies of the two peaks found at low level. The strains measured on the top and bottom beads were more nearly equal, with differences in level generally less than 3 db. Moreover the ratio of sound pressure to strain was more nearly consistent between panels. (In one notable exception, panel no. 5, the recorded pressure-strain ratio was 5 db smaller than the average of data for other panels.)

---

\*The largest of the strains in any of the beads was taken as the measure of panel response, since this study is concerned with fatigue lifetime and the largest strain causes the earliest failure.



Prolonged investigation of the responses of the panels at high levels of excitation would have destroyed their usefulness for gathering fatigue data. Moreover, such an investigation would have been a diversion from the purposes of this study. However, many response data were acquired in the course of the fatigue tests.

Response curves for panels numbered 17 through 20\* are shown in Fig. 13. Each curve represents the average of a large number of readings (from 23 to 162) taken at 2 db intervals of sound pressure level. The sound pressure was measured with the panel blocked. The nominal strain response is the rms of the signal from a gauge in a standard reference position, the same on each panel; this signal was recorded graphically and the value read later. Individual readings made on the same panel at the same pressure varied over a range of about  $\pm 0.5$  db centered on the average value. (In a few instances, particularly at lower amplitudes, variations of 1.0 to 1.5 db occurred.)

It appears from Fig. 13 that the strain in each panel is proportional to pressure, up to a pressure level of about 146 db. Beyond that point some nonlinearity appears. However, the measurements at the higher levels are not as reliable as those at lower levels; they were made during very short intervals of time. Measurements for the highest points for panels 19 and 20 were made in 2 seconds. There was not time for careful tuning of frequency to resonance. In view of the variations of the frequency of peak response with amplitude, as noted above, there exists some question whether the measurements were made at resonances. Therefore there is some question about the accuracy of the indicated amount of nonlinearity.

The response data of Fig. 13 which lie in a range of sound pressure levels from 140 to 146 db is summarized in Table III. We propose to use the average difference between sound pressure level and strain level as a "transfer function" in comparing various predictions of fatigue life.

TABLE III  
PURE-TONE RESPONSE OF PANELS AT RESONANCE

Data taken from Fig. 13. Pressure levels in db re 0.0002 microbar. Strain levels in db re $10^{-6}$ .	
Panel Number	Blocked Sound Pressure Level Less Nominal Strain Level
17	93.3 db
18	93.6
19	93.0
20	94.1
Average:	93.5 db

\*The numbers given panels are for identification only; they do not indicate order of testing.



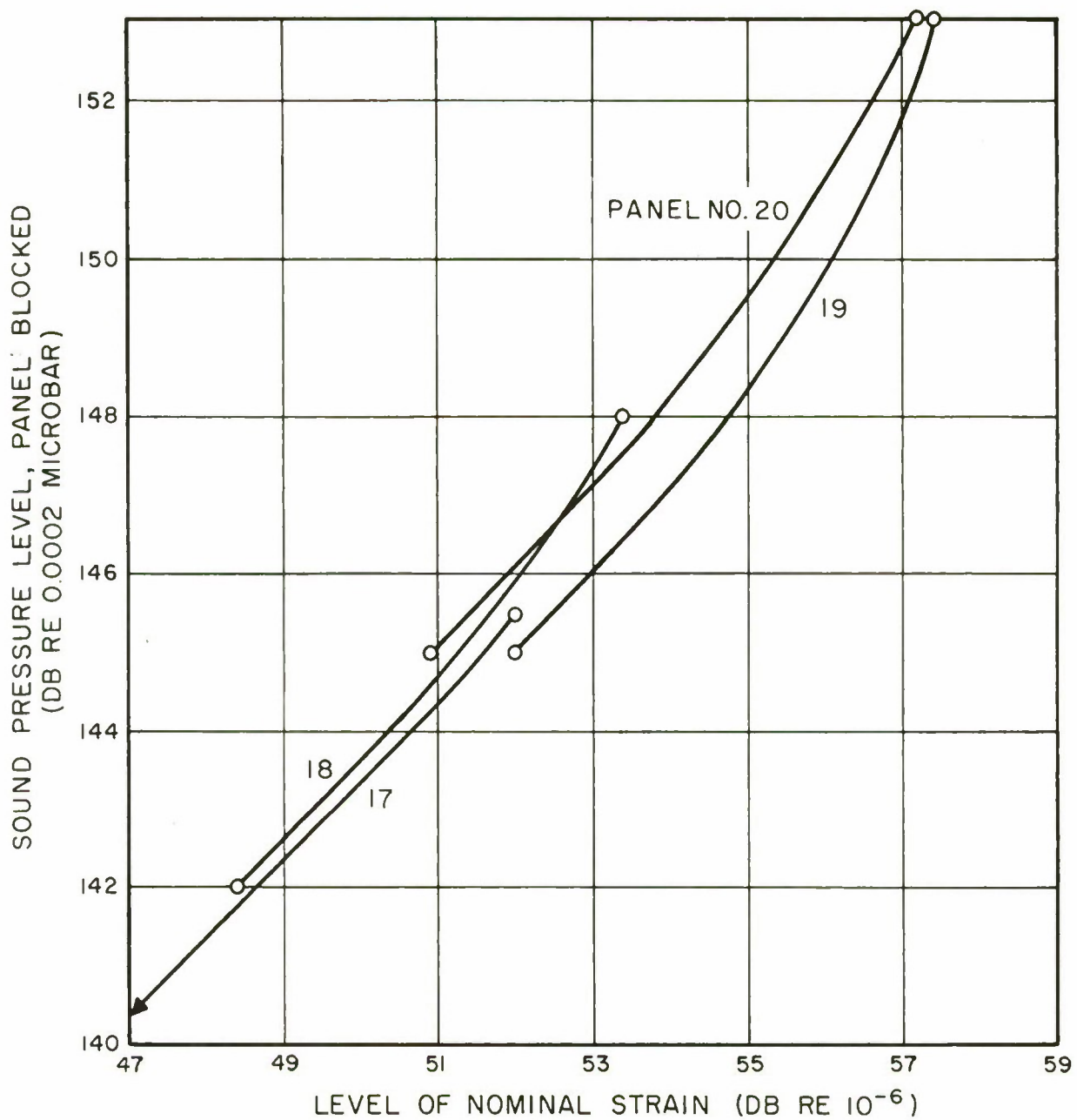


FIG. 13 PURE - TONE PANEL RESPONSE DATA

## 1. Loss Factor

Measurements and calculations were made to determine a loss factor for the panels when mounted in the side of the sound duct which leads from the siren. Casual observation indicated that the panel's motion was well damped in that location.

Determination of damping from the bandwidth of the resonance peak was made difficult by the close proximity of the two resonances. The peak with higher resonance frequency (twisting motion) was considerably narrower than the other (beam motion). From the average of measurements made on a number of panels, the loss factor was estimated as

pure-tone loss factor

from bandwidth measurements:  $\eta_t = 0.091$  ,

for the beam motion. On the other hand, both bandwidth and decay measurements on the higher mode (twisting motion) indicated that its loss factor was much less, about 0.015.

The large damping for beam motion and the much smaller damping for twisting motion strongly suggest that the beam motion is abnormally damped by virtue of its environment, i.e., that acoustic radiation damping dominates internal mechanical losses. An important corollary is that the response in the beam mode will increase markedly, by a factor of about 6, relative to that in the twisting mode when the panel is mounted in a realistic environment without the abnormal radiation loading.

The hypothesis of radiation loading can be checked by calculations. The radiation load upon the panel mounted in the duct consists of two impedances in parallel: (1) the impedance looking down the horn, and (2) the impedance looking back up the duct to the siren. The first can be estimated, by acoustic horn theory, to be a pure resistance (a specific acoustic resistance equal to  $\rho c$ , where  $\rho$  is air density and  $c$  is the speed of sound). The second impedance is not known because the effective impedance of the siren source has not been investigated.

Suppose that the impedance looking back at the siren is reactive (no power flow). Then the total resistive impedance presented to the panel can vary from zero, when this shunting reactance is zero, to the value computed for the horn loading alone, when the shunting reactance is large. This maximum resistive impedance leads to maximum acoustic radiation damping. From the dimensions of the panel and an assumed mode shape (fundamental mode of a pinned beam) we have computed that the maximum loss factor is

pure-tone loss factor

due to acoustic radiation:  $\eta_t \leq 0.154$  .

However, suppose that the acoustic impedance looking up the duct toward the siren is also a pure resistance equal to  $\rho c$  (i.e., a progressive wave with no reflections). Then the total radiation load will equal half the maximum load of the preceding paragraph. The resultant prediction of loss factor is half as large:

pure-tone loss factor

with  $(\rho c/2)$  acoustic loading:  $\eta_t = 0.077$  .

A final estimate of the pure-tone loss factor was based on comparisons of the pure-tone response and the random response measured in the laboratory. Details are given in the next subsection. For comparison, the result is given here:

pure-tone loss factor

inferred from random response:  $\eta_t = 0.13$  .

The four estimates for pure-tone loss factor have a range which is not greatly reassuring.

### C. RANDOM RESPONSE

The response of the panels to random noise was measured in an acoustic environment resembling that to be used in the jet-noise field tests. These measurements serve two purposes. First they determine the loss factor which is to be expected in the jet environment. Secondly, in the programmed-amplitude equivalence scheme (subsection II-D), they determine the scale factor by which one can translate from sound pressures used in the fatigue tests in the siren's duct to the equivalent sound pressures of jet noise.

Panels were mounted in one of the boxes described above in subsection A and were irradiated with steady random noise. Measurements were made of the rms value of the nominal strain (i.e., the strain at a standard location on the bead having the largest strain). The noise was generated by exciting a loudspeaker with the amplified signal from an electrical random noise generator, after filtering to a one-octave bandwidth (75 to 150 cps).

There was considerable difficulty in the way of a good experiment. A more powerful noise source would be required in order to fulfill the ideal requirements: a good "signal-to-noise" ratio in the strain signal; acoustic noise signal generated without peak clipping; sound pressure uniform over the panel's surface; and no objects in the close vicinity of the panel. The measurements reported here were made in a compromise situation in which the loudspeaker was six inches from the panel. The sound pressure level varied by several decibels over the face of the panel. The results of these random response measurements are given in Table IV.



TABLE IV

## RANDOM RESPONSE OF PANELS (LABORATORY MEASUREMENTS)

Pressure levels in db re 0.0002 microbar, measured in a third-octave band centered on 110 cps, with panel moving. Strain levels in db re  $10^{-6}$

Panel Number	Third-Octave Band Pressure Level Less Nominal Strain Level
15	87.5 db
16	88.5
17	88.3
18	90.7
19	89.9
20	<u>92.4</u>
Average:	89.5 db

Corresponding measurements of response were acquired in the course of the field tests behind a jet engine. The results of analysis of tape recordings are shown in Table V.

TABLE V

## RANDOM RESPONSE OF PANELS (FIELD MEASUREMENTS)

Pressure levels in db re 0.0002 microbar, measured in a third-octave band centered on 110 cps, with panel moving. Strain levels in db re  $10^{-6}$

Panel Number	Third-Octave Band Pressure Level Less Nominal Strain Level
10	86.8 db
11	87.1
12	88.0
13	<u>89.0</u>
Average:	87.7 db

The difference between the average responses found in these two sets of measurements may, in the absence of definitive information, be ascribed to any one of a number of causes: differences in the sound signals, variations to be expected in the average of a small number of measurements, variability between individual panels, differences in the acoustic radiation loading in the two tests. We favor the last two explanations. In any case, the difference between averages and the variations between measurements on individual panels are indicative of the precision which can be achieved in a measurement which is all-important in any fatigue life prediction scheme.

## 1. Loss Factor

The loss factor for the panel in the laboratory random environment was determined by measuring the rate of decay from steady-state resonant vibrations excited by a pure tone sound. Data for the six panels listed in Table IV result in an average value of loss factor

loss factor in

laboratory random environment:  $\eta_r = 0.0442 \pm 0.0057$  ,

where the number appended with  $\pm$  is the maximum range of variation.

The values of loss factor and response (Table IV) in this environment can be combined with the pure-tone response measured with the panel in the siren's duct (Table III) to predict a loss factor for the pure tone environment. This prediction is based on Eq. (17b). The spectral density of sound pressure is computed from the mean square pressure in the third-octave band and the bandwidth,  $f_o/3 \sqrt{2}$ . The predicted loss factor is

loss factor in pure tone environment predicted  
from response data and loss factor in laboratory

random environment:  $\eta_t = 0.13$  ,

which is in fair agreement with the previous estimates.

## 2. Statistics of Random Response

A 15-minute recording of the strain response to random noise excitation in the laboratory was analyzed on a Probability Density Analyzer. The rms strain response level was 16.6 db re  $10^{-6}$ . The results of the probability density analysis are shown in Fig. 14. They are seen to be in very close agreement with the Gaussian distribution curve appropriate to random response of a linear one-mode structure.

A similar analysis was made of the strain recorded in the field during the jet noise fatigue tests. In this case the rms strain level was 47.4 db. The probability density of this strain signal is compared with the ideal Gaussian distribution in Fig. 15. There is an indication of some response nonlinearity, the density being very slightly high near  $1\sigma$  and low at  $3\sigma$  and beyond. The probability density of extrema (strain peaks), being the negative slope of the strain signal density, appears from Fig. 15 to be very slightly higher than the Rayleigh distribution (the negative slope of the Gaussian curve) in the region above about  $1.5\sigma$ . These results are in qualitative agreement with the type of "nonlinearity" displayed in the pure-tone response curves of Fig. 13. However, the differences between these results and the Rayleigh distribution do not appear very large in the region of the "peak damage" strain which is  $2.2\sigma$  in the present case [Eq. (21), taking  $\alpha=4$  as validated below].

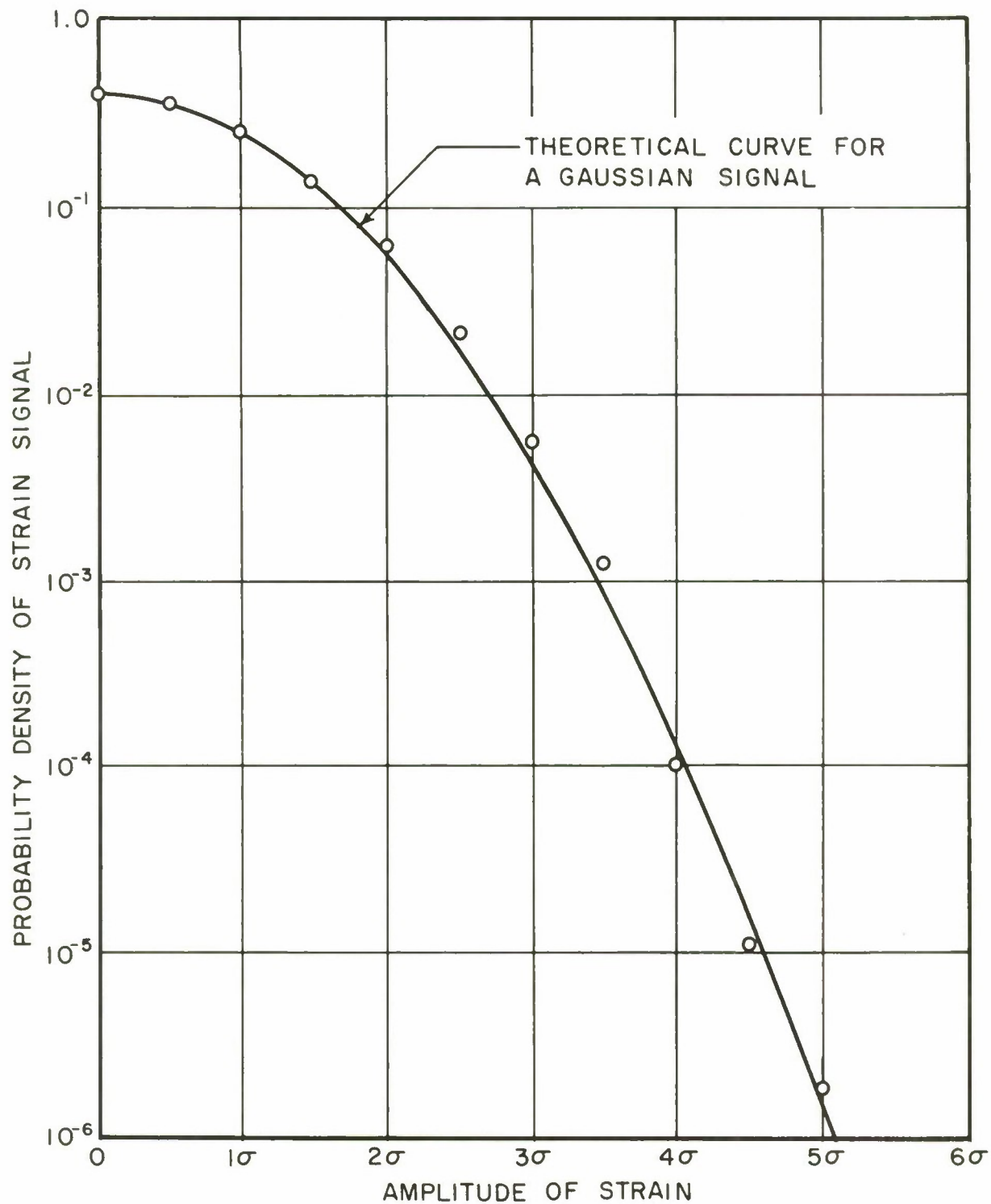


FIG.14 PROBABILITY DENSITY OF STRAIN IN  
PANEL EXPOSED TO RANDOM NOISE IN  
THE LABORATORY



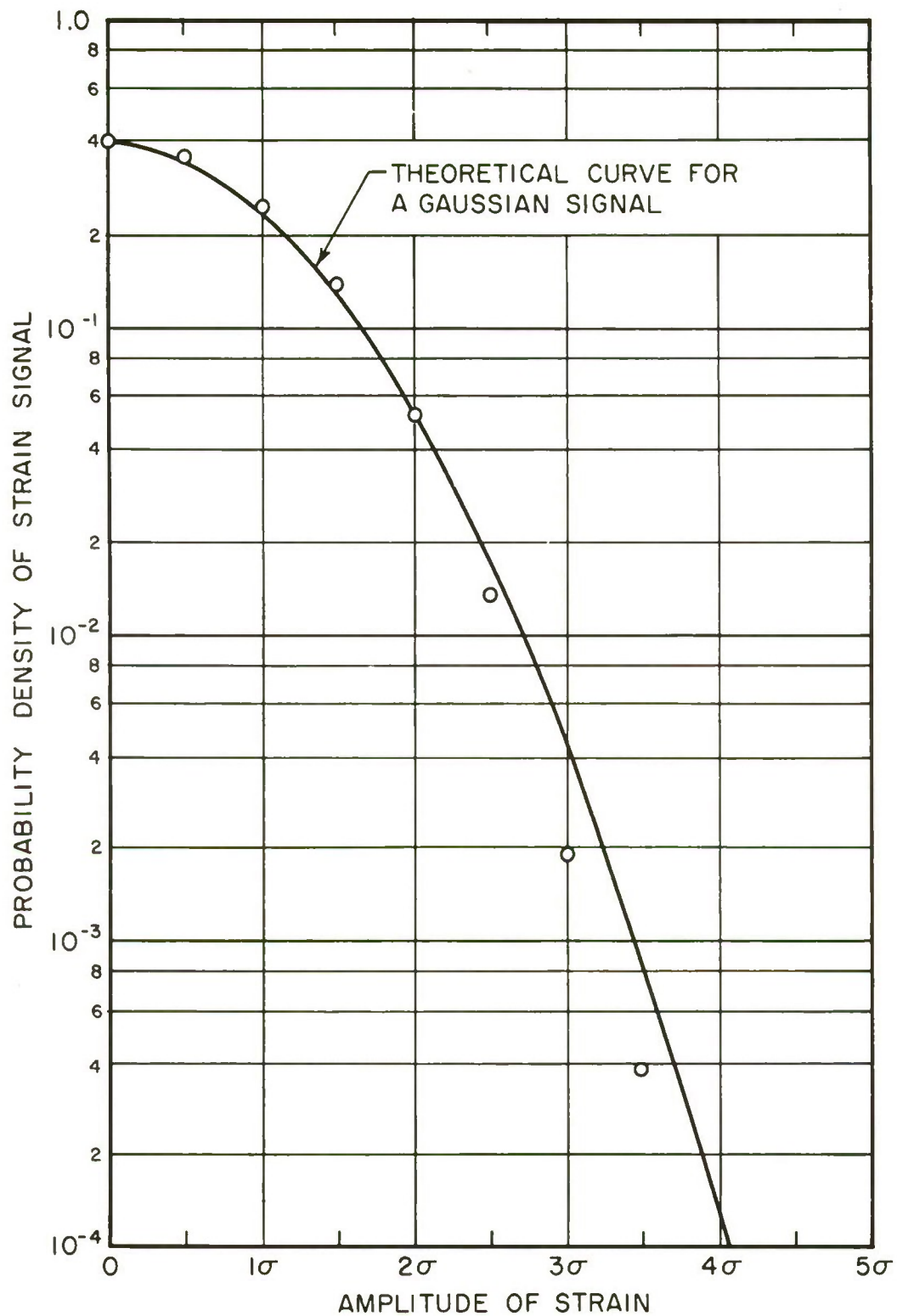


FIG. 15 PROBABILITY DENSITY OF STRAIN  
IN PANEL EXPOSED TO JET NOISE

#### D. COMMENTS ON NONLINEARITY

In these response studies, with siren or loudspeaker and with jet noise, there have been several indications of nonlinearity. Among these are the statistics of the response to jet noise and the curvature of the pure-tone response curves (Fig. 13) acquired in the course of the variable-amplitude fatigue tests. The latter indication is, as noted above, somewhat suspect because of the impossibility of tuning accurately to resonance. In contradiction to it, more careful but less numerous measurements made in some of the constant-amplitude fatigue tests, using the siren, seemed to indicate linearity at high levels of response. Specifically the ratio of blocked sound pressure to strain was constant ( $\pm 0.3$  db) from panel to panel, with the exception of one rogue panel for which the recorded ratio was 5 db lower (panel no. 5).

Other indications of nonlinearity are found at lower levels of response, as recorded above. These are the shift in resonance frequency and the merging of the two resonance peaks into one, as level is increased. The shifts in resonance frequency were much greater than can be explained by any appeal to the hard-spring resonator type of response appropriate to a pinned beam (ref. 16).

We wish to postulate a qualitative explanation for many of the observed peculiarities, in support of which there is not sufficient evidence. The two nearby modes of response found at low level should be nonlinearly coupled, in the potential energy, by virtue of their sharing a common membrane strain and tension. With increased excitation, this coupling tends to modify the pure tone response curve, making the two resonance peaks approach and eventually merge because the coupling increases. It is quite possible that changes of this sort are much more important, at moderate levels with nearby resonances, than any nonlinear effect on the strain amplitude at the resonance peaks. Above the level for critical coupling, that is, for merging of the peaks, the panel would behave much like a one-mode system, until at very high levels, nonlinearity began to have significant effects upon the amplitude of response. The validity of this postulated explanation should be investigated.

## SECTION V

### PROGRAMS FOR VARIABLE-AMPLITUDE FATIGUE TESTING

In this section we consider the ideal program and various modifications thereto which were found necessary as a result of limitations in the existing system for controlling sound pressure.

#### A. THE "IDEAL" PROGRAM

As explained in subsection II-D, it is desired that the sound pressure amplitude be cycled repetitively through a "block" in such a way as to reproduce the actual probability density of the response peaks in the response to low-level random noise. The measurements reported in section IV showed that density to be described by the Rayleigh distribution. We desire therefore a program in which the pressure envelope is a monotonic rising or falling function of time and has a density given by the Rayleigh distribution. Thus the envelope must satisfy the differential equation

$$dt = \pm (T/2) \times \exp[-x^2/2] dx \quad (22)$$

where  $x = p/\sigma$  is the ratio of the peak amplitude of pressure to the rms value, and

$$T = 2 \left| \int_{p=0}^{p=\infty} dt \right| .$$

The solution is

$$t = \pm (T/2) \exp[-p^2/2\sigma^2] , \quad 0 < \pm t < t \pm T/2 . \quad (23)$$

In the interval of time  $-T/2 < t < +T/2$ , the pressure given by this equation rises from zero to infinity (at  $t=0$ ) and then falls to zero again (Fig. 16). This defines the basic block of the program. The duration of one block is  $T$ . The quantity  $\sigma$  represents the long-time rms value of the pressure. The number of cycles in one block depends on the sound frequency.

The slope of the pressure envelope (Fig. 16) is infinite whenever the pressure is zero or infinite. Were such a pressure program used to drive a resonant structure, the structural response would not follow the pressure in a quasi-steadystate manner when the rate of change of pressure amplitude is very large. (We assume here that the sound pressure control system is ideal and unlimited.) Therefore the program must be truncated at a high level (in the range of  $4\sigma$ , say) and at a low level (at some small fraction of  $1\sigma$ ). These truncation levels must be chosen so that the omitted peaks would not



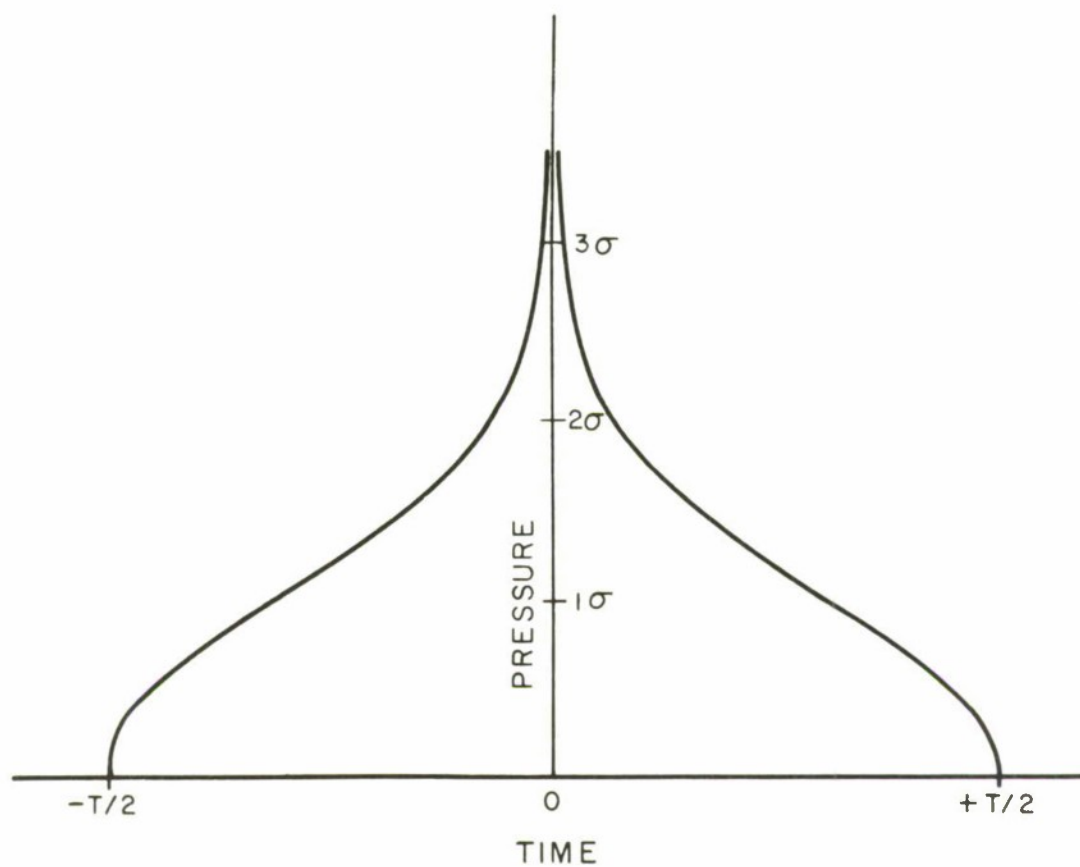


FIG. 16 ENVELOPE OF PRESSURE DURING ONE PROGRAM BLOCK

have made a significant contribution to the total fatigue damage. The major problem appears to be a proper choice of the upper truncation level.

# 1. Distortion from Truncation at High Levels

An analysis has been made of the distortion of the response envelope of a linear simple resonator (one mode) to an excitation envelope which is a pyramidal ramp (Fig. 17). The distortion includes (1) a time delay, which is not of importance, and (2) a depression of the maximum response amplitude below the expected maximum value. The amount of depression depends on the loss factor of the resonant system and the rate of change of pressure amplitude. (Our analysis assumed a constant rate of change; in the calculations we have used the maximum rate of change, as calculated from Eq. (22), which is a function of the truncation level.) For small values of depression, the depression in decibels is

$$\delta \approx 9.38 \exp[x^2/2]/x^2 \eta N_1 \text{ decibels,} \quad (24)$$

where  $x = p/\sigma$  is the truncation level,  $\eta$  is the loss factor, and  $N_1$  is the number of cycles in one block of the program.

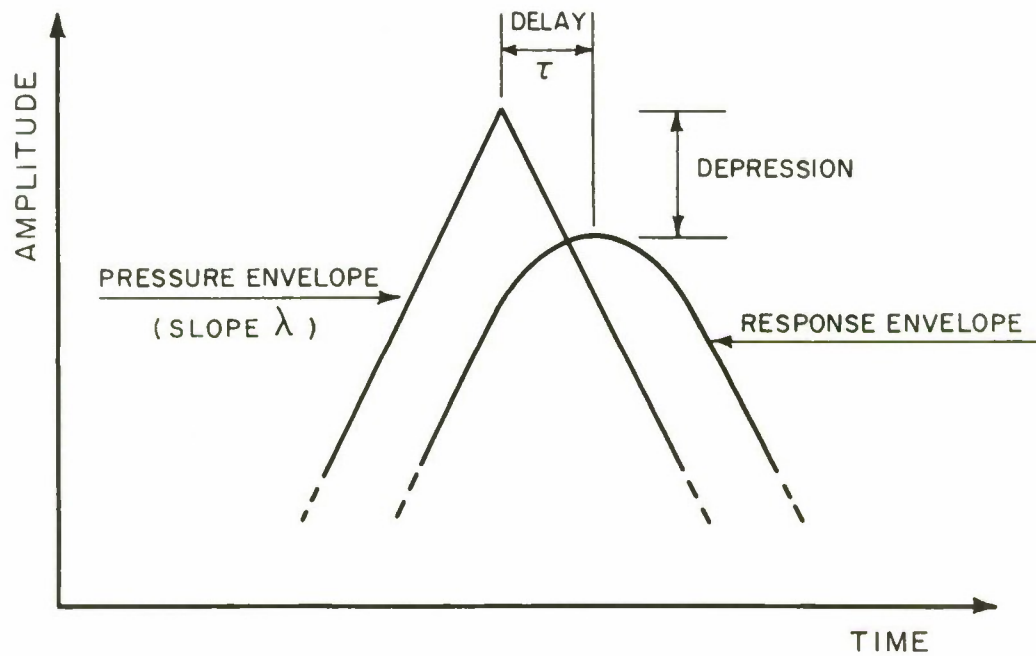
It can be seen that, for the depression to be small, either the truncation level must be low, or the number of cycles in a block must be large. Some numerical solutions of Eq. (24) are given in Table VI, for a loss factor  $\eta = 1/30$ , a typical value for aircraft structure, and for a depression  $\delta$  of 0.5 decibels.

TABLE VI  
RELATION BETWEEN BLOCK SIZE AND EXPECTED MAXIMUM RESPONSE

Calculated for 0.5 db depression of maximum with loss factor  $\eta = 1/30$

Expected Maximum Response linear:	db re $\sigma$ :	Depressed Maximum Response (Depression=0.5db)	Number of Cycles in One Block
$3\sigma$	9.5 db	$2.8\sigma$	$5.6 \times 10^3$
$3.5\sigma$	10.9 db	$3.3\sigma$	$2.2 \times 10^4$
$4\sigma$	12.0 db	$3.8\sigma$	$1.1 \times 10^5$
$5\sigma$	14.0 db	$4.7\sigma$	$6.1 \times 10^6$

A comparison of these numbers with theoretical distribution curves for damage in random response (Fig. 4) indicates that it may be necessary to omit the higher response peaks, which could account for some 20% of damage, in order to be able to get in 5 or more blocks before the structure fails. For example, with 2024 aluminum alloy, one might



$$\text{DELAY TIME: } \tau = 2 / \omega_0 \eta$$

$\omega_0$  = RESONANCE FREQUENCY

$\eta$  = LOSS FACTOR

$$\text{DEPRESSION} = 0.736 \lambda \tau$$

FIG. 17 DISTORTION OF RESPONSE ENVELOPE NEAR THE PEAK OF THE PRESSURE ENVELOPE



expect a total life of  $0.5$  to  $1.0 \times 10^6$  cycles with a slope of the fatigue curve (at the peak damage point) of  $\alpha \approx 8$ . Then if the pressure envelope is truncated at  $4\sigma$  (with a maximum response of  $3.8\sigma$ ), about 20% of damage will be omitted. There will be only 5 to 10 blocks in the total fatigue life. In order to get higher values of response, without severe distortion of the distribution of peak values, one would have to use a smaller number of blocks. But a large number of blocks are desirable in order to obtain a reasonable representation of the random response.

The considerations of the preceding paragraphs illustrate a fundamental physical limitation in the attempt to use programmed excitation with quasi-steadystate response of a highly resonant structure. The only alternatives are entirely different types of testing: either (1) excite transient response, which may require use of a jet engine as sound source, or (2) excite non-resonant, i.e. static, response, which promises formidable experimental difficulties with a large structure. Fortunately, very high maximum response levels (e.g.,  $5\sigma$ ) which require long blocks seem only to be required for long-life tests, where the slope of the fatigue curve is small.

## 2. Acceleration of Testing by Truncation at Low Level

We indicated earlier that there appears to be no difficulty in achieving controlled resonant response to values small compared with the rms value. However there is the possibility of saving considerable time and achieving an accelerated fatigue test by truncating at some low level. The only problem is choosing a level such that the effect on fatigue life will be small.

If fatigue interactions between strains of different amplitudes were small, the choice of lower truncation level is readily made with reference to the cumulative damage distribution curves, Fig. 4. From those curves, we see that only a few percent of total damage, or less, should be attributable to all peaks below the rms value for slopes of the fatigue curve greater than  $\alpha = 4$ . But these smaller peaks account for 39% of the time  $T$ . [See Eq. (23).] In Table VII we list the truncation levels corresponding to 10% damage, from Fig. 4, and the corresponding time savings, from Eq. (23), for a range of values of  $\alpha$ .

TABLE VII  
TIME SAVED BY TRUNCATION AT 10% DAMAGE LEVEL

Slope of Fatigue Curve, $\alpha$	Truncation Level (db re rms)	Time Saved (Percent)
4	+ 3.4 db	66.4%
8	+ 6.9	91.5%
16	+10.4	99.6%

Now, the choice of truncation level cannot be based on the slope  $\alpha$  of the constant-amplitude fatigue curve if interactions are important. (If interactions are not important, there is no need for a programmed test.) However the results available from research on fatigue interactions (refs. 17, 25) indicate that predictions based on a slope of 4 with vanishingly small endurance limit are probably safe, for 2024 and 7075 aluminum alloys. Precisely such a prediction is entailed in the first line of Table VII, indicating that the test may be run in one-third of the lifetime for random excitation, by eliminating all peaks below  $1.5\sigma(+3.4\text{db re } \sigma)$ .

It is quite possible that even more accelerated fatigue tests would be reasonably accurate when the expected lifetime is very large. However this should be verified experimentally, by performing two tests with different truncation levels.

## B. PRACTICAL SIREN CONTROL PROBLEMS

A variety of means was investigated in the attempt to achieve an adequately controlled sound pressure, continuously varying according to the program described above. These tests were made with the 24-in. diameter siren system described in reference 31.

Both flexibility and reliability are required of the control system. Flexibility is required because the modulator control of the siren has a nonlinear relation between input electrical signal and sound pressure output, and that relation depends upon the static air pressure in the supply plenum. Thus the control signal must be tailored to fit not only the function describing the desired program but also this nonlinear relation; the adjustment must be accomplished experimentally, by cut-and-try methods.

Reliability is required of the system because the rationale of the programmed fatigue test is based on the repetitive application of the same basic program of loading. If small errors were detected after running one block, they could (with suitable flexibility of control) readily be corrected, and even compensated for, before running the next block. However correction for large changes would require computation based on a fatigue theory, the very procedure which programmed testing is designed to avoid.

Several means for achieving a continuously varying sound pressure were investigated. An electronic cathode ray tube "Photoformer" was available which generates an electric voltage function proportional to the shape of an opaque cut-out placed in front of the cathode ray tube. Awkwardness in adjusting the shape of the cut-out, the imprecision in such adjustments, and long-time d.c. drift in the output voltage contraindicated the use of this instrument. An Arbitrary Function Generator (manufactured by American Measurement + Control Company) generates an electric voltage proportional to the height of a curve drawn on graph paper with conducting ink. Difficulties in achieving reliable signals,



changing with the rapidity required near the peak of the program, made us conclude investigations of its use.

The continuous program was then abandoned in favor of a stepped approximation thereto. A control device based on a stepping relay was designed, developed and proved by tests with the siren. This programmer steps up and down a total of 16 steps, including an "off" position. Both the dwell time and the level of the output signal at each step are adjustable. Various modes of operation were included: (1) continuous cycling; (2) stop at end of block; (3) stop and turn off at end of step; (4) manual control of time of stepping (for setting levels); (5) continuous recycling of any one step with 2 sec dwell between end and beginning (for setting time intervals). This instrument proved to have the requisite flexibility and precision. With it, changes in sound pressure level of less than 1 db per step can readily be achieved.

Unfortunately, the amplitude stability of sound pressure, with the siren controls fixed, was not adequate. This represented a deterioration of the siren's performance from its original state, apparently due to difficulties in the siren-modulator control system whose source was not readily apparent. There were short-time fluctuations in level of about  $1/2$  to 1 db either side of average and long-time drifts of about  $1/2$  to 1 db in an interval of about 15 minutes. Occasional surges in sound pressure have occurred; one surge in the middle of a fatigue test destroyed the specimen.

Detailed investigation and reworking of the siren control system was not possible in the course of this project. Therefore a simplified testing program was devised, with manual control of the sound pressure level and duration for each step.

### C. A SIMPLIFIED PROGRAM

The simplified program for sound pressure, which was used in the programmed-amplitude fatigue tests, was designed to be consonant with the capabilities of siren systems which do not include a sound pressure amplitude modulating device.

The basic program for one block, designed to be equivalent to  $10^5$  cycles of random response at 110 cps (i.e., 15 minutes), consists of 8 minutes of excitation in nine intervals (Fig. 18).<sup>\*</sup> The program was applied in the following manner: First the panel, mounted in the side of the duct leading from the siren, was blocked from vibrating by moderate pressure from a diagonal, sponge-coated bar. Then the

---

\* Please note the two ordinate scales in the figure. The "peak level" is the logarithmic measure of the maximum amplitude of the pressure cycle. The "rms level" is the rms value of the pressure cycle (3 db smaller) such as would be indicated on a sound level meter.



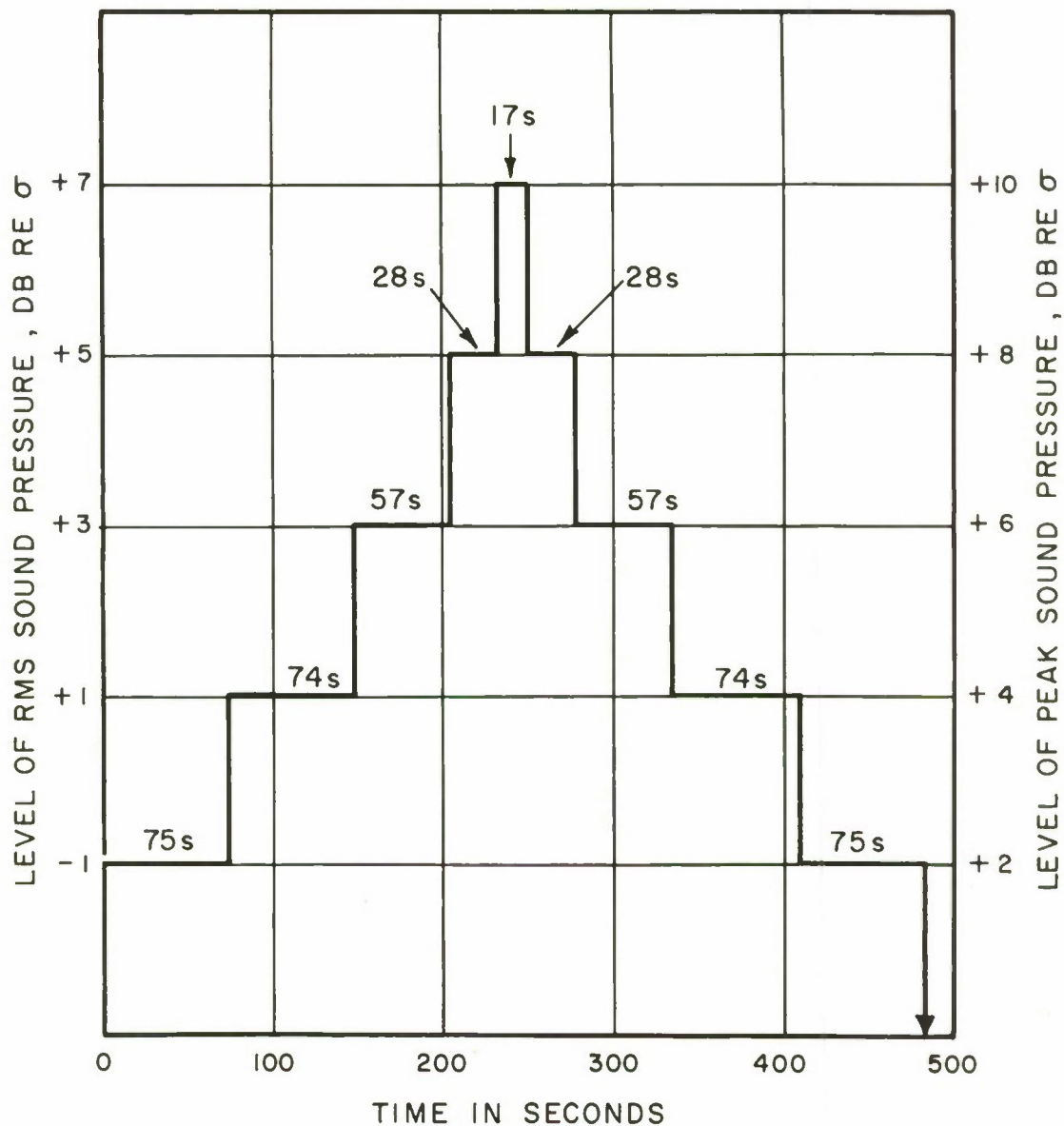


FIG. 18 ENVELOPE OF PRESSURE DURING ONE BLOCK OF THE SIMPLIFIED PROGRAM. (BLOCK EQUIVALENT TO  $10^5$  CYCLES OF RANDOM RESPONSE AT 110 CPS)

"blocked" sound pressure level was set to the appropriate value specified on the program. The blocking bar was removed for the prescribed time interval, and quickly replaced. The blocked sound pressure level was reset to the appropriate value for the next step, etc. This procedure is reasonably straight-forward, although tedious. Suitable experimental details for its easy use, depending upon the design of the "siren facility", are quickly discovered in the application.

The time scale of the basic program can be scaled to fit the expected fatigue life and the desired number of blocks; that is, the duration of each step can be changed by the same factor. There is, of course, some difficulty in maintaining precision in the length of the shortest interval for a short-life test. If the expected total life is  $4 \times 10^4$  cycles and 4 blocks are desired, the duration of the highest step should be only 1.7 seconds.

### 1. Design Basis for Program

The program shown in Fig. 18 was designed in this manner. Previous constant-amplitude fatigue tests and random tests in a jet noise environment had indicated that the slope of the fatigue curve for the panels (made of Alclad 2024 aluminum alloy) was very close to  $\alpha = 4$  in the range of interest. (See section VI below.) The lower truncation level was then chosen to be a peak level of +1 db re  $\sigma$ ; this corresponds to about the 4 percentile level on the cumulative damage distribution curve for  $\alpha = 4$  (Fig. 4).

After several tries, balancing the impracticability of very short intervals and of level changes of odd size against the desire for moderately small changes in level between steps, a decision was made to have steps differ in level by a uniform 2 decibels. The duration of each step was immediately determinable [from Eq. (23)] since, for example, the first step must last for the time spent by the ideal program in the interval from +1 to +3 db re  $\sigma$ . However the duration of the highest step was chosen to equal the total time spent by the ideal program above 9 db re  $\sigma$ .

The level of each step except the highest was chosen simply as the center of the range on the ideal program that it represents. Thus the first step, representing the interval from +1 to +3 db re  $\sigma$  on the ideal program, is run at a peak level of +2 db re  $\sigma$ . Any other procedure presumes prior knowledge of details of the response and fatigue mechanisms which are unavailable. (Were they available, a programmed test would be unnecessary.) Moreover any adjustment for a presumed damage distribution represents rather picayunish fiddling, since the adjustment would be very small in any interval where the damage density is large.

Only in determining the level of the highest step were fatigue and response mechanisms invoked; even there it was not necessary. If the highest step had been designed on the same basis as the others, to represent the interval +9 to +11 db re  $\sigma$ , it should have had a level of +10.0 db re  $\sigma$  and a duration of 15.5 sec. Instead

the duration (17 sec) was chosen to represent all peaks above +9 db re  $\sigma$ , and the level chosen to represent all that interval (assuming linear response, Miner's rule,  $\alpha = 4$ ). The calculated level, +10.04 db re  $\sigma$  was rounded off for use. The refinement does not make a great difference in the program, as a practical matter, and in theory it is probably unjustifiable.



## SECTION VI

### PANEL FATIGUE TESTS

Specimens of the structural panel whose design and response were described in section IV have been subjected to sonic excitation until they failed in fatigue. These tests were of three types: Pure-tone, constant-amplitude excitation at resonance by a siren; programmed variable-amplitude excitation at resonance by a siren; and excitation by jet noise.

The results of these tests are given in this section. Detailed comparisons and comments on the results are given in section VII, to follow.

#### A. CONSTANT-AMPLITUDE TESTS

Seven panels were tested with constant sound pressure levels under controlled conditions. (An eighth was sacrificed to familiarization.) Each panel cracked cleanly across one of the beads, approximately at midspan. No interval of crack growth was seen in spite of continuous observation under stroboscopic light. Each panel except number 2 cracked on an exterior bead, that is, near one of the free edges. (The crack in panel 2 passed through a small dent on an interior bead although prior response measurements had indicated that the highest nominal strain occurred in an exterior bead. This behavior may indicate that a dent in a bead affords significant strain concentration.) Except for panels 2 and 6, the crack appeared in that exterior bead which had been shown by prior response measurements to have slightly larger strain.

The fatigue lives for these panels are plotted in Fig. 19 against both the peak amplitude of strain at midspan and the exciting sound pressure level measured with the panel blocked.

On the strain-life plot is superposed a fatigue curve for Alclad 2024 aluminum alloy taken from the literature (ref. 32). (Values of stress were converted to strain by a value of Young's modulus equal to  $1.06 \times 10^7$  psi.) It was noted above that both panels 2 and 6 failed at unexpected points. Data are not available to predict the values of strain for these points, but they must be larger than the measured values used in plotting. The other data are in quite good agreement with the curve.

The pressure-life plot, by comparison, shows more scatter of the data. Note the peculiar results for panel 5, whose abnormally lively response was noted in section IV, above. Unfortunately, no reliable pressure measurement is available for panel 1.

All these tests were run with unmodified panels, as delivered by the manufacturer. During the subsequent field tests with jet noise, it was found expedient to drill 0.125-in. holes in the center

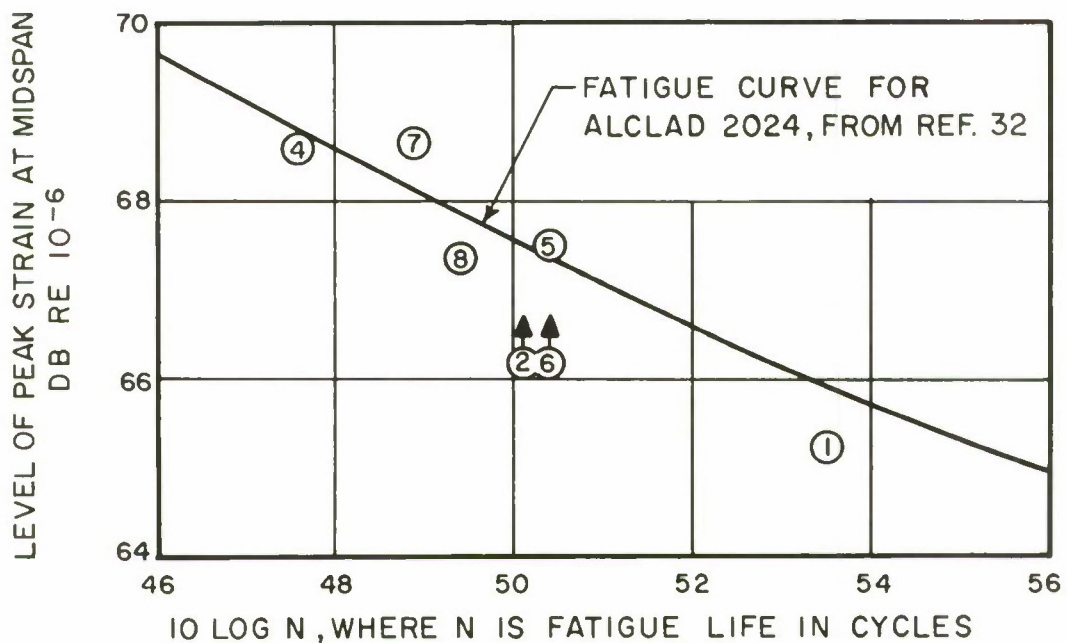
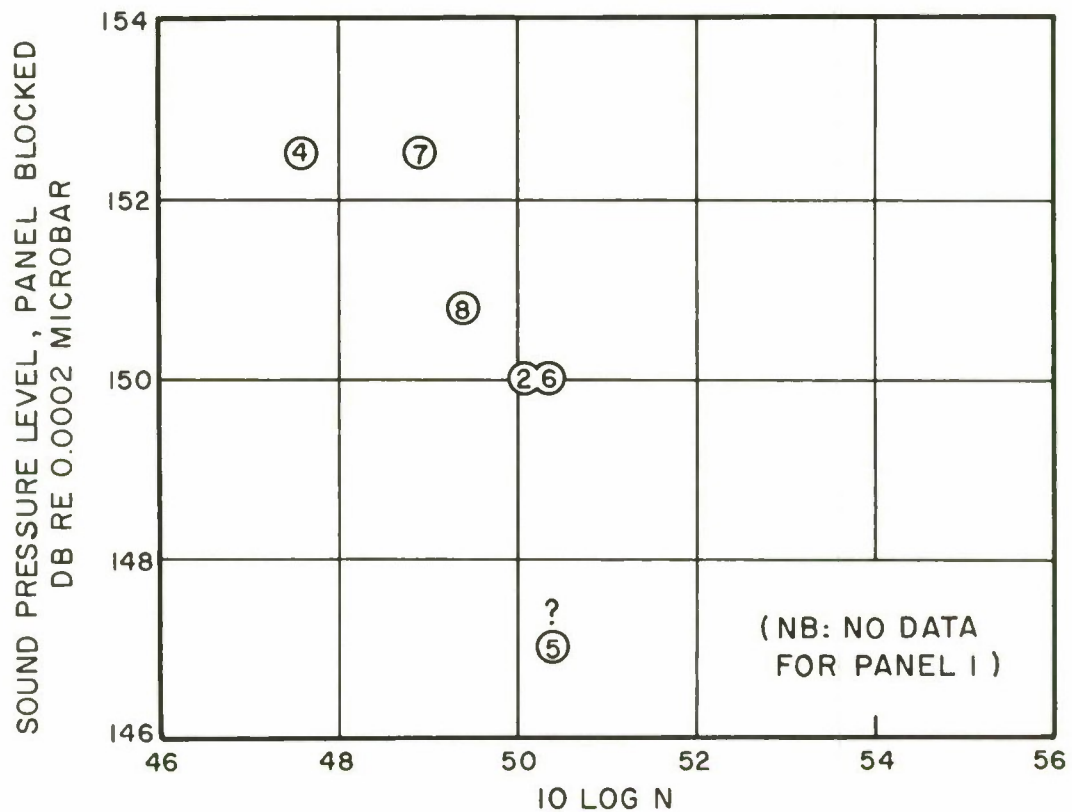


FIG. 19 FATIGUE LIVES WITH CONSTANT AMPLITUDE AS FUNCTIONS OF STRAIN AND BLOCKED SOUND PRESSURE (SEVEN PANELS, IDENTIFIED BY NUMBER)

of each bead at midspan. Two panels with such holes were fatigued with constant sound pressure from the siren. The data are given in Table VIII, along with the value of strain concentration factor inferred from comparison of these results with the smooth curve in Fig. 19.

TABLE VIII  
FATIGUE DATA FOR STRUCTURAL PANELS WITH 1/8-IN. HOLES  
IN BEADS; STRAIN CONCENTRATION FACTOR FOR HOLES

Panel Number	10 Log N (N = Life in Cycles)	Nominal Strain Level* (db re $10^{-6}$ )
14	52.7	50.1
15	<u>51.9</u>	<u>50.1</u>
Average	52.3	50.1
Conversion to level of peak strain at midspan*		<u>+8.2</u> 58.3
Strain level for failure at same life, panel without hole ( <u>from</u> curve in Fig. 19)		<u>66.5</u>
concentration factor		8.2 db
(in linear measure:		2.6)

\*Note: The "nominal strain level" in decibels is the logarithmic measure, read directly from the face of a calibrated meter, of the rms electrical signal from a bridge containing a strain gauge at a reference point on one of the beads. This reference point was not at midspan because gauges at midspan frequently failed before the panels did. However the conversion factor was repeatedly checked by measurements and found to be constant between panels. It includes 3.0 db for conversion from rms to peak level for a sine wave, and 5.2 db to account for the change in position of the gauge.



## B. PROGRAMMED VARIABLE-AMPLITUDE TESTS

Four structural panels, with 0.125-in. holes drilled in the centers of the beads, were fatigued according to the simplified programmed test described in subsection V-C, above. (One failed in the process of such a test due to a malfunction in the sound pressure control system.)

The use of the program given in Fig. 18 starts with a selection of the equivalent long-time rms sound pressure\*, that is, the value of  $\sigma$ . Then the duration of the block is chosen, based on the expected lifetime and the impracticability of short intervals. The duration of each step in the block is scaled in proportion. The panel is mounted in the duct of the siren and exposed to the programmed levels of blocked sound pressure in sequence, step by step as previously described, until a crack is observed.

Panel 17 lasted 18 blocks, each nominally having  $10^5$  cycles. Panel 18 lasted for 5 of these  $10^5$ -cycle blocks. Panels 19 and 20 were tested with blocks only one-eighth as long as that shown in Fig. 18, that is, nominally having  $1.25 \times 10^4$  cycles. These two panels cracked after 2-1/2 and 3 of these short blocks.

### 1. Correction of Raw Data

The short blocks call for very short durations at the higher steps (2.1, 3.5, 7.1 sec). Inevitably, there are errors. In fact, the graphic records of response show that the average times spent in the higher steps were too long. We propose to correct the measured lifetimes by means of a simple linear, non-interacting fatigue theory. The theory may not be accurate, but it should be accurate enough since the corrections are small. The correction formula is

$$N = N_{\text{design}} \frac{\sum \Delta_{\text{actual}} x^\alpha}{\sum \Delta_{\text{design}} x^\alpha}$$

- where  $N$  = number of cycles at which point is plotted  
 $N_{\text{design}}$  = number of blocks times nominal number of cycles per block  
 $\Delta$  = total time (design or actual) spent on step  $x$   
 $x$  = design value of peak amplitude of step  
 $\alpha$  = slope of constant amplitude fatigue curve.

In computation we took  $\alpha = 4$ . (See Fig. 19).

---

\* Because of the stepped approximation and the truncation of small values, the value of  $\sigma$  is not the actual long-time rms sound pressure.

The computed correction factors on life are:

panel no. 19: 1.16 (+0.6 in  $10 \log N$ )

panel no. 20: 1.12 (+0.5 in  $10 \log N$ )

These factors were applied before plotting data.

A second correction factor was applied to all data to correct for small variations between individual panels of the low-level resonance frequency. The nominal number of cycles per block was computed for a frequency of 110 cps. Actual frequencies ranged from 106 to 109 cps. A correction equal to the ratio of frequencies was made for each panel.

Note that the second correction would not be necessary if the fatigue life were measured in time units instead of cycles. Moreover the first correction would then have been different (smaller). However our results have been plotted with lifetime in cycles, for easy comparison with theoretical predictions and other data.

## 2. Results

The fatigue lifetime of the panels subjected to programmed sound from the siren are plotted in Fig. 20 as a function of the equivalent long-time rms sound pressure (measured with panel blocked). The results have a surprising consistency and show little scatter, in distinction to the constant-amplitude results plotted at the top of Fig. 19.

The curve on Fig. 20 labelled "predicted fatigue curve" requires some explanation. The basic fatigue information contained in the curve is the constant amplitude data reported elsewhere in the literature (ref. 32). From this we constructed a strain-life curve, a segment of which appears in the plot of our constant-amplitude results, Fig. 19. (The reasons for using strain as the variable in place of stress were explained in some detail in subsection II-A-2 and illustrated in section III, the report of our cantilever beam experiments.) However we found no data on which to base a strain-life curve for strains above the yield point, except the ultimate strain which causes failure in one cycle. D'Amato (ref. 7) has demonstrated the continuity of the strain-life curve (for plain 2024 aluminum) and we used his results in section III (e.g., Fig. 8). In the present case (Alclad 2024) interpolation over a rather wide gap was necessary. That part of the resultant curve which is pertinent to these results is shown in Fig. 21.

Also shown in Fig. 21 is a prediction from the constant-amplitude data of a random fatigue curve. This construction was based on the simple theory which assumes a Rayleigh distribution of peaks and the nonexistence of fatigue interactions.

The ordinate for the random fatigue curve is the level of the rms value of strain at the point of fatigue. This variable must be related to sound pressure level before the prediction can be

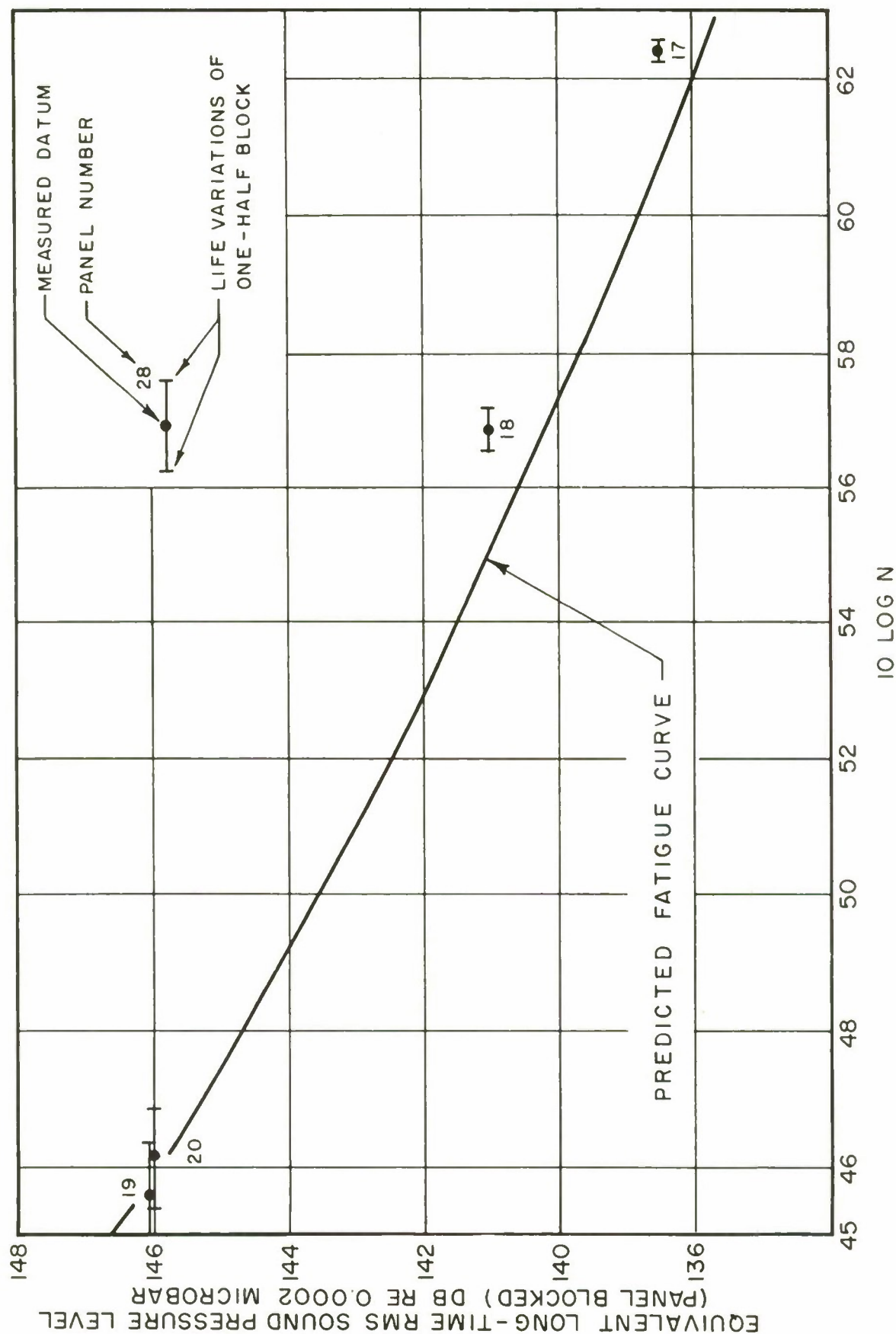


FIG. 20 FATIGUE LIVES WITH PROGRAMMED AMPLITUDE AS A FUNCTION OF BLOCKED SOUND PRESSURE



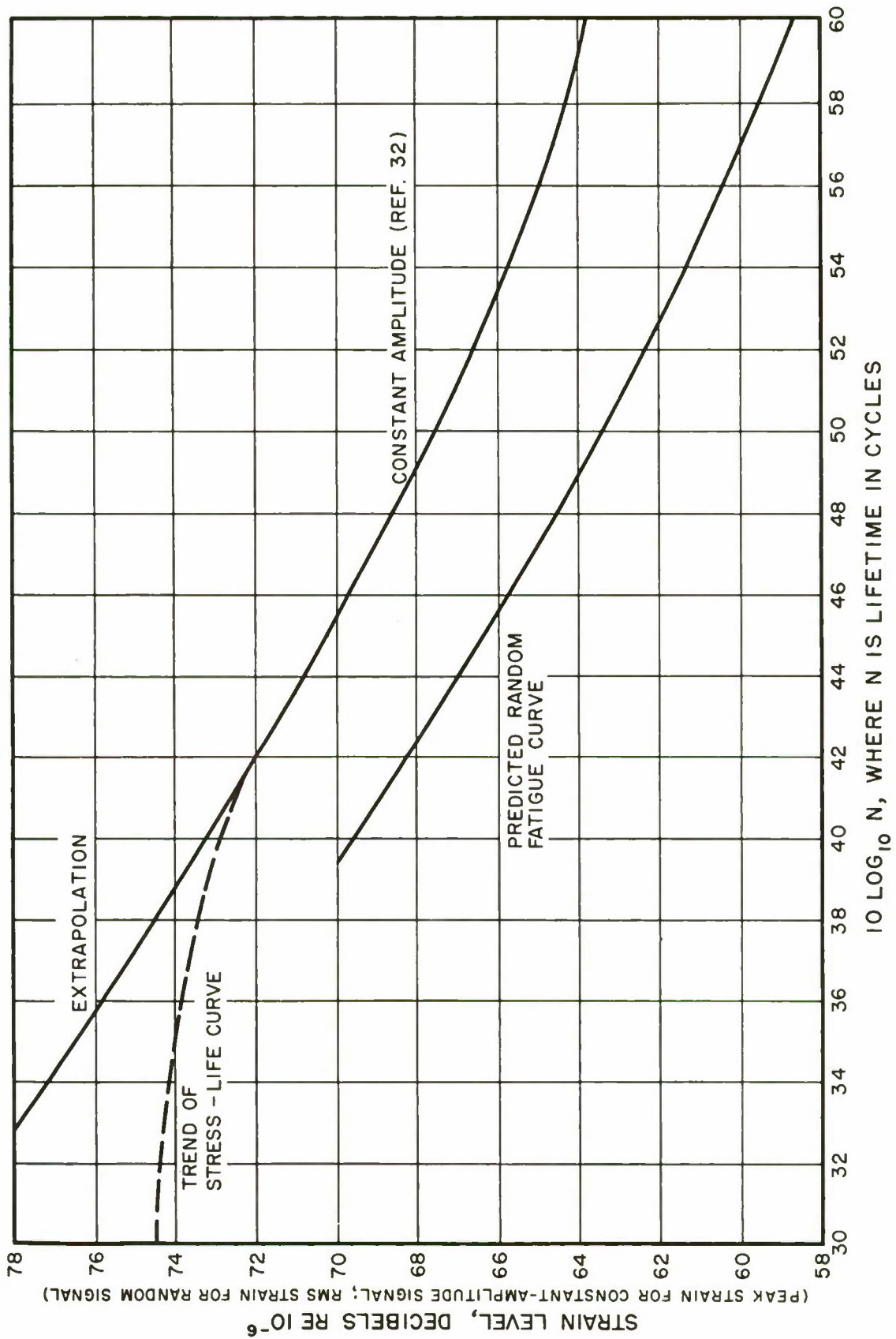


FIG. 21 FATIGUE CURVES FOR ALCLAD 2024 ALUMINUM

compared with the results of our programmed amplitude fatigue tests, Fig. 20. A constant conversion factor was used, whose value is based on the measured strain concentration factor (Table VIII) and the measured pure-tone response (Table III). The resulting prediction, plotted in Fig. 20, is in quite satisfactory agreement with the results of the programmed-amplitude fatigue tests.

### C. JET NOISE TESTS

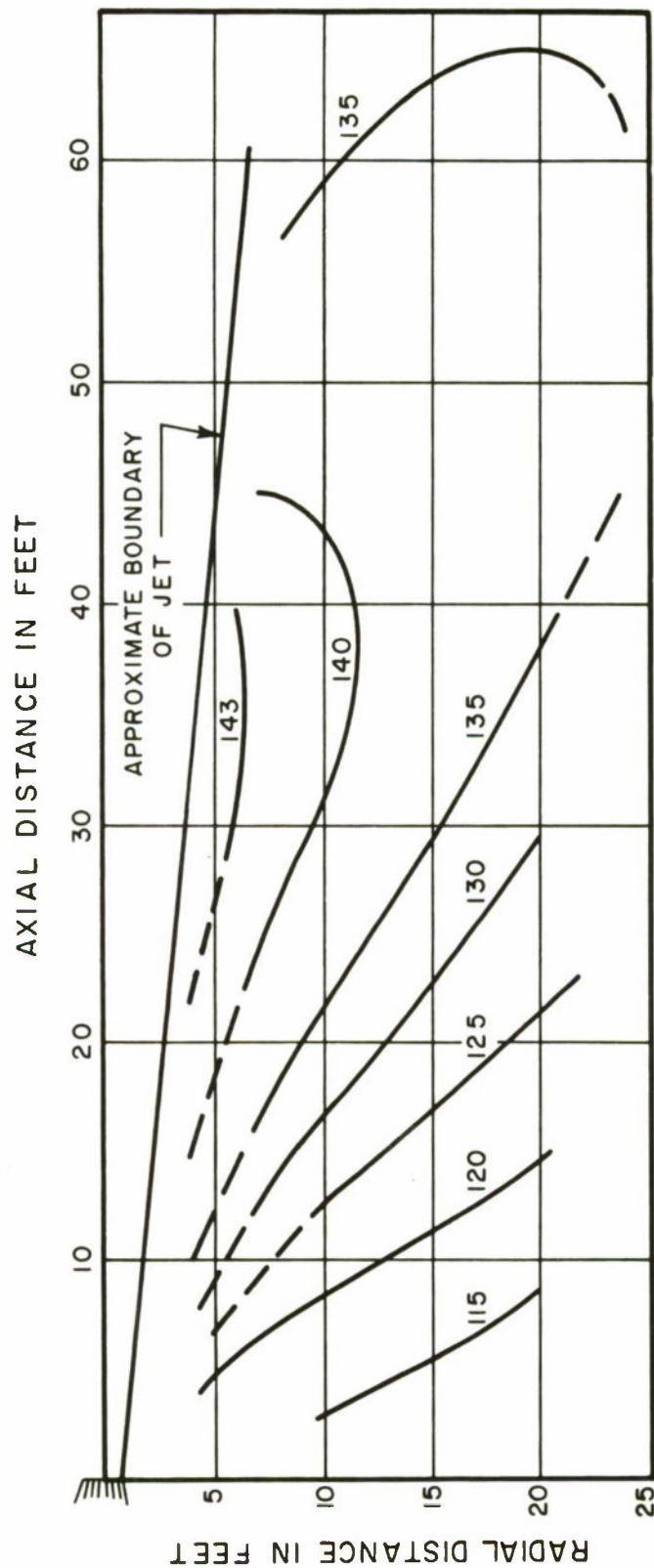
Five structural panels, with 0.125-in. holes drilled in the centers of the beads, were fatigued by exposing them to the noise from a jet engine. These measurements were made at a test stand at ASD where a J75-P19 engine was mounted horizontally above an extended, flat concrete surface. The center line of the engine was 6 ft above the concrete. The panel mounting was described in section IV and is illustrated in Fig. 12, above.

A survey of the sound pressure levels was made in the region aft, and of course to the side, of the engine. Contours of constant sound pressure levels in a third-octave band centered on 110 cps (engine at military power) are plotted in Fig. 22. For the fatigue tests, the panels were placed about 35 ft aft and 10 ft to the side of the exit nozzle. Different levels of excitation were achieved by running the engine at different speeds, from 100 percent to about 72 percent of full speed (rpm).

In a test, the engine speed was increased until the chosen sound pressure level was reached. If any change in the pressure occurred, the engine operator was instructed to adjust speed accordingly. Periodic inspections of the panels were attempted with the engine running at speed, but only inspections with the engine idling were relied upon for detection of cracks. These were made at intervals varying in accordance with expected lifetime.

During the tests, meter readings and tape recordings were made of the strain and acceleration of the panels and of the sound pressure level 3-in. above the center panel (overall level and level in a third-octave band centered on 110 cps). The recordings were analyzed later in the laboratory. The probability density analysis of the strain was shown above in Fig. 15. Some response data (pressure/strain ratios) were given in Table V.

Narrow-band (8%) spectra of the acceleration at the panel's center and the strain on a bead on one edge are shown in Figs. 23 and 24. The acceleration spectrum resembles very much the expected result for a one-mode system. However the height of the resonance peak cannot be used to determine the loss factor since the bandwidth of the analyzer (8%) is narrower than the bandwidth of the structure (estimated: 3%). The strain spectrum shows perturbations from the shape for one mode. The bump at about 60 cps probably is due to hum in the system.



ENGINE = 6 FT ABOVE FLAT CONCRETE SURFACE  
 MICROPHONE : 20 IN. ABOVE CONCRETE,  
 MEASUREMENTS AT 5 FT INTERVALS

FIG. 22 CONTOURS OF CONSTANT SOUND PRESSURE LEVEL IN A THIRD-  
 OCTAVE BAND CENTERED ON 110 CPS (J75-P19 JET ENGINE  
 AT MILITARY POWER )



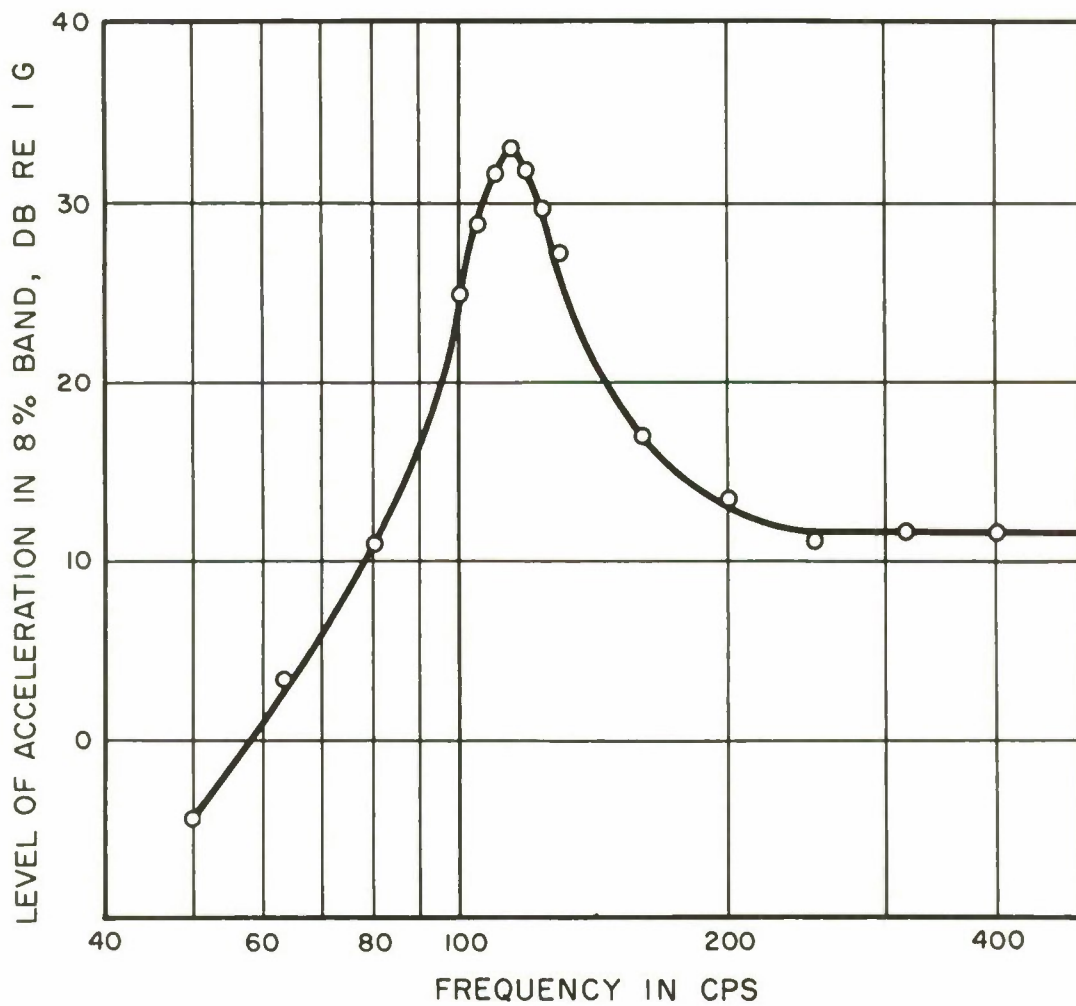


FIG. 23 NARROW - BAND SPECTRUM OF ACCELERATION  
RESPONSE OF PANEL TO JET NOISE  
(145 DB OVERALL)

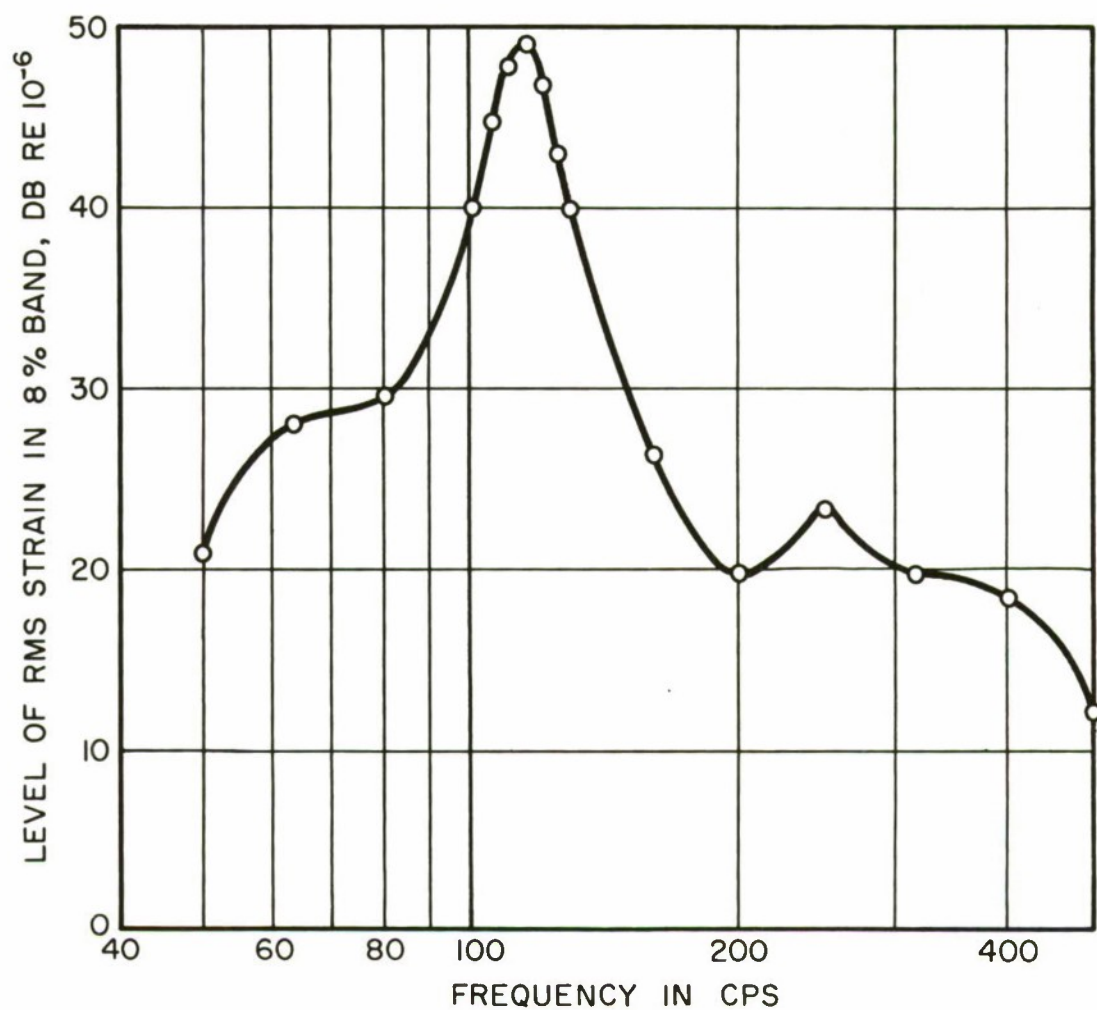


FIG. 24 NARROW-BAND SPECTRUM OF STRAIN  
RESPONSE OF PANEL TO JET NOISE  
(145 DB OVERALL)

The bump at about 250 cps probably reflects response in the second beam mode, whose resonance frequency was found by pure-tone measurements to be about 270 cps (section IV).

## 1. Results

Panel no. 9 was broken in an unknown time less than two minutes. Reliable measurements for it are not available; the data plotted in the following graphs are not reliable, representing attempts to use some fleeting observations of meters. Data for the other four panels (lifetimes: 4.5, 27, 65, and 65 minutes) have been taken with care from the tape recordings.

Strain-lifetime results are plotted in Fig. 25. That figure also contains a "predicted fatigue curve" which is based solely on (1) the computed random fatigue curve in Fig. 21, and (2) the strain concentration factor determined by pure-tone siren tests, Table VIII. Except in the case of panel no. 9, the agreement between prediction and measurements is quite good.

Sound pressure-lifetime results are plotted in Fig. 26. The "predicted fatigue curve" in this figure is based on Fig. 21 and Table VIII, as above, and upon the average pressure-strain ratio determined in the field (Table V). The differences between data and prediction are greater here than in Fig. 25. (The sound pressure plotted in Fig. 26 were measured with the panel vibrating, as were the data used in Table V. With the panel blocked, the sound pressure levels in a third-octave band centered on the resonance averaged 1 db higher.)



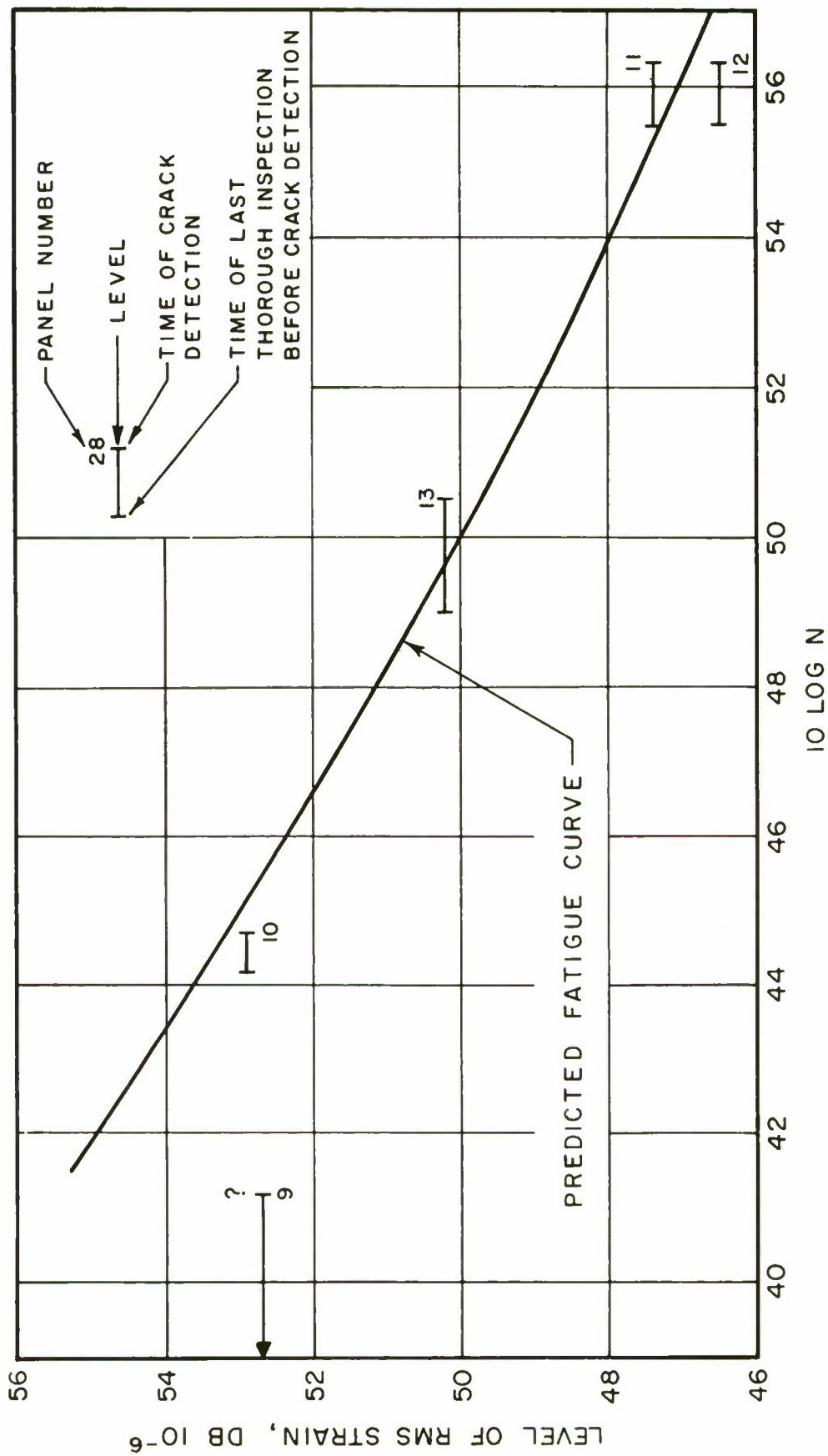


FIG. 25 STRAIN - LIFE FATIGUE DATA WITH JET NOISE EXCITATION

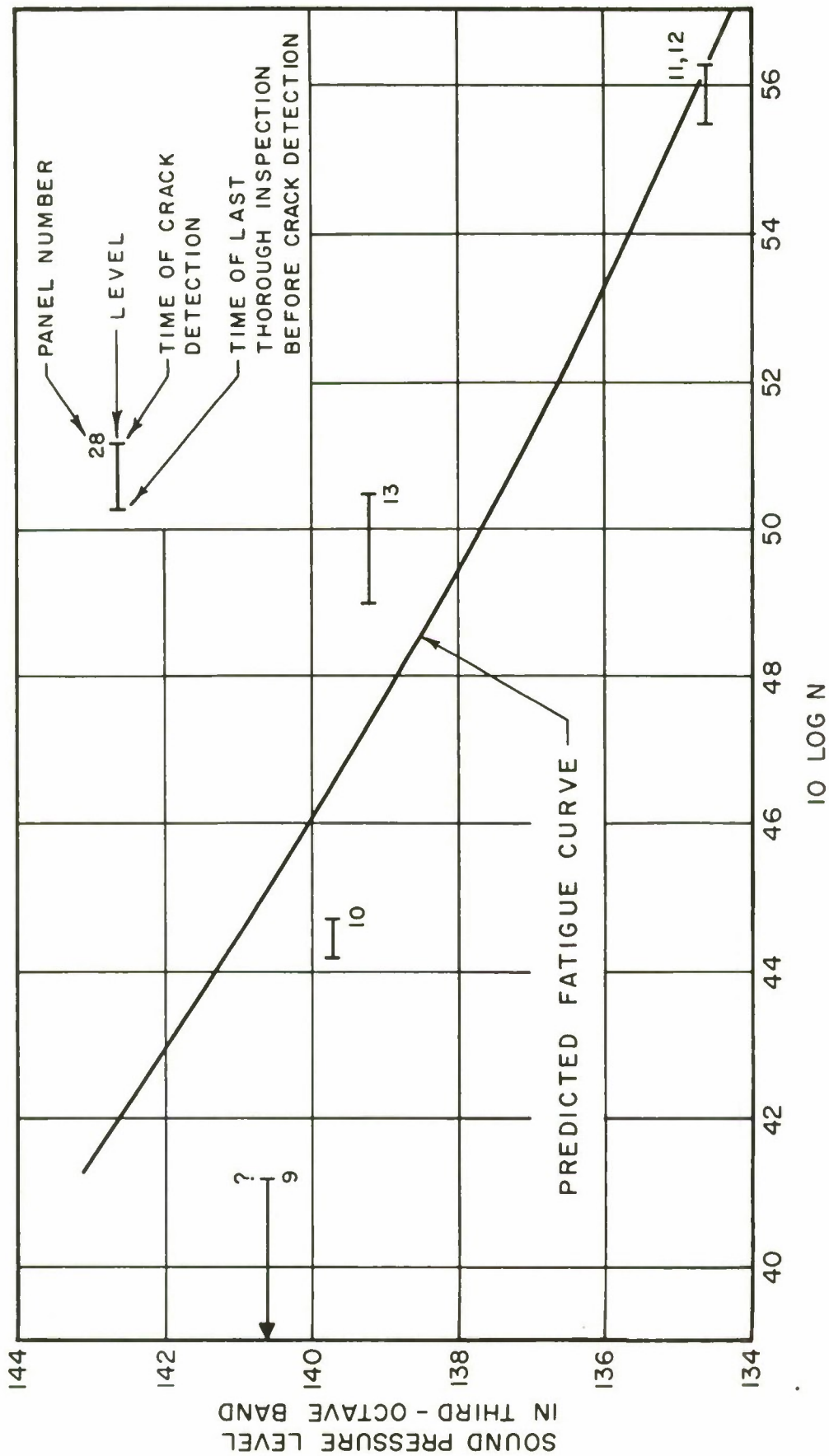


FIG. 26 SOUND PRESSURE - LIFE FATIGUE DATA WITH JET NOISE EXCITATION

## SECTION VII

### EVALUATIONS AND COMPARISONS

When the evaluation of prediction schemes has been promised, there comes a time when equivocation over the detailed significance of data must be set behind one and straightforward predictions compared with test results.

We shall compare the measured fatigue lives of panels exposed to various levels of jet noise with predictions obtained by two schemes. The first prediction scheme is that described in subsection II-D. It is based on measurements of fatigue lifetime under excitation by a program of varying sound pressures generated by a siren. The equivalent random noise level for a specific program is found by random-noise response measurements (ratio of rms strain to rms pressure.)

The second prediction scheme is based on computations from fatigue curves taken from the literature, assuming a Rayleigh distribution of strain peaks, and making no allowance for fatigue interactions between different peaks. Experimental measurements include (1) constant-amplitude fatigue tests, using a siren, to determine a strain concentration factor, and (2) random-noise response measurements. This prediction scheme is essentially that described in subsection II-D, except that measurements of random-noise response are used in place of computations, for reasons discussed below.

The first comparisons are shown in Fig. 27. The two prediction schemes give very nearly the same results, the predicted lifetimes being, on the average, long by a factor of from 2 to 4 while the predicted sound pressure levels for a given life are high by about 2 db. The random-noise response data on which these predictions are based are the results of laboratory measurements (Table IV).

When the predictions are based on random-noise measurements made in the same environment as the jet-noise fatigue tests (Table V) a different picture emerges (Fig. 28). Each prediction scheme appears to define a very satisfactory trend curve for the jet-noise fatigue data.

The dashed curve in Fig. 28 is plotted with the slope determined by fatigue tests of randomly excited cantilever beams (Table II). It is evident that those results are in essential agreement with results of the other tests. Therefore these cantilever beam tests are an acceptable means for designing accelerated life tests.



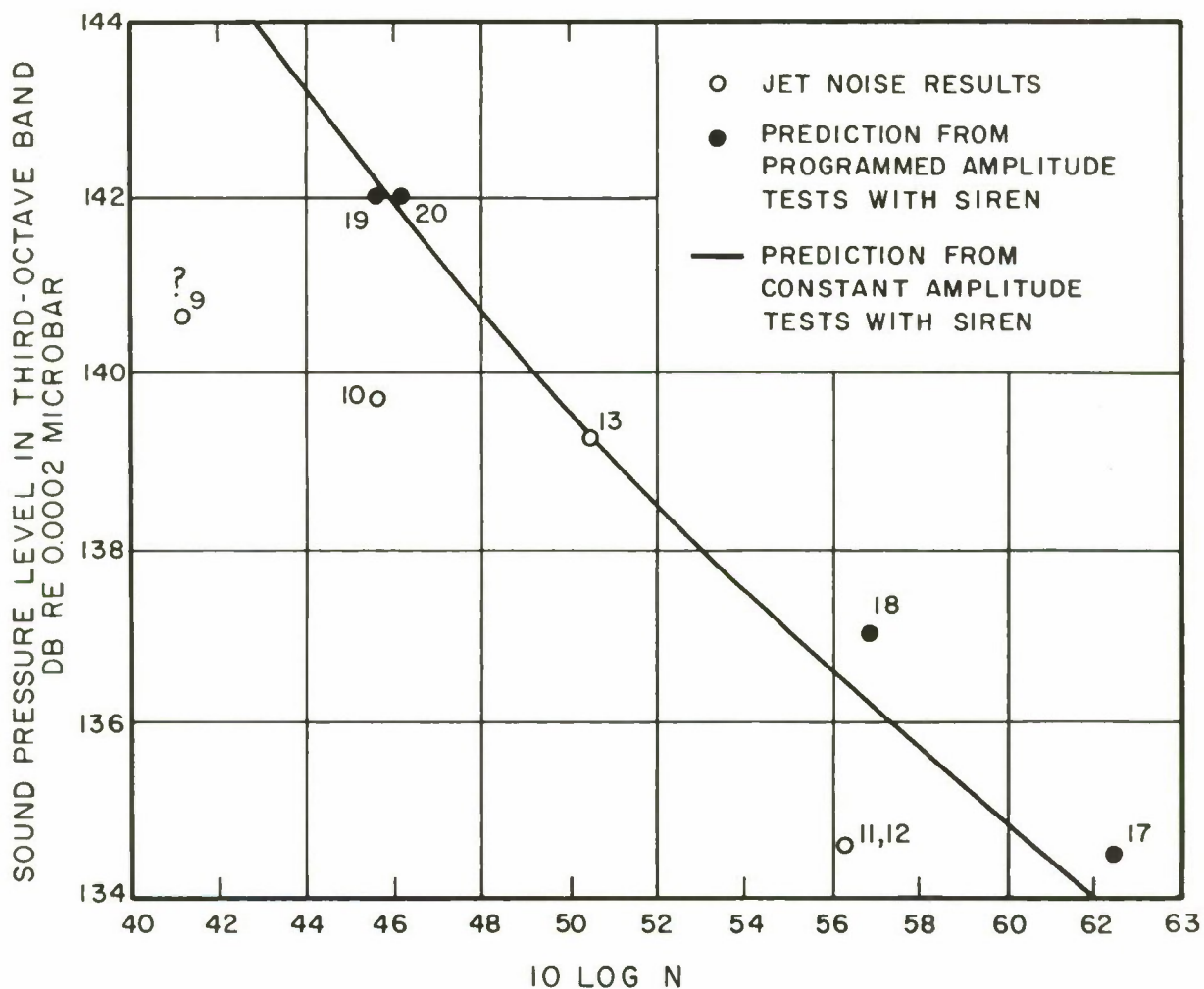


FIG. 27 JET NOISE FATIGUE DATA COMPARED WITH PREDICTIONS BASED ON LABORATORY MEASUREMENTS OF RANDOM RESPONSE

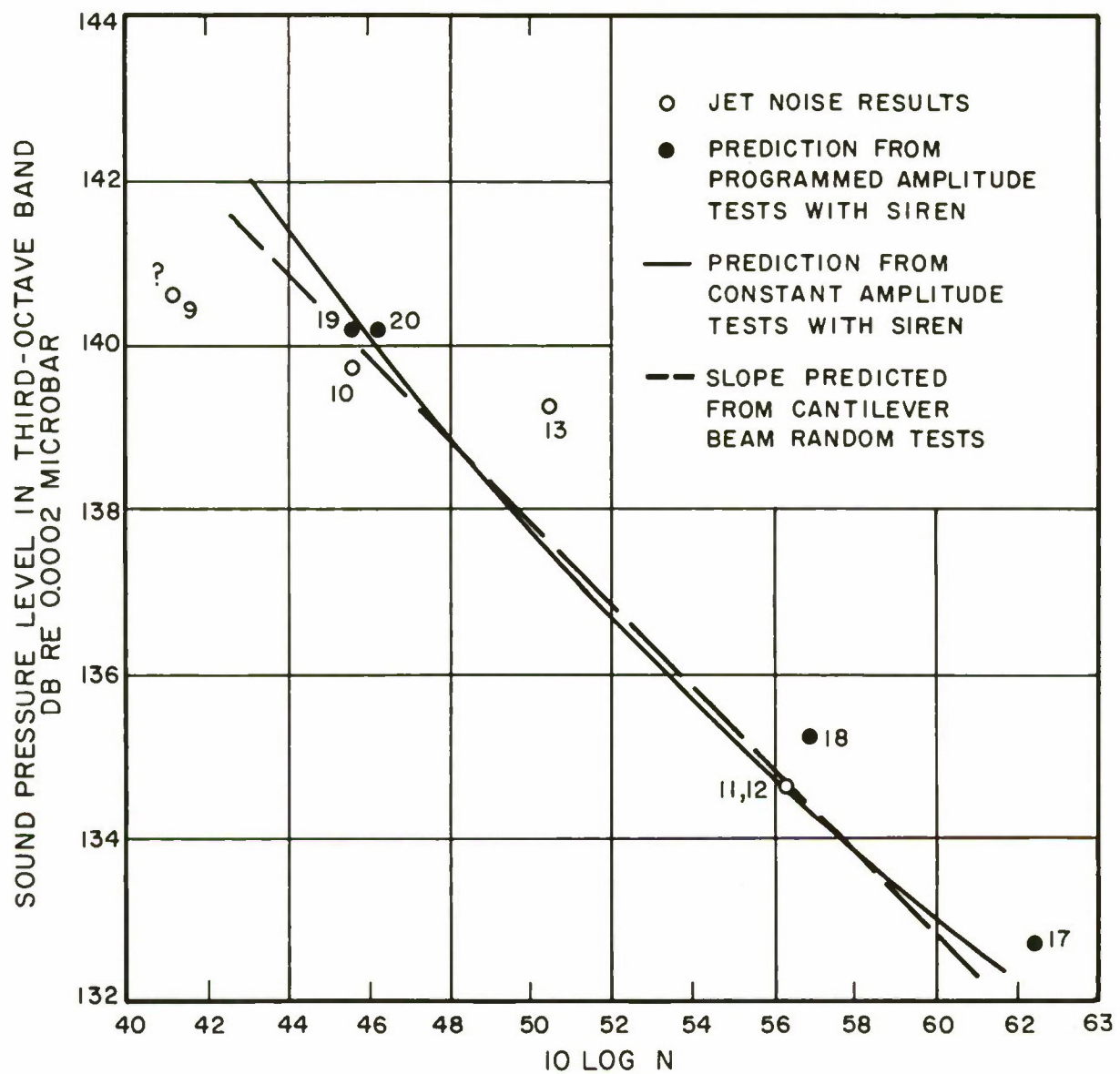


FIG. 28 JET NOISE FATIGUE DATA COMPARED WITH PREDICTIONS BASED ON FIELD MEASUREMENTS OF RANDOM RESPONSE

## A. GENERAL COMMENTS

We present here a number of comments on the implications of these results.

The extent of the agreement between predictions and measurements apparent in Fig. 28 must be considered a little bit fortuitous. The predictions are based on a series of measurements, each of which is somewhat inaccurate for many reasons. The number of samples used in both laboratory and field tests is not large and changes of 0.5 to 1 db, or perhaps more, might be expected in a repeat test. Nevertheless, satisfactory agreement has been achieved.

The basic problem in these tests was in achieving a satisfactory measurement of response. For example, fatigue curves plotted in terms of measured strains showed excellent agreement. (See Figs. 20 and 25, remembering that the measurements for panel 9 are suspect.) To some extent this problem was probably due to variations between characteristics of individual panels. It was very much accentuated by the presence in low level response of two nearby modes, one of whose importance was unrealistically magnified in the pure-tone tests by the abnormal acoustic radiation damping of the other.

A particularly important aspect of the response problem is the determination of the response to random noise. The direct experimental approach in the laboratory has its difficulties (abnormal radiation loading, non-uniform pressure distribution, etc.) discussed in the section on response. Measurement in a suitable field environment may not always be feasible. The other alternative of calculation from measured values of damping, using Eq. (17), appears from the present experience to be particularly poor. Loss factors could not be determined with as much accuracy as the pressure-strain ratio.

It is for this reason that a computational procedure based on measured loss factors and Eq. (17) was not included in the predictions exhibited above. Four determinations were made of the loss factor for the panel in the pure-tone environment (Section IV above). The resulting predictions for fatigue curves would have ranged from 1.2 db lower than the predictions in Fig. 27 to 3.2 db higher. It is felt that the procedure adopted, using the laboratory measurement of random pressure-strain ratio, was the most accurate.

Finally, this investigation illustrates the advantages in making many measurements of response on many specimens. Accumulated errors of 2 to 4 db or more could easily have resulted from reliance on particular individual measurements.



## B. PROGRAMMED AMPLITUDE TEST SCHEMES - PRO AND CON

The programmed amplitude test schemes proposed and tested in this study have various advantages and disadvantages.

The simplified program, with 2 db steps, proved feasible and gave good results. It is a good way to achieve an average pure tone response without actually making measurements. If it had been applied blindly, without so much study of response at a low level, many of the worries about the two modes of response would have been avoided. On the other hand, it requires much more test time than constant-amplitude fatigue tests, and could become quite a chore for long lifetimes.

A continuous program, such as is described in subsection V-A, was not necessary in the present tests, to judge from the results. However with reliable automatic control of sound pressure amplitude and of frequency, a continuous program would be quite a bit simpler. Continuous and automatic control would probably be essential for determinations of short lifetimes.

## C. FATIGUE INTERACTIONS

The fatigue measurements made on the panels, made of Alclad 2024 aluminum alloy, indicate that fatigue interactions were not a significant factor. Therefore no judgement can be made of the effectiveness of the programmed amplitude tests in simulating this aspect of random fatigue.

However, the results of the cantilever beam tests on plain 2024 aluminum alloy (section III) indicate a difference between random measurements and predictions which may be ascribable to fatigue interactions.

## D. NONLINEARITY

Nonlinearity of response is not believed to have been a strong factor in the present tests, except in respect to its mode coupling effects. There is some suggestion, both in the programmed-amplitude tests and in the jet tests, that nonlinearity may have accounted for a flattening of about 1 db at the high levels in the fatigue curves of Figs. 27 and 28. However, a definitive conclusion is not appropriate in view of the experimental accuracy.

## SECTION VIII

### RESEARCH ON SIREN FATIGUE TESTING

The results of this investigation indicate a number of areas where research is needed in order to validate and improve the reliability of fatigue testing with siren excitation. These areas are listed here with brief discussions of the information that is desired.

#### A. EXPERIMENTAL INVESTIGATION OF VARIABILITY FOR TYPICAL CONSTRUCTION

It is extremely important that quantitative limits be set on the accuracy required of a testing scheme. Quite probably, these limits will be set by variability in the response and fatigue characteristics for nominally identical samples of the same structure. What are typical values for these variations? If the variations seem too large, can they be reduced, in practical construction, by suitable quality control techniques?

The panels used in this investigation afford one example of variation in the low-level response characteristics. Yet this variation seemed to disappear at larger response amplitudes (section IV). Thus predictions of life based on the low-level response to pure tones would have been much more inaccurate than predictions based either on the high-level response or on the rms response to noise.

How much variability is there in the relations between fatigue lifetime and nominal response? In the panels used in this investigation, the strain concentrations were quite uniform, from panel to panel, and the strain-lifetime relations show little scatter. But much more scatter is likely if the fatigue occurs at some sharp bend, on a rivet line, etc.

#### B. EXPERIMENTAL COMPARISONS OF CONSTANT AMPLITUDE, PROGRAMMED AMPLITUDE, AND RANDOM-RESONANT FATIGUE LIFETIMES

The tests made in this study afford some comparisons of the fatigue lifetimes of a resonant structure excited by constant amplitude, programmed amplitude, and random signals. Many more such comparisons could be desired. Especially valuable would be very carefully controlled comparisons made with quite idealized specimens. A shaker-excited resonant beam is one likely design. The experiments should be refined to include controlled force of excitation and controlled nonlinearities of response (both in stiffness and damping). They should include careful response studies and a moderately large number of tests, including some with quite long lifetime. Various materials should be tested.



More experience with variable amplitude fatigue testing of structures would be desirable. These should include tests with other designs and other materials. The practicability of long-life tests should be studied; the lower truncation level of the program can be much higher in such tests with a consequent saving of time. In any test with lifetime less than about  $10^5$  cycles, it appears that automatic control of the program and of the frequency should be incorporated; such control devices should be developed and tested.

#### C. RANDOM RESPONSE OF ONE-MODE RESONATOR WITH NONLINEAR DAMPING

Available results from this and other investigations have indicated the practical importance of nonlinear damping in governing the response of structures. It is a disturbing fact that there is neither experimental nor theoretical information on which to base an estimate of the effects of nonlinear damping on fatigue life. Both experimental and theoretical investigations should be started. Information on the probability density of response peaks is essential.

#### D. RESPONSE OF NONLINEARLY COUPLED PROXIMATE MODES

The peculiar behavior of the panel used in this study (section IV) has been tentatively explained as resulting from the presence of two resonant modes with closely adjacent resonance frequencies and from their nonlinear coupling through the potential energy. According to this hypothesis, the coupling results in essentially one-mode response when the amplitude of vibration is large, even though the force-response relations are not noticeably nonlinear.

Practical structures very often show two such proximate modes in their response curves. Theory indicates that they should be nonlinearly coupled. Both theoretical and experimental studies of such systems are required for adequate understanding and prediction of their response. If the explanation proposed here is right, prediction of the fatigue lifetime of such a system would be greatly simplified.

#### E. EXPERIMENTS ON FATIGUE LIFE OF A STRUCTURE WITH TWO DISTINCT MODES

Structures with two distinct resonant modes, well separated in resonance frequencies, are also common. Much discussion, little analysis, and apparently no experimentation have been applied to the question of the fatigue life of such a structure. Some carefully controlled experiments, with associated analyses, are required to investigate this area. Both constant amplitude and random excitation should be used, with different levels at the two frequencies.



## F. FEW-MODE MODELS OF PRACTICAL STRUCTURES

Reports of detailed, careful experimental investigations of the response of practical structures to excitation by sound are seldom found. Since theories based on the presence of but one mode are simple and available, evidence is often found to confirm the dominance of a single mode of response. The evidence is not always sufficient: A single peak in the spectrum of response to random noise could indicate only a clumping of modes in a limited frequency region.

Experiments and analyses should be made to define the response characteristics of reasonably simple structures in considerable detail. This work might well start with pure-tone studies, leading to the description of an idealized (possibly nonlinear) model with a few modes. The response of the model to random forces could then be studied by analyses and analog experiments.

## REFERENCE LIST

1. J. W. Miles, J. Aeronaut. Sci. 21, 753-762 (1954).
2. W. D. Dorland, NASA TN D-611 (August, 1961).
3. A. K. Head and F. H. Hooke, Proc., Int'l. Conf. on Fatigue, sponsored by Inst. Mech. Engrs. (Gt. Brit.) and Am. Soc. Mech. Engrs., November 1956, pp. 301-304.
4. A. L. Karnesky and H. C. Schjelderup, Shock and Vibration Bulletin No. 25, Part II, pp. 39-54, Office of the (U.S.) Secretary of Defense, Washington, D. C., December 1957; A. L. Eshleman, Jr., J. VanDyke, Jr., and P. Belcher, ASME Paper No. 59-AV-48, presented at the ASME Aviation Conference, Los Angeles, March 1959; P. M. Belcher, J. D. VanDyke, Jr., and A. L. Eshleman, Jr., Aero/Space Engineering 18 (No. 6), 24-30 (June 1959); H. C. Schjelderup, pp. 19-25 in Acoustical Fatigue, ASTM Special Technical Publication No. 284 (American Society for Testing Materials, Philadelphia, Pennsylvania, 1960).
5. R. W. Fralich, NASA Memo 4-12-59L (June 1959).
6. K. Gunn, Aeronaut. Q., 6, 277-294, (1955).
7. R. D'Amato, WADD TR 60-175 (April 1960).
8. A. M. Freudenthal, R. A. Heller, and P. J. O'Leary, WADC TN 55-273, Part I (June 1955).
9. R. H. Lyon, "On the Vibration Statistics of a Randomly Excited Hard Spring Oscillator. II", J. Acoust. Soc. Am., 1395-1403 (1961). (Prepared under Contract AF 33(616)-7147.)
10. I. Dyer, P. W. Smith, Jr., C. I. Malme, and C. M. Gogos, ASD TR 61-262 (March 1961).
11. Reference 10, Section III.
12. Reference 10, Section II.
13. S. H. Crandall, Chap. 4 in S. H. Crandall, editor, Random Vibration (The Technology Press of the Massachusetts Institute of Technology, Cambridge, Massachusetts, 1958).
14. Reference 10, Fig. 44.
15. R. W. Hess, L. W. Lassiter, and H. H. Hubbard, NACA RM L55E13c (July 1955); L. W. Lassiter and R. W. Hess, NACA Report 1367 (1958).
16. P. W. Smith, Jr., J. Acoust. Soc. Am. 33, 752-756 (1961); ibid, 814-815 (1961). (Prepared under Contract AF 33(616)-7147.)

# REFERENCE LIST (CONT)

17. A. M. Freudenthal and R. A. Heller, WADC TR 58-69 Part I (June 1958).
18. R. H. Lyon, J. Acoust. Soc. Am. 33, 815 (1961).
19. Karl Pearson, Tables of the Incomplete  $\Gamma$  - Function, (Cambridge University Press, Cambridge, England, 1946).
20. P. W. Smith, Jr., "Response of Nonlinear Structures to Random Excitation," presented at SAE National Aeronautic and Space Engineering and Manufacturing Meeting, Los Angeles, 12 October 1961, Paper No. 430E.
21. P. W. Smith, Jr., C. I. Malme, and C. M. Gogos, J. Acoust. Soc. Am. 33, 1476-1482 (1961).
22. A. M. Freudenthal and R. A. Heller, Chapter 8 in Fatigue in Aircraft Structures, edited by Freudenthal (Academic Press, New York, 1956).
23. A. M. Freudenthal and R. A. Heller, WADC TN 55-273, Part II, (October, 1956).
24. A. M. Freudenthal and R. A. Heller, WADC TR 58-69, Part II, (January, 1960).
25. R. A. Heller, WADD TR 60-752 (February, 1961).
26. H. F. Hardrath and E. C. Naumann, pp. 125-138 in Fatigue of Aircraft Structures, ASTM Special Technical Publication No. 274 (American Society for Testing Materials, Philadelphia, 1960).
27. R. H. Lyon, J. Acoust. Soc. Am. 32, 716-719 (1960).
28. P. J. Roark, Formulas for Stress and Strain, (McGraw-Hill Book Company, New York, 1954), Table XVII, p. 344.
29. R. E. Peterson in WADC TR 59-507 (August, 1959).
30. Reference 10, Section VIII.
31. G. W. Kamperman, C. H. Allen, J. R. Sharp, and L. J. Williams, WADD TR 59-12 (December, 1959).
32. H. N. Cummings, WADD TR 60-42 (July, 1960), Fig. 96.



Aeronautical Systems Division, Dir/Aero-  
mechanics, Flight Dynamics Lab, Wright-  
Patterson AFB, Ohio.

Rpt Nr ASD-TR 61-639 SONIC FATIGUE LIFE  
DETERMINATION BY SIREN TESTING. Final  
report, May 62, 87 p. incl illus., tables, 32 refs.

Unclassified Report

Experimental and theoretical researches were  
made on the problem of predicting the fatigue  
life of a resonant structure exposed to jet noise  
by testing it with intense sound from a siren. One  
panel design of Alclad 2024 aluminum was tested  
to fatigue with constant-amplitude and variable  
amplitude siren sounds and with jet noise. A

( over )

close correlation of all three results was found.

A comparison was also made of fatigue lifetimes  
of a resonant cantilever beam, of plain 2024  
aluminum, measured with constant excitation  
amplitude (pure tone) and with random excitation.  
Random lifetimes were found to be shorter than  
predictions from constant-amplitude data.

1. Sonic fatigue

I. AFSC Project 1370,  
Task 137001

II. Contract AF 33(616)-  
7147

III. Bolt Beranek and  
Newman, Inc.

IV. P. W. Smith, Jr.,  
and C. I. Malmé

V. In ASTIA collection  
VI. Aval fr OTS

Aeronautical Systems Division, Dir/Aero-  
mechanics, Flight Dynamics Lab, Wright-  
Patterson AFB, Ohio.

Rpt Nr ASD-TR 61-639 SONIC FATIGUE LIFE  
DETERMINATION BY SIREN TESTING. Final  
report, May 62, 87 p. incl illus., tables, 32 refs.

Unclassified Report

Experimental and theoretical researches were  
made on the problem of predicting the fatigue  
life of a resonant structure exposed to jet noise  
by testing it with intense sound from a siren. One  
panel design of Alclad 2024 aluminum was tested  
to fatigue with constant-amplitude and variable  
amplitude siren sounds and with jet noise. A

( over )

close correlation of all three results was found.

A comparison was also made of fatigue lifetimes  
of a resonant cantilever beam, of plain 2024  
aluminum, measured with constant excitation  
amplitude (pure tone) and with random excitation.  
Random lifetimes were found to be shorter than  
predictions from constant-amplitude data.